



---

# RENORMALISATION GROUP FOR GRAVITY AND DIMENSIONAL REDUCTION

---

## MASTER THESIS

zur Erlangung des akademischen Grades eines  
Master of Science  
an der Naturwissenschaftlichen Fakultät der  
Karl-Franzens-Universität Graz

Natália Alkofer, BSc

*Advisor:* Prof. Dr. Daniel F. Litim  
*Co-advisor:* Priv.-Doz. Dr. Bernd-Jochen Schaefer

2013



# Abstract

The functional renormalisation group for the Einstein-Hilbert action is investigated for the case of four infinite (or large) and one compact dimension.

The motivation for this study is given by the suggestion that gravity in more than four dimensions might be able to solve the so-called hierarchy problem of the Standard Model of elementary particle physics because the assumed extra dimensions allow to unify the true Planck scale with the electroweak scale. In a first step the Einstein-Hilbert theory for the functional renormalisation group treatment of Quantum Gravity is introduced. To set the scene for the following investigation including a compact dimension first some corresponding calculations for four and more large dimensions are performed and the results are found to be in agreement with already known ones.

The equations determining the renormalisation group flows are then derived for the case of one compact dimension. These dimensionally reduced renormalisation group equations are then numerically solved for the case of four large and one compact dimension. Results for the four- to five-dimensional crossover are then discussed employing two forms of the background field flow in the Einstein-Hilbert theory for the case of one extra compact dimension. Renormalisation group trajectories allowing for a significant lowering of the true Planck scale to the electroweak scale are identified. The behaviour of the running gravitational coupling at the four- to five-dimensional crossover and the true Planck scale is displayed. Potential phenomenological implications are briefly discussed.



# Kurzfassung

Die funktionale Renormierungsgruppe für die Einstein-Hilbert-Wirkung wird für den Fall von vier unendlich großen und einer kompakten Dimension untersucht.

Die Motivation für diese Untersuchung liegt in dem Vorschlag begründet, dass Gravitation in mehr als vier Dimensionen in der Lage ist, das sogenannte Hierarchieproblem des Standardmodells der Elementarteilchenphysik zu lösen, da die hypothetischen extra Dimensionen es erlauben, die tatsächliche Planck-Skala mit der elektroschwachen Skala zu identifizieren. In einem ersten Schritt wird hierzu die Einstein-Hilbert-Theorie für die funktionale Renormierungsgruppe der Quantengravitation eingeführt. Um einen Vergleich zur späteren Untersuchung mit einer kompakten Dimension zu ermöglichen, werden zuerst Berechnungen in vier und höheren Dimensionen durchgeführt und die gefundenen Ergebnisse mit bereits bekannten Resultaten verglichen.

Die den Renormierungsgruppenfluß bestimmenden Gleichungen werden für den Fall einer zusätzlichen kompakten Dimension abgeleitet. Diese dimensional reduzierten Renormierungsgruppengleichungen werden dann für vier nicht-kompakte und eine kompakte Dimension numerisch gelöst. Die entsprechenden Ergebnisse für den vier- zu fünf-dimensionalen Crossover werden für zwei Formen des Hintergrundfeldflusses in der Einstein-Hilbert-Theorie diskutiert. Es werden Renormierungsgruppen trajektorien präsentiert, die eine signifikante Erniedrigung der tatsächlichen Planck-Skala bis hin zur elektroschwachen Skala erlauben. Das Verhalten der laufenden Gravitationskopplung beim vier- zu fünf-dimensionalen Crossover und bei der tatsächlichen Planck-Skala wird angegeben. Potentielle phänomenologische Implikationen werden kurz diskutiert.



# Contents

<b>1</b>	<b>Introduction</b>	<b>1</b>
1.1	Motivation . . . . .	1
1.2	Extra Dimensions . . . . .	4
1.2.1	The Hierarchy Problem . . . . .	4
1.2.2	Exploring Extra Dimensions . . . . .	5
1.2.3	The ADD Model . . . . .	5
1.3	Asymptotic Safety Scenario . . . . .	7
1.3.1	Weinberg’s Conjecture and Criteria . . . . .	7
1.3.2	Renormalisation Group Flows and Fixed Points . . . . .	7
<b>2</b>	<b>Renormalisation Group for Einstein-Hilbert Quantum Gravity</b>	<b>9</b>
2.1	Functional Renormalisation Group . . . . .	9
2.2	Einstein-Hilbert Quantum Gravity . . . . .	11
2.2.1	Background Field Formalism for Gravity . . . . .	11
2.2.2	Einstein-Hilbert Theory . . . . .	13
2.2.3	Gauge Fixing and DeDonder Gauge . . . . .	14
2.3	$\beta$ -Functions and Analytic Flows . . . . .	14
<b>3</b>	<b>Quantum Gravity in <math>D \geq 4</math></b>	<b>19</b>
3.1	Fixed Points in $D \geq 4$ . . . . .	19
3.2	Phase Diagrams in $D \geq 4$ . . . . .	24
<b>4</b>	<b>Dimensional Reduction for Einstein-Hilbert Gravity</b>	<b>29</b>
4.1	Matsubara Formalism and Kaluza-Klein modes . . . . .	30
4.2	Dimensionally Reduced Renormalisation Group Equations . . . . .	32
4.3	$\beta$ -Functions and Effective Coupling . . . . .	35
4.4	Discussion of the Limits . . . . .	37
4.5	Renormalisation Group Flows and Phase Diagrams in $D = 4 + 1$ . . . . .	40
4.5.1	Results for the Background Field Flow . . . . .	40
4.5.2	Results following from the Exact Functional Identity . . . . .	43
<b>5</b>	<b>Conclusions</b>	<b>47</b>
5.1	Phenomenological Implications . . . . .	47
5.2	Concluding Remarks and Outlook . . . . .	48

<b>A</b>	<b>Notations and Definitions</b>	<b>51</b>
<b>B</b>	<b>Derivation of the Functional Renormalisation Group Equations</b>	<b>53</b>
	B.1 An exact functional identity for the effective average action . . . . .	53
	B.2 Background field flow in proper-time regularisation . . . . .	55
<b>C</b>	<b>Second Variation of the Effective Action</b>	<b>57</b>
	C.1 Basic Variations . . . . .	57
	C.2 Tensor Decomposition of $\Gamma_k^{(2)}$ . . . . .	58
<b>D</b>	<b>Trace Evaluations and Heat Kernel Expansion</b>	<b>61</b>
	D.1 Background Field Flow . . . . .	61
	D.2 Exact Functional Identity . . . . .	65
	D.3 Tracing with a Compact Dimension . . . . .	67
	D.4 Dimensionally Reduced Background Field Flow . . . . .	69
	D.5 Exact Functional Identity: Dimensional Reduction . . . . .	71
<b>E</b>	<b>Threshold Functions</b>	<b>73</b>
<b>F</b>	<b>Numerical treatment</b>	<b>75</b>
	<b>References</b>	<b>77</b>
	<b>Acknowledgements</b>	<b>81</b>

# List of Figures

1.1	An illustration of different scales relevant for gravity. . . . .	6
3.1	Condition for the UV fixed point values for $D = 4$ and $D = 5$ for the background field flow. . . . .	21
3.2	Conditions for the UV fixed point values for $D = 4$ for the exact functional identity and the background field flow with $m = 3/2$ . . . . .	23
3.3	The extended phase diagram for the background field flows in $D = 4$ . . . . .	25
3.4	The phase diagram for $D=4$ from the exact functional identity. . . . .	26
3.5	$g_k$ , $\lambda_k$ and $\eta_k$ for two different trajectories in $D=5$ for the exact functional identity. . . . .	27
4.1	Comparison between three different values of $L$ . . . . .	40
4.2	Two examples for the RG scale dependence of coupling constants. . . . .	41
4.3	A further example for the RG scale dependence of coupling constants. . . . .	42
4.4	Same example as in Fig. 4.2 for the RG scale dependence of coupling constants but now for the $\beta$ -functions derived from the exact functional identity. . . . .	43
4.5	Similar to Fig. 4.3 but now for the coupling constants derived from the exact functional identity, and for $\lambda_k$ several starting conditions are displayed. . . . .	44
4.6	Phase diagram for the running gravitational coupling $g_{k,\text{eff}}$ and the cosmological constant $\lambda_k$ in 4+1 dimensions with physical trajectories in function of $\ln(kL/2\pi)$ . . . . .	46



# List of Tables

3.1	<b>D = 4:</b> UV fixed points within the background field flow for various values of the cutoff parameter $m$ . . . . .	22
3.2	<b>D = 5:</b> UV fixed points within the background field flow for various values of the cutoff parameter $m$ . . . . .	22
3.3	<b>D = 8:</b> UV fixed points within the background field flow for various values of the cutoff parameter $m$ . . . . .	22
3.4	The scaling exponents for some values of the cutoff parameter $m$ and number of dimensions $D$ . . . . .	22
3.5	UV fixed points for different number of dimensions for the two considered forms of the FRG. . . . .	24
3.6	The $k$ -independent product $\tau_*$ and the scaling exponents for $D = 4$ and $D = 5$ . . . . .	24



# Chapter 1

## Introduction

*“No question about quantum gravity is more difficult than the question, “what is the question?”.”*

*(J. Wheeler)*

### Contents

---

<b>1.1</b>	<b>Motivation</b>	<b>1</b>
<b>1.2</b>	<b>Extra Dimensions</b>	<b>4</b>
1.2.1	The Hierarchy Problem	4
1.2.2	Exploring Extra Dimensions	5
1.2.3	The ADD Model	5
<b>1.3</b>	<b>Asymptotic Safety Scenario</b>	<b>7</b>
1.3.1	Weinberg’s Conjecture and Criteria	7
1.3.2	Renormalisation Group Flows and Fixed Points	7

---

## 1.1 Motivation

Almost a hundred years ago, in 1915, Einstein proposed a theory of gravity. This theory is based on the principle of invariance of general coordinate transformations (diffeomorphism invariance), and Einstein called it therefore *Allgemeine Relativitätstheorie (General Theory of Relativity)* [1]. It is a classical field theory which allows to understand gravity only on the basis of the geometry of space-time. In the last decades General Relativity (GR) has been experimentally verified from length scales ranging from  $\mu\text{m}$  to cosmological distances. The corresponding coupling constant, Newton’s gravitational constant  $G_N$ , has been measured in laboratory experiments on scales of about  $50 \mu\text{m}$  to  $1\text{m}$ , see *e.g.*, [2] but also the footnote on Table 1.1 in the Particle Physics Booklet July 2012 [3]. Nowadays we know that a further constant, the so-called cosmological constant  $\Lambda$ , has to be considered in the classical theory of gravity. Introduced by Einstein in the early twenties to allow for a static universe it was abandoned by him after Hubble’s discovery of an expanding universe. As recent measurements indicate that this expansion is accelerating one reintroduces

this constant for a phenomenological description of cosmology. The corresponding value of  $\Lambda$  is so small that it plays a role only on cosmological distances.

The classical theory of gravity, *i.e.*, GR, can be formulated via the Einstein-Hilbert (EH) action. Varying this action with respect to the metric field provides Einstein's equation<sup>1</sup>. In this thesis I will choose the EH action, including the term with the cosmological constant, as a basis. More precisely, as it will be explained below, I will work within the EH theory in which the effective action is always projected on two terms [4].

Treating the EH theory as a Quantum Field Theory faces several problems. As an exhaustive description of the corresponding challenges is well beyond the scope of this thesis let me focus on the problem whose potential solution provides one of the starting points of this thesis: The perturbation series derived from the EH action is not renormalisable, *i.e.*, in every order of perturbation theory new types of divergencies appear which make then the perturbation series unpredictable. This can be inferred already from a simple power counting argument (for details on the notation see Appendix A): Newton's gravitational constant  $G_N$  possesses in four space-time dimensions a mass dimension -2, one has  $G_N = 1/m_{Pl}^2$  with  $m_{Pl} \approx 10^{19}$  GeV [3]. The enormous size of this number tells us that in a standard picture with four space-time dimensions gravity is in the classical regime not only at cosmological, astrophysical and every-day length scales but also at every current experiment including those at the Large Hadron Collider (LHC). Nevertheless, in order to progress on our understanding of gravity and quantum physics a quantum theory of gravity is highly desirable.

Returning to the problem of the potential non-renormalisability of a gravity action it might actually turn out that the above described problem is one of the methods, *i.e.*, the perturbative expansion, and not one of the theories. Already in the 70's Weinberg conjectured that Einstein gravity becomes renormalisable when treated non-perturbatively [5]. Based on different methods, but hereby especially on the Functional Renormalisation Group (FRG) [?, 6, 7, 9, 10], convincing evidence has been gathered for this fact which is known nowadays as asymptotic safety scenario [11–19]. Hereby it is important to note that asymptotic safety is quite distinct from the asymptotic freedom of four-dimensional quantum gauge field theories which renders them perturbatively renormalisable. Asymptotic freedom requires the dimensionless running coupling(s) of the theory to go to zero in the ultraviolet (UV). This special property allows then to re-express in the UV (*i.e.*, in practice well above a characteristic scale as, *e.g.*,  $\Lambda_{QCD}$ ) the perturbative series for a  $S$ -matrix element such that it contains only finite terms dependent on renormalised parameters, *i.e.*, all UV divergencies can be removed in a controlled way from the perturbative expressions. Therefore gauge field theories as, *e.g.*, Quantum Chromodynamics (QCD),

---

<sup>1</sup>Varying the EH action with respect to the metric and the Christoffel symbols provides Einstein's equation plus the metric compatibility constraint  $D_\rho g_{\mu\nu} = 0$  (Palatini formalism) and therefore leads to the same classical physics. This makes evident that not necessarily the metric coefficients alone are the dynamical degrees of freedom in a complete theory of gravity.

are perturbatively renormalisable. Asymptotic safety shares with asymptotic freedom the requirement of the existence of a non-trivial UV fixed point. However, in the asymptotic safety scenario the coupling constant(s) can take any finite value. Candidate theories for the asymptotic safety scenario possess typically (a) coupling constant(s) with negative mass dimensions. Rendering it (them) dimensionless by multiplying appropriate powers of the renormalisation scale, and thus generating arbitrary numerical values in dependence of the employed units, makes plain that a perturbative treatment close to an UV fixed point cannot work. Therefore we are confronted with the quest for an appropriate non-perturbative method.

The non-perturbative method chosen for this thesis is the FRG.<sup>2</sup> Hereby, I will use the background field formalism and two forms of the FRG, an exact functional identity and an approximated background field flow. For the latter I use proper-time regularisation and for the exact identity, the Wetterich equation [22], Litim’s optimised regulator [23–28]. Both forms of the FRG can be described as a mathematical tool which allows to treat quantum fluctuations step-by-step by varying the resolution scale. Hereby one starts with the classical action in the UV and solves the differential equations for the  $\beta$  functions of the theory, for details see Chapters 3 and 4 of this thesis.

Noting that gravity is not at all special in four dimensions (again in contrast to quantum gauge field theories which are exactly renormalisable in precisely four dimensions) I will investigate first the asymptotic safety scenario for a larger number of dimensions, hereby verifying previously obtained results [29, 30]. These extra dimensions will then be compactified such that the corresponding length scales can be continuously decreased from infinity to zero. The corresponding observed change of the fixed point values of the coupling constants demonstrates the possibility of going continuously from higher-dimensional fixed point values to lower-dimensional ones.

However, considering compact extra dimensions has an important other motivation. As mentioned above the enormous size of the Planck mass indicates that gravity will be in its classical regime up to truly huge energy scales. Together with today’s knowledge on elementary particle physics this creates a severe problem in our understanding of the relation of gravity to electroweak (EW) physics. As the renormalisation of masses of scalar fields is not protected by any known mechanism, the question arises why the mass of the Higgs is only (approximately) 125 GeV and not close to the Planck mass. This problem is called the hierarchy problem, for more details see Subsection 1.2.1 below. Quite recently there has been an interesting speculation [31, 32] which shifts the problem from the EW theory to gravity, resp., the geometry of space-time. At short distances gravity is not tested below  $10^{-4}$  m, so there is ample space for ”new” physics. Especially, the Arkani-Hamed, Dimopoulos and Dvali (ADD) model [?, 32] suggests that there might exist “large” extra dimensions with up to a  $\mu\text{m}$  compactification scale. One can easily verify,

---

<sup>2</sup>An approach which comes closest to Lattice Quantum Gravity is dynamical triangulation, see, e.g., [20, 21] and references therein.

see Subsection 1.2.3 below, that this would allow to unify the true gravity with the EW scale. In case such a scenario would be true this would not only solve the hierarchy problem<sup>3</sup> but opens up the exciting possibility to probe quantum gravity at the LHC. For a phenomenological description of corresponding cross sections (*e.g.*, graviton-mediated Drell-Yan processes) it is vital to know how the gravitational coupling runs in the energy domain relevant to the experiment [33–35]. In this thesis it is intended to describe the first few steps in a potential calculation of the scale dependence of the gravitational coupling constants in a space-time with compactified but “large” extra dimension(s).

## 1.2 Extra Dimensions

Before describing the ADD model [31, 32] and extra dimensions one of the original motivations for it will be described in the following subsection.

### 1.2.1 The Hierarchy Problem

Last year CERN announced the discovery of a particle with a mass of approximately 125 GeV. It is generally expected that this particle is the long-sought Higgs boson. If confirmed this will be the only fundamental scalar field in the Standard Model (SM) of particle physics. The discrepancy between its mass and the Planck or a possible Grand Unified Theory (GUT) scale leads to a fine tuning problem which is called the hierarchy problem<sup>4</sup>.

Contrary to the case of Dirac fermions and vector particles where either chiral symmetry or gauge invariance limits the divergence of mass renormalisation to a logarithmic one, the mass renormalisation of a scalar is quadratic:

$$m_H^2 = m_{H,0}^2 + \delta m_H^2 \quad \text{with} \quad \delta m_H^2 \propto \Lambda_{UV}^2 . \quad (1.1)$$

Therefore to achieve the physical Higgs mass there must be a very precise cancellation between  $m_{H,0}^2$  and  $\delta m_H^2$ .

Several explanations have been proposed to solve the hierarchy problem, *e.g.*, in technicolor models the Higgs is a bound state of TeV scale techniquarks. In this thesis, however, I build on another suggestion to circumvent the hierarchy problem, namely large extra dimensions.

---

<sup>3</sup>More precisely, it is solved on the expense that one would like to explain the size of the extra dimensions.

<sup>4</sup>As a matter of fact there are several hierarchy problems in physics. However, it is generally agreed upon that the question why the EW scale is so much smaller than the cutoff scale given by the Planck or GUT scale, is the most prominent hierarchy problem in particle physics.

## 1.2.2 Exploring Extra Dimensions

The above mentioned extra dimensions are assumed to be large as compared to the EW length scale. This is due to the following argument: In  $D = 4 + n$  dimensions (with Euclidean signature) the EH action<sup>5</sup> is given by

$$S_{EH}^{(D)} = -\frac{M_D^{n+2}}{16\pi} \int d^{4+n}x \sqrt{\det g_{\mu\nu}^{(D)}} R^{(D)} = -\frac{V_n M_D^{n+2}}{16\pi} \int d^4x \sqrt{\det g_{\mu\nu}^{(4)}} R^{(4)} \quad (1.2)$$

with  $M_D$  being the Planck scale in  $D$  dimensions and  $V_n$  the volume taken by the  $n$  extra dimensions. Here it was assumed that matter is restricted to our four-dimensional hypersurface, *i.e.*, the space constituted by the extra dimensions is flat. It is evident that one reproduces Einstein gravity if one identifies  $M_{Pl}^2 = M_D^{n+2} V_n$ .

Assuming the simplest compactification, namely a torus with periodic boundary conditions such that  $x_i = x_i + L$  with  $i = 5, 6, \dots, 4+n$ , one has  $V_n = L^n$ . Thus, if the size of the extra dimensions is large as compared to the EW scale the fundamental scale of gravity can be as low as the EW scale. To make this quantitative we rewrite the above formula as

$$M_{Pl}^2 = M_D^2 (M_D L)^n. \quad (1.3)$$

To avoid the hierarchy problem one requires  $M_D$  to be of the order of the EW scale, *i.e.*, 1 TeV. As  $M_{Pl} \approx 10^{16}$  TeV this implies  $(M_D L)^n \approx 10^{32}$  and therefore an enormously large separation of scales,

$$1/L \ll M_D \approx 1\text{TeV} \approx m_{EW}. \quad (1.4)$$

From this discussion it is evident that for  $n = 1$  there are approximately 32 orders of magnitude between  $1/L$  and  $M_D$ . One recognises then that  $n = 1$  is excluded because this would imply deviations from Newtonian gravity over solar system distances: Using  $\hbar c = 1 = 0.2 \cdot 10^{-18} \text{ m TeV}$  one estimates then  $L \approx 0.2 \cdot 10^{14} \text{ m}$ . Nevertheless, for illustrational purposes I will use  $n = 1$  in this thesis, and leave the cases  $n \geq 2$  for later studies.

## 1.2.3 The ADD Model

In the simplest version of the ADD model [31, 32] of large extra dimensions it is required that the fields of the SM are constraint to a four-dimensional hypersurface (our visible universe) whereas gravity propagates to additional dimensions. This subspace of extra dimensions has to be orthogonal to the four-dimensional hypersurface, and it is assumed to be compact. Nevertheless, due to Einstein's equation the space spanned by the extra dimensions is flat.

As detailed above the ADD model provides a solution to the hierarchy problem of particle physics. However, the prize to be paid is, at least, two further undetermined parameters, namely  $n$  and  $L$ . From the theoretical point of view the problem of explaining the fine-tuning of the Higgs mass has been reformulated to the question

---

<sup>5</sup>For simplicity the cosmological constant is neglected in this argument.

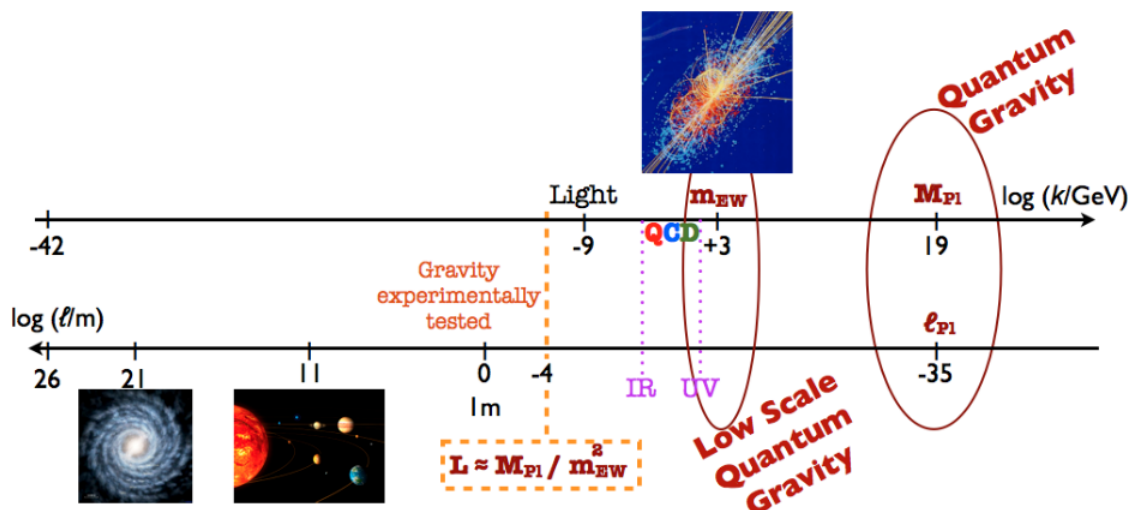


Figure 1.1: An illustration<sup>6</sup> of different scales relevant for gravity. On the right side, *i.e.*, for small distance and large momentum scales one has the (conventional) quantum gravity region. On the left side, with the distance scale equal to the Hubble scale there is the extreme infrared (IR) region.

why extra dimensions with a typical size smaller than 0.1 mm and larger than 1 fm (depending on the number of compactified extra dimensions) exist. From the experimental point of view the ADD model is highly interesting: It leads to measurable consequences for scattering processes at LHC energies, see *e.g.*, [33–39]. However, details of related observables will depend on the coupling strength of gravitons at the EW and the fundamental Planck scale. To this end one is interested in the Renormalisation Group (RG) running of Newton’s gravitational coupling in the ADD model geometry.

The situation is summarised in Fig. 1.1: A description of gravity in the conventional picture needs to cover at least sixty orders of magnitude from the Planck scale in the UV (in the figure on the right side) to the Hubble scale in the IR. Gravity is experimentally tested above scales of approximately 0.1 mm. This allows to introduce additional compact dimensions with corresponding sizes denoted by  $L$  as displayed in the figure. (The presented formula is valid for  $n = 2$ .) This results in a quantum gravity scale of the order of the EW scale  $m_{EW}$ . This region is marked as “Low Scale Quantum Gravity” in Fig. 1.1. It will be tested by the LHC in the coming years. An important constraint for the purpose of this thesis is the following: To achieve the lowering of the quantum gravity scale by 15 - 16 orders of magnitude one needs to have

$$1/L \ll m_{EW}. \quad (1.5)$$

<sup>6</sup>Images credits: NASA, ESA and CERN.

## 1.3 Asymptotic Safety Scenario

Here I will briefly review a few general aspects of the asymptotic safety scenario and a non-trivial UV fixed point in Quantum Einstein Gravity [5].

### 1.3.1 Weinberg's Conjecture and Criteria

The first and main criterium of the asymptotic safety scenario is the existence of a non-trivial fixed point at short distances. Such an UV fixed point can be considered as the generalisation of a non-interacting UV fixed point in asymptotically free theories as, *e.g.*, QCD. Whereas asymptotically free theories are perturbatively renormalisable, the non-vanishing value of the coupling constant(s) at the UV fixed point exclude a perturbative treatment. Secondly, it is indispensable that the UV fixed point is continuously connected with the IR behaviour of the theory by a well-defined RG trajectory. Otherwise, the UV fixed point would be disconnected from the observed semi-classical physics at large distances. Thirdly, it is mandatory that the UV fixed point possesses at most a finite number of IR unstable directions. Or else, the predictive power would be lost: An infinite number of unstable directions would necessitate the input of infinitely many parameters to obtain a trajectory reaching the IR limit.

These three criteria being fulfilled the UV fixed point together with a specific RG trajectory provides a fundamental definition of the theory. Such a theory is then called asymptotically safe. The existence of such theories have been conjectured by Weinberg in the seventies of the last century [5].

### 1.3.2 Renormalisation Group Flows and Fixed Points

To move on, the RG flow for Newton's gravitational constant  $G_N$ , will be discussed. Hereby, the number of dimensions  $D$  will be kept general. In a first step one introduces the renormalised dimensionless coupling as

$$g = \mu^{D-2} Z_G^{-1}(\mu) G_N \tag{1.6}$$

where the momentum scale  $\mu$  denotes the renormalisation scale.  $Z_G(\mu)$  is the graviton wave function renormalisation factor normalised at some  $\mu = \mu_0$  such that  $Z_G(\mu_0) = 1$ .

The renormalisation scale  $\mu$  can be chosen as a typical energy scale  $E$  or as a typical momentum transfer  $p$ . However in this thesis I will follow the Wilsonian approach, and  $\mu$  will be identified with the corresponding momentum cutoff  $k$ , see below.

It will turn out that an important quantity is given by the graviton anomalous dimension

$$\eta_N = -\mu \frac{\partial}{\partial \mu} \ln Z_G(\mu) . \quad (1.7)$$

$\eta_N$  is a non-trivial function of  $g$  and the other couplings appearing in the theory. The RG flow reads then

$$\mu \frac{\partial}{\partial \mu} g = (D - 2 + \eta_N) g . \quad (1.8)$$

Eq. (1.8) especially implies the existence of the non-interacting (Gaussian) fixed point  $g_* = 0$ . For this fixed point one has then  $\eta_N = 0$ , *i.e.*, classical scaling. Looking instead for a non-trivial fixed point  $g_* \neq 0$  one has to solve

$$\eta_* = 2 - D . \quad (1.9)$$

Therefore a non-trivial fixed point of quantum gravity in  $D > 2$  leads to a negative integer value for the UV limit of the graviton anomalous dimension  $\eta_N$ . Note that its numerical value is such that it precisely counter-balances the canonical dimension of Newton's coupling constant  $G_N$ .

The non-trivial UV fixed point of quantum gravity, if it exists, has two important consequences. First, Newton's coupling constant  $G_N$  scales as

$$G_N(\mu) = Z_G^{-1}(\mu) G_N(\mu_0) \xrightarrow{\mu \rightarrow \infty} \frac{g_*}{\mu^{D-2}} \quad (1.10)$$

when the UV fixed point is approached. This implies that Newton's coupling constant  $G_N(\mu)$  becomes infinitesimally small. Second, the spectral dimension<sup>7</sup> of space-time at very short distances becomes equal to two, see, *e.g.*, [18] and references therein.

Equipped with this general background I will present in the next two chapters the knowledge on EH quantum gravity and on the corresponding use of the FRG relevant for this thesis. In Chapter 4 dimensional reduction is introduced and then applied to EH quantum gravity. The derivations and results presented in this chapter constitute the main part of this thesis. In Chapter 5 some potential phenomenological implications are described as well as some concluding remarks and an outlook are presented. A number of technical details is deferred to six appendices.

---

<sup>7</sup>The spectral dimension is defined via the average return probability in a random walk, a concise explanation can be, *e.g.*, found in Appendix A.1 of [18].

# Chapter 2

## Renormalisation Group for Einstein-Hilbert Quantum Gravity

*“As far as extra dimensions are concerned, very tiny extra dimensions wouldn’t be perceived in everyday life, just as atoms aren’t: We see many atoms together but we don’t see atoms individually.”*  
(E. Witten)

### Contents

---

<b>2.1</b>	<b>Functional Renormalisation Group . . . . .</b>	<b>9</b>
<b>2.2</b>	<b>Einstein-Hilbert Quantum Gravity . . . . .</b>	<b>11</b>
2.2.1	Background Field Formalism for Gravity . . . . .	11
2.2.2	Einstein-Hilbert Theory . . . . .	13
2.2.3	Gauge Fixing and DeDonder Gauge . . . . .	14
<b>2.3</b>	<b><math>\beta</math>-Functions and Analytic Flows . . . . .</b>	<b>14</b>

---

In this chapter the use of non-perturbative RG methods for EH gravity will be shortly reviewed. The RG is well suited for such an investigation for several reasons: Firstly, the investigation of gravity should cover approximately sixty orders of magnitude, see Fig. 1.1, which makes a continuum method preferential. Secondly, as explained in Chapter 1 gravity is perturbatively non-renormalisable and might be renormalisable non-perturbatively. Therefore a non-perturbative method is required. Thirdly, the asymptotic safety scenario requires an UV fixed point, a notion directly referring to the RG.

Most of the material presented in this chapter follow closely the seminal paper by Reuter [11]. For further use in the following chapters the presentation has been reordered and new definitions have been introduced.

### 2.1 Functional Renormalisation Group

In this as in the following two chapters I will employ two forms of the FRG: An exact functional identity and an approximated background field flow. For the FRG

there exist several versions of exact functional identities. In this thesis I will use the Wetterich equation [22] with the optimised regulator of [23], called Litim regulator from here on. Both versions are functional differential equations for the effective action. Before providing expressions specific to EH gravity I will summarise the basic idea of the FRG, see Appendix B for a brief summary of corresponding derivations.

Denoting by “Tr” all occurring integrals and sums leads to the compact notation for the Wetterich equation [22]

$$\partial_t \Gamma_k = \frac{1}{2} \text{Tr} \left( \left( \Gamma_k^{(2)} + R_k \right)^{-1} \partial_t R_k \right) \quad (2.1)$$

with

$$\Gamma_k^{(2)} := \frac{\delta^2 \Gamma_k[\bar{\Phi}]}{\delta \bar{\Phi}(q) \delta \bar{\Phi}(-q)}. \quad (2.2)$$

The exact functional identity (2.1) is the basic equation to be used in this thesis. As already mentioned, I will use the Litim regulator

$$R_k(q^2) = (k^2 - q^2) \Theta(k^2 - q^2). \quad (2.3)$$

Its scale derivative is given by

$$\partial_t R_k(q^2) = 2 k^2 \Theta(k^2 - q^2). \quad (2.4)$$

As we will see later in this thesis the step function  $\Theta(k^2 - q^2)$  will allow for some significant simplifications in the appearing integrals.

In this thesis a background field formalism will be used. To this end one introduces a non-propagating background field  $\Phi_0$  into the effective action,  $\Gamma_k[\bar{\Phi}] \rightarrow \Gamma_k[\bar{\Phi}, \Phi_0]$ , and couples the fluctuating field  $\bar{\Phi} - \Phi_0$  to the external current and to the regulator. When deriving the flow the background field acts as kind of “spectator”, and one obtains Eq. (2.1) with the replacement

$$\Gamma_k^{(2)}[\bar{\Phi}] \rightarrow \frac{\delta^2 \Gamma_k[\bar{\Phi}, \Phi_0]}{\delta \bar{\Phi}(q) \delta \bar{\Phi}(-q)}, \quad (2.5)$$

see *e.g.*, [40] and references therein. Eventually, the background field  $\Phi_0$  is identified with the physical mean field,  $\Phi_0 = \bar{\Phi} = \langle \Phi \rangle_J$  thereby leading to an effective background independence. In this way one has arrived at the background field flow for an effective action  $\Gamma_k[\bar{\Phi}] \equiv \Gamma_k[\bar{\Phi}, \bar{\Phi}]$ . The main difference between standard and background flows is given by the presence of the background field at an intermediate step of the calculation which amounts to a re-organisation of the flow.

In addition, it will prove useful to substitute  $q^2 \rightarrow \Gamma_k^{(2)}[\Phi_0, \Phi_0](q^2)$  in the regulator function  $R_k(q^2)$ . Note that  $R_k$  is chosen to depend on the background field and to be independent of the fluctuating field. As we will see in the following sections this will introduce the covariant background Laplacian and the wave function renormalisation function into the regulator.

The background field formalism has also been used for a derivation of generalised proper-time flows [41, 42], a concise summary (followed here) is given in [43]. Using the notation  $x := \Gamma_k^{(2)}[\bar{\Phi}, \bar{\Phi}]$  and  $x_0 := \Gamma_k^{(2)}[\Phi_0, \Phi_0]$  background-dependent regulators of the form  $R_k(q^2) \rightarrow x_0 r(x_0)$  are introduced. With a special choice of an one-parameter family of regulator functions  $r_m(x)$  one can derive the background field flow

$$\partial_t \Gamma_k = \text{Tr} \left( \frac{k^2}{k^2 + x/m} \right)^m + \frac{1}{2} \text{Tr} \left( \frac{r_m}{x(1+r_m)} - \frac{1}{x} \left( \frac{k^2}{k^2 + x/m} \right)^m \right) \partial_t x \quad (2.6)$$

with  $m \in [1, \infty]$ .<sup>1</sup> If the term  $\sim \partial_t x$  is neglected (*i.e.*, the additional terms due to the scale dependence in the regulator function are dropped), and if one uses for the numerator of the first term a proper-time integral representation the exact functional flow Eq. (2.1) reduces to the proper-time flow of [44]:

$$\partial_t \Gamma_k[\Phi] = -\frac{1}{2} \text{Tr} \int_0^\infty \frac{ds}{s} \partial_t f_k^m(s) e^{-s\Gamma_k^{(2)}} + \mathcal{O} \left( \partial_t \Gamma_k^{(2)} \right). \quad (2.7)$$

Hereby the regulator functions  $f_k^m(s)$  take the form as defined in Appendix B. This way of deriving the approximate background field flow equation (2.7) make it plausible that already this simpler equation, as compared to the exact functional identity (2.1), provides qualitatively correct and quantitatively almost correct results.

In Appendix B also an alternative way [45] how to arrive at the background field flow equation (2.7) is given. Taking into account (non-dynamical) ghost contributions the background field flow reads then

$$\partial_t \Gamma_k[\Phi] = -\frac{1}{2} \text{Tr} \int_0^\infty \frac{ds}{s} \partial_t f_k^m(s) \left( e^{-s\Gamma_k^{(2)}} - 2 e^{-sS_{gh}^{(2)}} \right). \quad (2.8)$$

Here  $S_{gh}^{(2)}$  is the second variation of the tree-level ghost action. The form (2.8) of the background field flow equation (with ghost quantum corrections neglected, see also Subsection 2.2.2) will be used in the following section for EH gravity.

## 2.2 Einstein-Hilbert Quantum Gravity

### 2.2.1 Background Field Formalism for Gravity

Throughout this thesis it is assumed that the metric  $g_{\mu\nu}$  represents the dynamical degrees of freedom in gravity. To be more precise, from the  $\frac{1}{2}D(D+1)$  coefficients of the symmetric rank-2 tensor  $g_{\mu\nu}$  only  $\frac{1}{2}D(D-3)$  represent propagating degrees of freedom. The remaining  $2D$  coefficients have to be dealt with by adding a gauge fixing and a Faddeev-Popov ghost term to the action.

---

<sup>1</sup>Convergence of the integrals require a dimension-dependent and in general more restrictive lower bound on the parameter  $m$ , see below.

The generating functional is represented by an integral over all metrics  $\gamma_{\mu\nu}$ , *e.g.*, for vanishing sources one has

$$Z = \int \mathcal{D}\gamma_{\mu\nu} \exp(-S[\gamma_{\mu\nu}]) , \quad (2.9)$$

where  $S$  is an arbitrary diffeomorphism-invariant classical action. In the background field formalism one splits now the metric into a background  $\bar{g}_{\mu\nu}$  and a fluctuation  $h_{\mu\nu}$  which is not necessarily small [11]:

$$\gamma_{\mu\nu} = \bar{g}_{\mu\nu} + h_{\mu\nu} . \quad (2.10)$$

Correspondingly, the gauge fixing term  $S_{gf}[h; g]$  needs to be of the background type, *i.e.*, it is invariant under a *combined* transformation of  $\bar{g}_{\mu\nu}$  and  $h_{\mu\nu}$ . This invariance requirement ensures that the effective action will be invariant under diffeomorphisms.

The Faddeev-Popov ghosts are vector fields, and I will denote them by  $c_\mu$  and the antighosts by  $\bar{c}_\mu$ . With  $S_{gh}$  being the ghost action the functional integral reads then

$$Z = \int \mathcal{D}h_{\mu\nu} \mathcal{D}c_\mu \mathcal{D}\bar{c}_\mu \exp(-S[\bar{g}_{\mu\nu} + h_{\mu\nu}] - S_{gf} - S_{gh}[h_{\mu\nu}, c_\mu, \bar{c}_\mu; \bar{g}_{\mu\nu}]) . \quad (2.11)$$

In a next step one introduces a source coupled to the fluctuating part of the metric and performs the Legendre transform of the connected generating functional  $\ln Z$  to obtain the effective action  $\Gamma[\bar{h}_{\mu\nu}; \bar{g}_{\mu\nu}]$  where  $\bar{h}_{\mu\nu} := \langle h_{\mu\nu} \rangle$  denotes the expectation value of the fluctuating part of the metric. The expectation value of the total metric  $\gamma_{\mu\nu}$  is called from here on  $g_{\mu\nu}$ , and one has

$$g_{\mu\nu} := \langle \gamma_{\mu\nu} \rangle = \bar{g}_{\mu\nu} + \langle h_{\mu\nu} \rangle = \bar{g}_{\mu\nu} + \bar{h}_{\mu\nu} . \quad (2.12)$$

Usually the effective action  $\Gamma$  is considered to be a functional of  $g_{\mu\nu}$  and  $\bar{g}_{\mu\nu}$  instead of  $\bar{h}_{\mu\nu}$  and  $\bar{g}_{\mu\nu}$ . It can be shown [8, 11, 46–48] that the effective action in the usual formalism, *i.e.*, the generating functional of the one-particle irreducible Green functions,  $\Gamma[g_{\mu\nu}]$ , is obtained by setting  $g_{\mu\nu} = \bar{g}_{\mu\nu}$  or, equivalently,  $\bar{h}_{\mu\nu} = 0$ .

A further advantage of the background formalism is the fact that the background metric can be used in the following way in the regulator function: One constructs first the background covariant Laplacian  $-\bar{D}^2$  and use its eigenmodes<sup>2</sup> to define the cutoff at a momentum scale  $k^2 = -\bar{D}^2$ . This implies that the regulator function  $R_k$  depends on the background metric. The background is then eliminated by identifying it with the physical average metric in the final equations. This dynamical adjustment of the background metric implements in an approximate way the background independence required for a theory of quantum gravity.

---

<sup>2</sup>These eigenmodes are only used implicitly because the operator traces will be evaluated within a heat-kernel expansion in first order.

## 2.2.2 Einstein-Hilbert Theory

The EH action including a cosmological constant term is given by

$$S_{EH} = \int d^D x \sqrt{\det g_{\mu\nu}} \left( \frac{-R + 2\Lambda}{16\pi G_N} \right), \quad (2.13)$$

where  $R(g_{\mu\nu})$  is the Ricci scalar,  $\Lambda$  denotes the cosmological constant (with canonical mass dimension  $[\Lambda] = 2$ ), and  $G_N$  is Newton's coupling constant. Its canonical mass dimension is  $[G_N] = 2 - D$ . For later use I define

$$\kappa = (32 \pi G_N)^{-1/2}. \quad (2.14)$$

The Wilsonian effective action of Quantum Einstein Gravity can be written as

$$\Gamma_k = \Gamma_{k,EH} + \Gamma_{k,gf} + \Gamma_{k,gh} + \Gamma_{k,matter}. \quad (2.15)$$

In the truncation employed in this thesis the matter part is completely neglected and quantum corrections to the ghosts are not considered, *i.e.*, the anomalous dimension of the ghosts is set to zero,  $\eta_{gh} = 0$ .<sup>3</sup> The gauge fixing term will be discussed in the next subsection.

Under the RG flow higher order interactions in the metric field will be generated. In the EH theory these are neglected and only the couplings in Eq. (2.13) become running couplings and thus functions of the momentum scale  $k$ . As long as this scale  $k$  is much smaller than the  $D$ -dimensional Planck scale  $M_D$  gravity is well approximated by the EH action with a slowly running  $G_k$ . This justifies the use of the EH theory for the purpose of this thesis.

Introducing the running of the cosmological constant and of Newton's constant one writes

$$\Gamma_{k,EH} = 2 \kappa^2 Z_{Nk} \int d^D x \sqrt{\det g_{\mu\nu}} (-R(g) + 2 \bar{\lambda}_k). \quad (2.16)$$

In this notation the running gravitational coupling constant is reexpressed as  $G_k = G_N/Z_{Nk}$  where  $Z_{Nk}$  is the running graviton wave function renormalisation constant.

In addition, as usual in this context, an additional approximation will be used: To simplify the expression for the second variation of the effective average action I will employ for the background metric a maximally symmetric space in which the Riemann and the Ricci tensors can be expressed in function of the background metric and the Ricci scalar. Note that a space, respectively, space-time is maximally symmetric if and only if the Riemann tensor can be written as

$$\bar{R}_{\rho\mu\nu\sigma} = \frac{1}{D(D-1)} (\bar{g}_{\rho\nu} \bar{g}_{\mu\sigma} - \bar{g}_{\rho\sigma} \bar{g}_{\mu\nu}) \bar{R}, \quad (2.17)$$

and the Ricci tensor is then given by

$$\bar{R}_{\mu\nu} = \frac{1}{D} \bar{g}_{\mu\nu} \bar{R}, \quad (2.18)$$

with the Ricci scalar being defined as usual as  $\bar{R} = \bar{g}^{\mu\nu} \bar{R}_{\mu\nu}$ , *cf.*, Appendix A.

---

<sup>3</sup>Dynamical ghosts have been considered in [49–51].

### 2.2.3 Gauge Fixing and DeDonder Gauge

Following Ref. [11] in this thesis I will use deDonder gauge. The corresponding gauge fixing functional is given in Appendix A. This results in the ghost action

$$\Gamma_{gh}[h, c, \bar{c}; \bar{g}] = -\sqrt{2} \int d^D x \sqrt{\det \bar{g}_{\mu\nu}} \bar{c}_\mu \mathcal{M}[\gamma; \bar{g}]^\mu{}_\nu c^\nu \quad (2.19)$$

where the Faddeev-Popov operator is given by

$$\mathcal{M}[\gamma; \bar{g}]^\mu{}_\nu = (\bar{g}^{\mu\beta} \bar{g}^{\alpha\gamma} \bar{D}_\gamma \gamma_{\beta\nu} D_\alpha + \bar{g}^{\mu\beta} \bar{g}^{\alpha\gamma} \bar{D}_\gamma \gamma_{\alpha\nu} D_\beta - \bar{g}^{\mu\lambda} \bar{g}^{\sigma\rho} \bar{D}_\lambda \gamma_{\rho\nu} D_\sigma) . \quad (2.20)$$

## 2.3 $\beta$ -Functions and Analytic Flows

For deriving the  $\beta$ -Functions I followed for the general part Ref. [11], for the background field flow in proper-time regularisation Ref. [45] and for the Wetterich equation (except the usage of the regulator function) again Ref. [11]. All technical details are given in Appendix D.

Before going to the detailed expressions a few definitions are in order. One introduces the dimensionless Newton's constant

$$g_k \equiv k^{D-2} G_k \equiv k^{D-2} Z_{Nk}^{-1} G_N \quad (2.21)$$

and the dimensionless cosmological constant

$$\lambda_k \equiv k^{-2} \bar{\lambda}_k \quad (2.22)$$

as well as the anomalous dimension

$$\eta_{Nk} \equiv -\partial_t \ln Z_{Nk} . \quad (2.23)$$

As remarked at the end of Sect. 2.1 the approximate background field flow equation (2.7), although being the simpler equation as compared to the exact functional identity (2.1), is expected to provide qualitatively correct and quantitatively almost correct results. In the following always the simpler approximate background field flow equation will be treated first in order to allow a focus on the important qualitative features.

### Background Field Flow

Following the explicit steps as detailed in Appendix D one finds

$$\begin{aligned} \eta_{Nk} &= g_k B_0(\lambda_k) \quad \text{with} \quad (2.24) \\ B_0(\lambda_k) &= 4(4\pi)^{-D/2+1} \frac{\Gamma(m+2-D/2)}{\Gamma(m+1)} \times \\ &\times \left( \frac{1}{(1-2\lambda_k)^{(m+2-D/2)}} \frac{1}{12} (-5D+7)D - \frac{1}{3}(D+6) \right). \quad (2.25) \end{aligned}$$

For the two  $\beta$ -functions in the background field flow one finally obtains

$$\partial_t \lambda_k = \beta_\lambda(g_k, \lambda_k) = \eta_{Nk} \lambda_k - 2 \lambda_k + g_k A_0(\lambda_k) \quad (2.26)$$

with

$$A_0(\lambda_k) = (4\pi)^{-D/2+1} \frac{\Gamma(m+1-D/2)}{\Gamma(m+1)} \left( \frac{D(D+1)}{(1-2\lambda_k)^{(m+1-D/2)}} - 4D \right) \quad (2.27)$$

and

$$\partial_t g_k = \beta_g(g_k, \lambda_k) = (D-2 + \eta_{Nk}) g_k. \quad (2.28)$$

## Exact Functional Identity

As already mentioned several times in the context of the exact functional identity (2.1) I am using exclusively the Litim regulator which for a scalar field theory is given by Eq. (2.3). As one sees in the discussion on the background field flow above for EH gravity one employs the cutoff on the modes of the background covariant Laplacian,  $-\bar{D}^2$ . The details, including the employed heat kernel expansion, are given again in Appendix D, see also Eqs. (D.18) and (D.19).

The exact functional identity for EH theory is given in Eq. (D.23). Introducing as before dimensionless constants one arrives from this equation at

$$\partial_t \lambda_k = \beta_\lambda(g_k, \lambda_k) = \eta_{Nk} \lambda_k - 2 \lambda_k + g_k \left( A_0(\lambda_k) - \eta_{Nk} A_1(\lambda_k) \right) \quad (2.29)$$

with

$$A_0(\lambda_k) = 8\pi \frac{(4\pi)^{-D/2}}{\Gamma(D/2)} \left( \frac{(D+1)}{(1-2\lambda_k)} - 4 \right) \quad (2.30)$$

and

$$A_1(\lambda_k) = 8\pi \frac{(4\pi)^{-D/2}}{\Gamma(D/2)} \left( \frac{(D+1)}{(D+2)} \frac{1}{(1-2\lambda_k)} \right), \quad (2.31)$$

where

$$\partial_t g_k = \beta_g(g_k, \lambda_k) = (D-2 + \eta_{Nk}) g_k. \quad (2.32)$$

Using a Hartree-Fock type resummation, one obtains for the anomalous dimension

$$\eta_{Nk} = \frac{g_k B_0(\lambda_k)}{1 + g_k B_1(\lambda_k)}, \quad (2.33)$$

with

$$B_0(\lambda_k) = 16\pi \frac{(4\pi)^{-D/2}}{\Gamma(D/2)} \left( -(D-1) \frac{1}{(1-2\lambda_k)^2} + \frac{D(D+1)}{12} \frac{1}{(1-2\lambda_k)} - \left( \frac{4}{D} + \frac{D}{3} \right) \right) \quad (2.34)$$

and

$$B_1(\lambda_k) = -16\pi \frac{(4\pi)^{-D/2}}{\Gamma(D/2)} \left( \frac{(D-1)}{(D+2)} \frac{1}{(1-2\lambda_k)^2} - \frac{(D+1)}{12} \frac{1}{(1-2\lambda_k)} \right). \quad (2.35)$$

Before using these expressions in the next chapter to discuss the fixed points and the phase diagrams it is worthwhile to compare the two different versions of the  $\beta$ -functions.

## Comparison of the $\beta$ -Functions and discussion of the RG flows

When comparing the two forms of  $\beta_\lambda$  (2.26) and (2.29) one recognises that they are quite similar, the difference is the term  $-g_k\eta_{Nk}A_1(\lambda_k)$  on the r.h.s. of the  $\beta$ -function following from the exact functional identity. In addition, the flow of the cosmological constant  $\lambda_k$  is of smaller significance than the flow of the coupling constant  $g_k$  for the physics along a phenomenologically acceptable RG trajectory. Due to this one may conclude that the differences between the two types of RG flow for  $\beta_\lambda$  are of minor importance.

At first sight Eqs. (2.28) and (2.32) for  $\beta_g$  look identical, however, the expressions (2.24) and (2.33) for the anomalous dimension  $\eta_{Nk}$  are distinctively different. Whereas the expression within the approximate background field method for the anomalous dimension  $\eta_{Nk}$  is strictly linear in  $g_k$  this is not the case for the  $\eta_{Nk}$  derived from the exact equation. The origin of the denominator appearing in the expression (2.33) can be directly traced back to the fact that (as anticipated from the derivation of the background field flow) the scale derivative of the regulator function contains a term proportional to  $\eta_{Nk}$ , see Eq. (D.19). Neglecting the first term on the r.h.s. of Eq. (D.19) would result in vanishing functions  $A_1(\lambda_k)$  and  $B_1(\lambda_k)$  as can be verified straightforwardly from the steps of the calculation which are explicitly given in Appendix D. As the scale derivative of the approximate background field regulator function, see Eq. (B.20), does not contain a term proportional to the anomalous dimension  $\eta_{Nk}$  the appearance of a simpler structure in the respective  $\beta$ -functions than in the ones from the exact equation is evident.

Due to the non-linear dependence of  $\eta_{Nk}$  on  $g_k$  in the case of the exact equation one might expect some significant differences in the flows generated by the approximate and the exact functional equation. As will be discussed in the next chapter it turns out that the differences in the two RG flows are restricted to regions in the  $(\lambda_k, g_k)$  plane close to a line where the anomalous dimensions  $\eta_{Nk}$  diverges. (A detailed discussion will be given in Sect. 3.2.) For all physical RG trajectories discussed in this thesis neglecting the functions  $A_1(\lambda_k)$  and  $B_1(\lambda_k)$  is qualitatively and semi-quantitatively good approximation.

As already stated above the limit  $\lambda_k \rightarrow 0$  has no significant impact on the  $\beta$ -function for  $g_k$  and thus the qualitative behaviour of the coupling and the anomalous dimension are not changed. On the other hand, the limit  $\lambda_k \rightarrow -\infty$  is an interesting one. As the functions  $A_1(\lambda_k)$  and  $B_1(\lambda_k)$  go in this case to zero the discussion applies to the two different forms of the flow alike. Due to the terms originating from the ghost action the functions  $A_0(\lambda_k)$  and  $B_0(\lambda_k)$  take a finite non-vanishing limit. In addition, it is important to note that  $B_0$  is also in this limit negative, therefore the

anomalous dimension will be non-positive and goes to zero only for  $g_k \rightarrow 0$ . As also  $A_0$  is in this limit negative one arrives at the consistent conclusion that  $\beta_\lambda$  is always negative and thus the absolute value of  $\lambda_k$  increases towards the IR. Furthermore, a finite non-vanishing value of  $g_k$  leads to a contradiction. This leaves the possibilities  $g_k \rightarrow 0^+$  and  $g_k \rightarrow +\infty$ . (Note that negative and thus unphysical values of  $g_k$  are discarded anyhow.) In the first case, the anomalous dimension vanishes and both,  $g_k$  and  $\lambda_k$ , approach with classical scaling laws ( $k^{D-2}$  and  $k^{-2}$ , respectively) this IR fixed point when  $k$  is lowered. In the second case,  $\eta_{Nk} \rightarrow -\infty$  and the dominant term in  $\beta_g$  is  $B_0 g_k^2$ . The resulting approximate differential equation has the solution

$$g_k = \frac{1}{\text{const.} - B_0 \ln k} \quad (2.36)$$

and one recognises that the flow will stop at a finite value of  $k$ ,  $k = e^{\text{const.}/B_0}$ , because both,  $g_k$  and  $\eta_{Nk}$  diverges. As  $\beta_\lambda$  diverges then too, also  $\lambda_k$  diverges but now with an infinite scale derivative. The limits discussed here will be numerically verified in Sect. 3.2, the interested reader may peak ahead to Fig. 3.3.

At this point a remark is in order: The  $\beta$ -functions become singular when  $\lambda_k \rightarrow \frac{1}{2}$ . In addition, as already mentioned the expression (2.33) for the anomalous dimension diverges at a boundary line which in the case of the exact functional identity also restricts the values of  $\lambda_k$  for RG trajectories starting at negative or small positive values of  $\lambda_k$ .<sup>4</sup> Therefore in this thesis all trajectories with  $\lambda_k > \frac{1}{2}$  (or to the right of the above mentioned boundary line) will be not considered.

Last but not least, the limit  $g_k \rightarrow 0^+$  will be discussed here. Then the anomalous dimension also goes to zero,  $\eta_{Nk} \rightarrow 0^-$ , and the  $\beta$ -functions contain basically only the canonical dimensions. Considering now a flow from the UV to the IR one has then three possibilities to obtain  $g_k \rightarrow 0$ :

- There is exactly one RG trajectory, the so-called separatrix, for which both  $g_k$  and  $\lambda_k$  will vanish with the classical scaling law for  $g_k$ . To flow into this IR fixed point a precise cancelation in  $\beta_\lambda$  is required which makes plain that one and only one RG trajectory ends up in this IR fixed point. As all the couplings vanishes in this fixed point it is called a Gaussian fixed point.
- In the IR the RG trajectory may end up in  $g_k \rightarrow 0^+$  and  $\lambda_k \rightarrow -\infty$ , see the discussion above.
- As the flows end at a singular boundary line there is one RG trajectory with  $g_k = 0$  not yet covered by the previous cases: If one starts a RG trajectory with  $g_k = 0$  and  $0 < \lambda_k < 1/2$  this trajectory will stop at  $(g_k, \lambda_k) = (0, 1/2)$  which is then a degenerate fixed point.

---

<sup>4</sup>A RG trajectory cannot cross a line where the  $\beta$ -functions diverges.



# Chapter 3

## Quantum Gravity in $D \geq 4$

*“If I take the theory as we have it now, literally, I would conclude that extra dimensions really exist. They’re part of nature. We don’t really know how big they are yet, but we hope to explain that in various ways.”*

*(E. Witten)*

### Contents

---

<b>3.1</b>	<b>Fixed Points in <math>D \geq 4</math></b>	<b>19</b>
<b>3.2</b>	<b>Phase Diagrams in <math>D \geq 4</math></b>	<b>24</b>

---

In the last chapter the expressions for the  $\beta$ -functions and the graviton anomalous dimension have been derived for two forms of the RG. In this chapter I am going to discuss the RG trajectories in  $D = 4$  and higher dimensions<sup>1</sup> to set the scene for the investigation of the ADD model scenario with a “large” compact dimension. Besides confirming results already known in the literature, the presentation in this chapter is intended to provide the background for a meaningful comprehension of the novel results to be presented and discussed in Chapter 4.

Before discussing the flow it is instructive to discuss the fixed point structure.

### 3.1 Fixed Points in $D \geq 4$

Fixed points are zeros of the  $\beta$ -functions. As thus they are sources and sinks of RG trajectories. Defining the flow to run from large to small  $k$  an UV fixed point is a source whereas an IR fixed point is a sink of RG trajectories. Having UV and IR fixed points special trajectories connecting an UV to an IR fixed point exist, those trajectories are called separatrices. From the discussion at the end of Chapter 2 it is evident that both versions of the  $\beta$ -functions as derived in the last chapter possesses always a Gaußian fixed point at  $(g_*, \lambda_*) = (0, 0)$  for every value  $D$  of the number of space-time dimension. For the cases discussed here ( $D \geq 4$ ) this is always an IR fixed point. Therefore in the following we will concentrate on the discussion of the non-trivial fixed point which will turn out to be an UV fixed point. Note also that

---

<sup>1</sup>For a brief description of the numerical treatment see Appendix F.

for  $D > 2$  there can be no non-trivial fixed point in the classical regime because  $\beta_g$  will vanish for  $g_k \neq 0$  only if  $\eta_{Nk} = 2 - D$  and thus the absolute value of the anomalous dimension and therefore quantum effects are large.

The  $\beta$ -function for  $g_k$  reads:

$$\partial_t g_k = \beta_g(g_k, \lambda_k) = (D - 2 + \eta_{Nk}) g_k , \quad (3.1)$$

for both forms as derived from the approximate and the exact functional identity. For a non-trivial fixed point, *i.e.*, for  $g_* \neq 0$  a necessary condition is

$$\eta_* = 2 - D . \quad (3.2)$$

Therefore this relation and

$$\beta_\lambda|_{\eta_{Nk}=2-D} = 0 \quad (3.3)$$

will be used to find the non-trivial UV fixed point.

In addition, I will compute the scaling exponents at the UV fixed point from the stability matrix

$$B = \begin{pmatrix} \frac{\partial \beta_\lambda}{\partial \lambda} & \frac{\partial \beta_\lambda}{\partial g} \\ \frac{\partial \beta_g}{\partial \lambda} & \frac{\partial \beta_g}{\partial g} \end{pmatrix} \quad \text{evaluated at} \quad (g_*, \lambda_*) . \quad (3.4)$$

The scaling exponents are the real and imaginary part of the negative eigenvalues of  $B$  (*i.e.*,  $BV = -\theta V$ )

$$\theta = \theta' \pm i\theta'' . \quad (3.5)$$

Solving the linearised flow equations one obtains

$$\begin{pmatrix} g_k \\ \lambda_k \end{pmatrix} = \begin{pmatrix} g_* \\ \lambda_* \end{pmatrix} + \begin{pmatrix} \sum_{l=1}^2 c_l V_{1l}(k_0/k)^{\theta_l} \\ \sum_{l=1}^2 c_l V_{2l}(k_0/k)^{\theta_l} \end{pmatrix} \quad (3.6)$$

with some appropriate constants  $c_l$  and  $k_0$  being some reference scale. One recognises that if the real part of the scaling exponent is positive then the coupling constants approach with corresponding power laws the UV fixed point values. Therefore a positive value of  $\theta'$  indicates an attractive fixed point. On the other hand, a negative value would indicate a repulsive fixed point in contradiction to the anticipated result. Thus, it is important to check that the real parts of the scaling exponents come out positive. As one sees below one obtains for the cases considered in this thesis a complex-conjugate pair of scaling exponents, *i.e.*, only one value for the real part. The imaginary part of the scaling exponent leads to oscillations around the fixed point values, the RG trajectory ‘spirals’ into the fixed point.

It is also important to note that a change of the regulator function leaves the scaling exponents invariant, see *e.g.*, Sect. 5 of Ref. [14]. Quantities which are unchanged under a variation of the cutoff scheme, like the scaling exponents, are called universal.

## Approximate Background Field Flow

Using Eqs. (2.24) and (2.26) for the background field flow Eqs. (3.2) and (3.3) can be written as

$$\begin{aligned} 2 - D &= g_* \frac{1}{3} (4\pi)^{-D/2+1} \frac{\Gamma(m+2-D/2)}{\Gamma(m+1)} \left( \frac{(-5D+7)D}{(1-2\lambda_*)^{(m+2-D/2)}} - 4(D+6) \right) \\ &= g_* B_0(\lambda_*) \end{aligned} \quad (3.7)$$

$$\begin{aligned} D\lambda_* &= g_* (4\pi)^{-D/2+1} \frac{\Gamma(m+1-D/2)}{\Gamma(m+1)} \left( \frac{D(D+1)}{(1-2\lambda_*)^{(m+1-D/2)}} - 4D \right) \\ &= g_* A_0(\lambda_*). \end{aligned} \quad (3.8)$$

The resulting condition

$$g_* = (2-D)/B_0(\lambda_*) = D\lambda_*/A_0(\lambda_*) \quad (3.9)$$

is graphically displayed for  $D=4$  and  $D=5$  ( $m=2$ ) in Fig. 3.1.

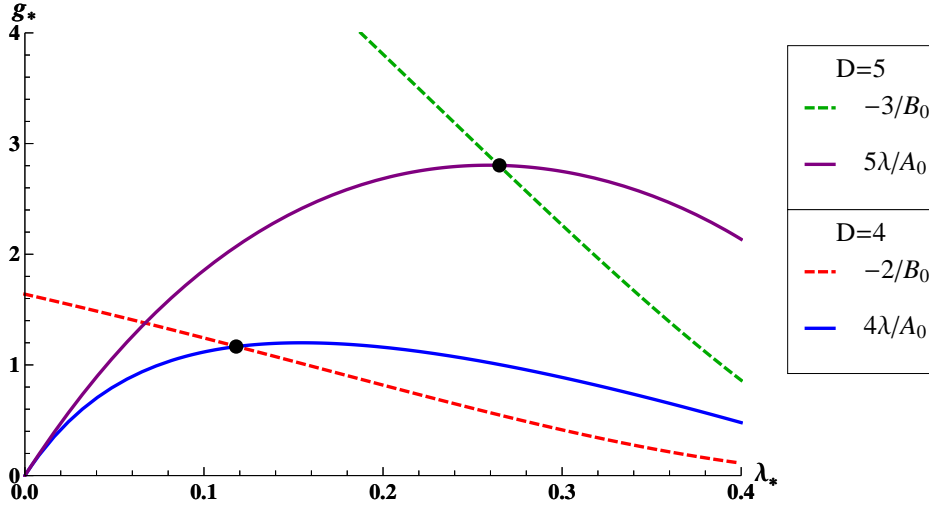


Figure 3.1: Condition (3.9) for the UV fixed point values for  $D=4$  and  $D=5$  for the background field flow ( $m=2$ ). The crossings of the curves, marked by the black points, provides the fixed point values  $g_*$  and  $\lambda_*$ .

In Table 3.1 some results for the resulting UV fixed point in  $D=4$  using several values of  $m$  are given. As the fixed point values  $g_*$  and  $\lambda_*$  are scheme dependent they cannot possess a direct physical meaning. On the other hand, in  $D=4$   $g_* \lambda_*$  is an universal, *i.e.*, scheme-independent, quantity, and the product  $g_k \lambda_k = (k^{D-2} Z_{Nk}^{-1} \bar{G}) (k^{-2} \bar{\lambda}_k) \propto k^{D-4}$  is independent of the RG scale  $k$ . For general  $D$  one generalises this consideration and defines the  $k$ -independent product

$$\tau_* = \lambda_* g_*^{2/(D-2)} \quad (3.10)$$

which can be shown to be an universal quantity. Therefore in an exact treatment the value of  $\tau_*$  has to be the same for all cutoff schemes. Deviations for different regulators are thus an indication of truncation errors.

In Tables 3.2 and 3.3 results for the UV fixed point values in  $D = 5$  and  $D = 8$  are displayed. In the three considered cases  $D = 4$ ,  $D = 5$  and  $D = 8$  one sees a reasonably weak dependence of the universal quantity  $\tau_*$  indicating the robustness of physical quantities under a change of the cutoff function.

$m$	$g_*$	$\lambda_*$	$\tau_*$
3/2	0.764	0.193	0.147
2	1.166	0.118	0.138
3	1.890	0.0663	0.125
4	2.589	0.0460	0.119
5	3.281	0.0352	0.115
6	3.971	0.0285	0.113
10	6.719	0.0162	0.109
40	27.27	0.00381	0.104

Table 3.1:  $\mathbf{D} = 4$ : UV fixed points within the background field flow for various values of the cutoff parameter  $m$ .

$m$	$g_*$	$\lambda_*$	$\tau_*$
2	2.803	0.265	0.527
3	7.254	0.141	0.528
4	12.40	0.0958	0.513
5	18.27	0.0726	0.504
6	24.80	0.0585	0.497
10	56.55	0.0329	0.485
40	479.1	0.00767	0.470

Table 3.2:  $\mathbf{D} = 5$ : UV fixed points within the background field flow for various values of the cutoff parameter  $m$ .

$m$	$g_*$	$\lambda_*$	$\tau_*$
4	862.3	0.235	2.24
5	2474	0.156	2.11
6	5217	0.117	2.03
10	33432	0.0584	1.88
40	$2.875 \times 10^6$	0.0123	1.75

Table 3.3:  $\mathbf{D} = 8$ : UV fixed points within the background field flow for various values of the cutoff parameter  $m$ .

For some selected cases the scaling exponents are given in Table 3.4. The sizeable imaginary part,  $\theta''$ , leads to the fact that the RG flows will “spiral” into the fixed point, see also next section.

	$\theta'$	$\theta''$
$D = 4, m = 3/2$	2.004	1.659
$D = 4, m = 2$	1.835	1.299
$D = 5, m = 2$	3.595	2.896

Table 3.4: The scaling exponents for some values of the cutoff parameter  $m$  and number of dimensions  $D$ .

## Exact Functional Identity

Using Eqs. (2.29) and (2.33), Eqs. (3.2) and (3.3) can be written as

$$D \lambda_* = 8 \pi g_* \frac{(4 \pi)^{-D/2}}{\Gamma(D/2)} \left( \frac{(D+1)}{(D+2)} \frac{2D}{(1-2\lambda_*)} - 4 \right), \quad (3.11)$$

$$2 - D = \frac{g_* B_0(\lambda_*)}{1 + g_* B_1(\lambda_*)}, \quad (3.12)$$

with the functions  $B_0(\lambda_k)$  and  $B_1(\lambda_k)$  given in Eqs. (2.34) and (2.35), respectively. The condition for the UV fixed point can be also written as

$$g_* = \frac{2 - D}{B_0(\lambda_*) + (D - 2)B_1(\lambda_*)} = \frac{D\lambda_*}{A_0(\lambda_*) + (D - 2)A_1(\lambda_*)}. \quad (3.13)$$

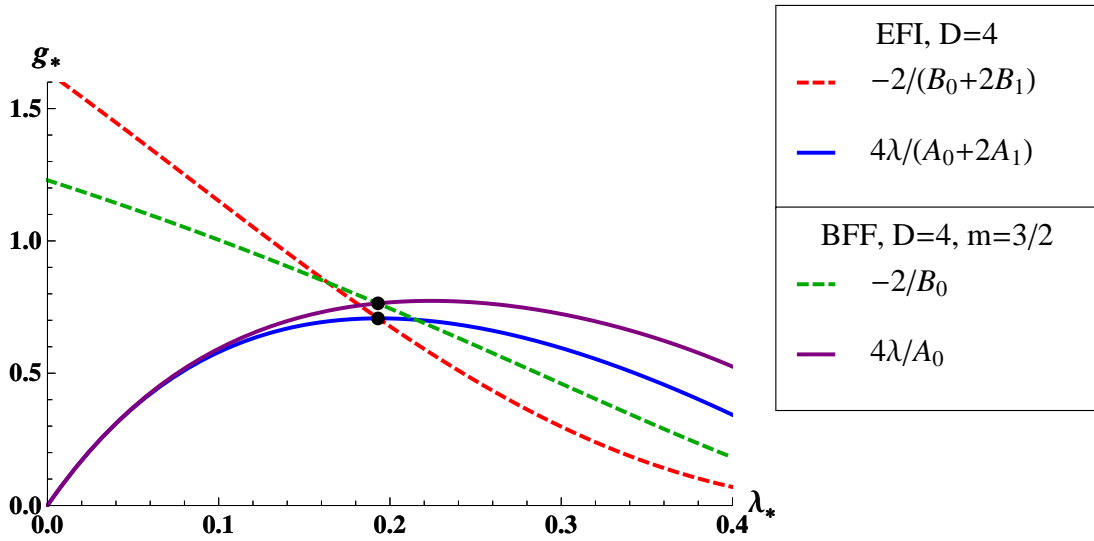


Figure 3.2: Conditions (3.13) for the UV fixed point values for  $D = 4$  for the exact functional identity (dashed red and full blue lines) and (3.9) for the background field flow with  $m = 3/2$  (dashed green and full purple lines). The crossing of the curves, marked by the black points, provides the fixed point values  $g_*$  and  $\lambda_*$ .

A comparison with the results for the non-trivial UV fixed point shows that the corresponding values are almost identical to the one of the approximate background field flow with the minimally possible half-integer value of  $m$ , *cf.*, Table 3.5. Note that convergence of the integrals requires  $m > (D/2) - 1$ , and therefore  $m = (D-1)/2$  is the smallest half-integer number such that the integrals are well-defined.

D	4		5		8	
	$g_*$	$\lambda_*$	$g_*$	$\lambda_*$	$g_*$	$\lambda_*$
Exact functional identity	0.707	0.193	2.853	0.237	461.4	0.284
Background flow, $m = (D - 1)/2$	0.764	0.193	2.803	0.265	379.9	0.316

Table 3.5: UV fixed points for different number of dimensions for the two considered forms of the FRG.

	$\tau_*$	$\theta'$	$\theta''$
$D = 4$	0.137	1.475	3.043
$D = 5$	0.478	2.687	5.154

Table 3.6: The  $k$ -independent product  $\tau_*$  and the scaling exponents derived from the exact functional identity for  $D = 4$  and  $D = 5$ . These values are identical to the ones given in [30, 52].

## 3.2 Phase Diagrams in $D \geq 4$

In this section the RG flows in the  $(\lambda_k, g_k)$  plane will be displayed for  $D = 4$  and  $D = 5$  for both considered forms of the FRG. Such “phase portraits” are called phase diagrams. They will be shown here because the comparison to them will make the  $5D$ - $4D$  crossover evident in the latter studied case of one compactified dimension, see the next chapter.

### Background Field Flow

A selection of results obtained from the approximate background field flow will be displayed first. As  $m = 2$  will be used for  $D = 4$  and  $D = 5$  as well as in the case of dimensional reduction I will specialise to this case.

For  $\mathbf{D} = 4$  and  $\mathbf{m} = 2$  one obtains for the functions  $A_0$  (2.27) and  $B_0$  (2.25):

$$A_0(\lambda_k) = \frac{-4 + 5c_k}{2\pi} \quad \text{and} \quad B_0(\lambda_k) = \frac{-10 - 13c_k^2}{6\pi} \quad (3.14)$$

with

$$c_k = \frac{1}{(1 - 2\lambda_k)}. \quad (3.15)$$

For  $\mathbf{D} = 5$  and  $\mathbf{m} = 2$  one obtains for the functions  $A_0$  (2.27) and  $B_0$  (2.25):

$$A_0(\lambda_k) = \frac{-10 + 15\sqrt{c_k}}{8\pi} \quad \text{and} \quad B_0(\lambda_k) = \frac{(-11/3) - 7.5\sqrt{c_k}}{8\pi} \quad (3.16)$$

with  $c_k$  as defined in Eq. (3.15).

Note that due to the singularities in the  $\beta$ -functions the line  $\lambda_k = \frac{1}{2}$  provides a boundary line which cannot be crossed by the flows. To make the flows visible in the

full physically relevant range  $\lambda_k \in (-\infty, 1/2)$  and  $g_k \in (0, \infty)$  in Fig. 3.3 the phase diagram is shown with compactified axes. This allows to identify several interesting points in the phase diagram.<sup>2</sup>

In Fig. 3.3 the point **A** marks the previously discussed UV stable fixed point with coordinates  $(g_*, \lambda_*) = (1.166, 0.118)$  in 4D (see Fig. 3.3) and  $(g_*, \lambda_*) = (2.803, 0.265)$  in 5D. **B** is the already mentioned IR fixed point with coordinates  $(g_*, \lambda_*) = (0, 0)$  present for all  $D > 2$ . Furthermore, **C** is a degenerate IR fixed point at  $(g_*, \lambda_*) = (0, \frac{1}{2})$ . And **D** is an IR attractive fixed point located at negative cosmological constant with coordinates  $(g_*, \lambda_*) = (0, -\infty)$ . Finally, **E** is a degenerate IR fixed point located at  $(g_*, \lambda_*) = (+\infty, -\infty)$ .

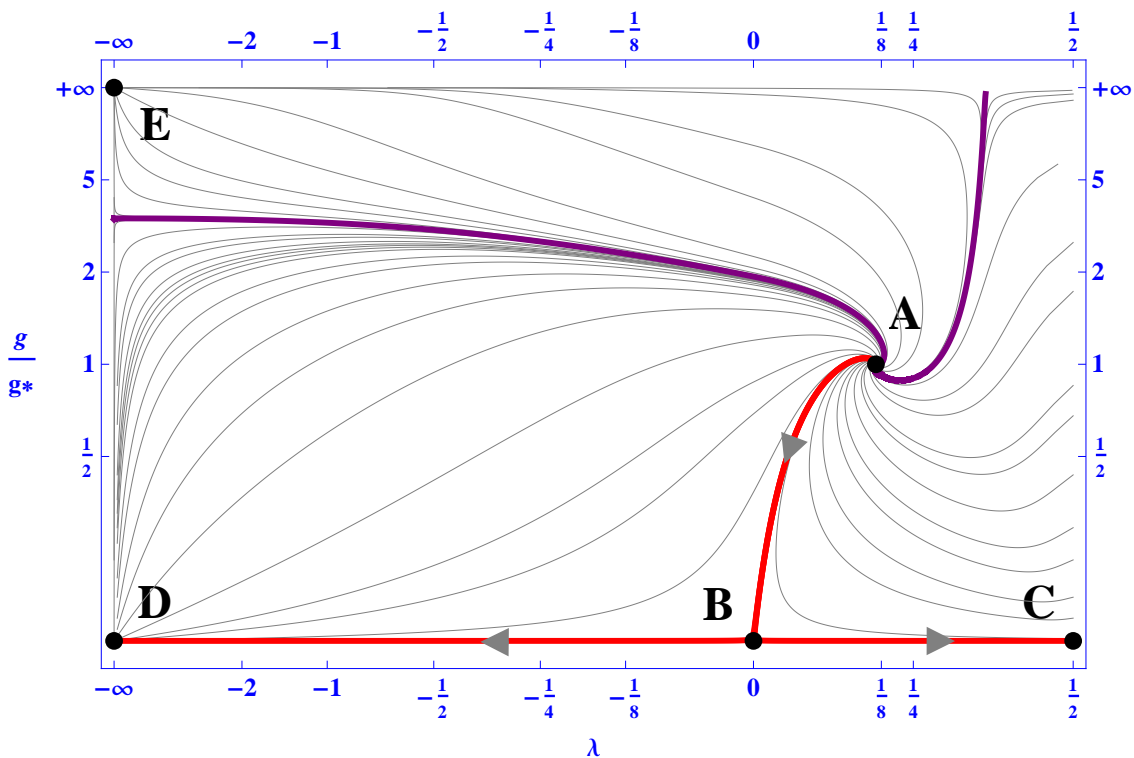


Figure 3.3: The extended phase diagram for the background field flows in  $D = 4$ . For the meaning of the different points see the text above. To obtain this plot the differential equations (2.26) and (2.28) have been solved with the functions (3.14) as input. The different trajectories are generated by different starting conditions.

The existence of these fixed point leads to several dividing lines or separatrices. Note that a physical RG trajectory is expected to pass close to the separatrix from **A** to **B**. Further separatrices run from **B** to **C** and from **B** to **D**. The purple lines originating from **A** are the limits of a region where the RG trajectories are completely disconnected from a weak-coupling and thus semi-classical regime.<sup>3</sup>

<sup>2</sup>As this type of plot looks very similar for the cases  $D = 4$  and  $D = 5$  the phase diagram is displayed only for  $D = 4$ . Furthermore, the notation for these points follows the one in Ref. [53].

<sup>3</sup>A phase diagram where the strong-gravity region is shielded by separatrices from regions which admit an extended semi-classical regime has been obtained recently from a truncation of the exact functional identity based on the graviton propagator [54].

## Exact Functional Identity

Here the corresponding phase diagrams following from the exact functional identity are discussed.

For  $\mathbf{D} = 4$  Eqs. (2.30-2.31) and (2.34-2.35) simplify to

$$A_0(\lambda_k) = \frac{5c_k - 4}{2\pi}, \quad A_1(\lambda_k) = \frac{5c_k}{12\pi}, \quad (3.17)$$

$$B_0(\lambda_k) = \frac{-9c_k^2 + 5c_k - 7}{3\pi}, \quad B_1(\lambda_k) = \frac{-6c_k^2 + 5c_k}{12\pi},$$

with  $c_k$  as defined in Eq. (3.15).

The resulting flows are shown in Fig. 3.4. Here an additional remark is in order: Whereas for the approximate background field flow the  $\beta$ -functions became singular for  $\lambda_k = 1/2$  the corresponding boundary is, based on the exact functional identity, another line. It is determined from the divergence of the anomalous dimension:

$$\frac{1}{\eta_{Nk}} = 0 \implies g_{\text{bound}}(\lambda_k) = 21\pi^2 \frac{(1 - 2\lambda_k)^2}{1 + 14\lambda_k} \quad (3.18)$$

and displayed in Fig. 3.4 as the dotted line.

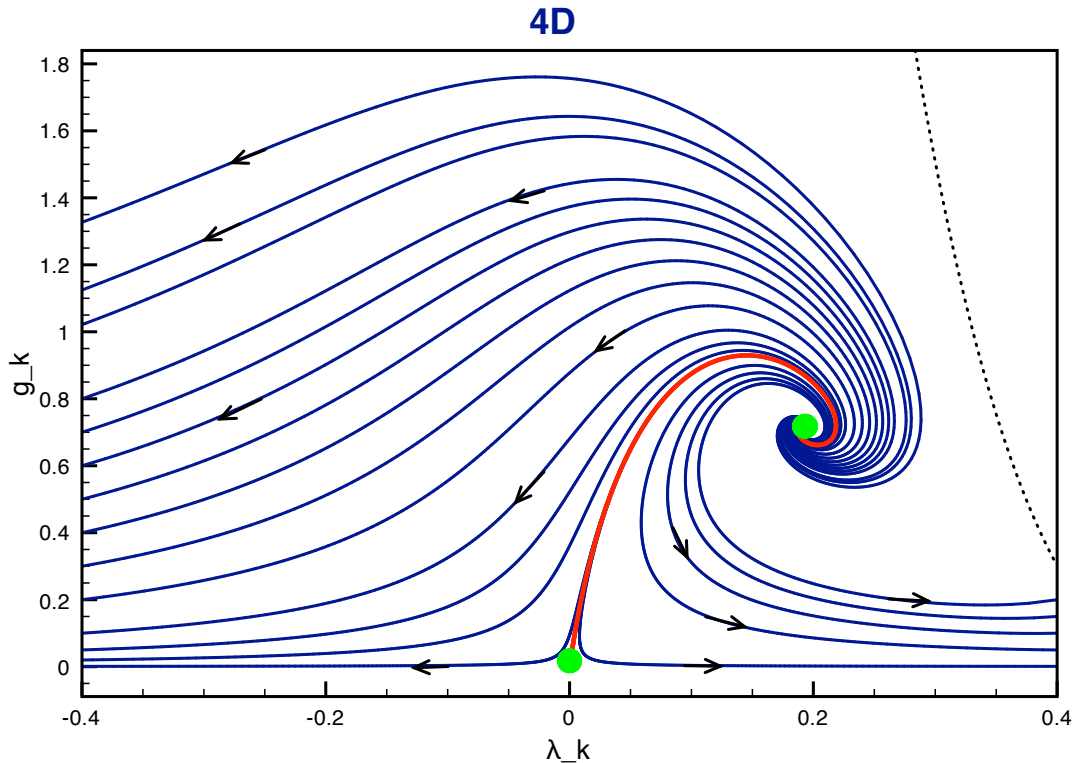


Figure 3.4: Shown is the phase diagram for the running gravitational coupling  $g_k$  and the cosmological constant  $\lambda_k$  in four dimensions from the exact functional identity. The RG trajectories are solutions for different starting conditions of the differential equations (2.29) and (2.32) with the functions (3.17) as input. The separatrix (full red line) connects the UV and the IR fixed points marked by green dots. Arrows indicate the direction of the RG flow with decreasing  $k \rightarrow 0$ . The dotted black line indicates the boundary  $g_{\text{bound}}(\lambda_k)$  where  $1/\eta_{Nk} = 0$ , see Eq. (3.18).

For  $D = 5$  the corresponding formulae read

$$\begin{aligned}
A_0(\lambda_k) &= \frac{6c_k - 4}{3\pi^2}, & A_1(\lambda_k) &= \frac{2c_k}{7\pi^2}, \\
B_0(\lambda_k) &= \frac{-8c_k^2 + 5c_k - 74/15}{3\pi^2}, & B_1(\lambda_k) &= \frac{-8c_k^2 + 7c_k}{21\pi^2},
\end{aligned}
\tag{3.19}$$

with  $c_k$  as defined in Eq. (3.15). Furthermore,

$$\frac{1}{\eta_{Nk}} = 0 \implies g_{\text{bound}}(\lambda_k) = 21\pi^2 \frac{(1 - 2\lambda_k)^2}{1 + 14\lambda_k}
\tag{3.20}$$

which leads then to a phase diagram very similar to the four-dimensional case.

In both cases one can make an interesting observation for the RG trajectories which pass close to the boundary line.

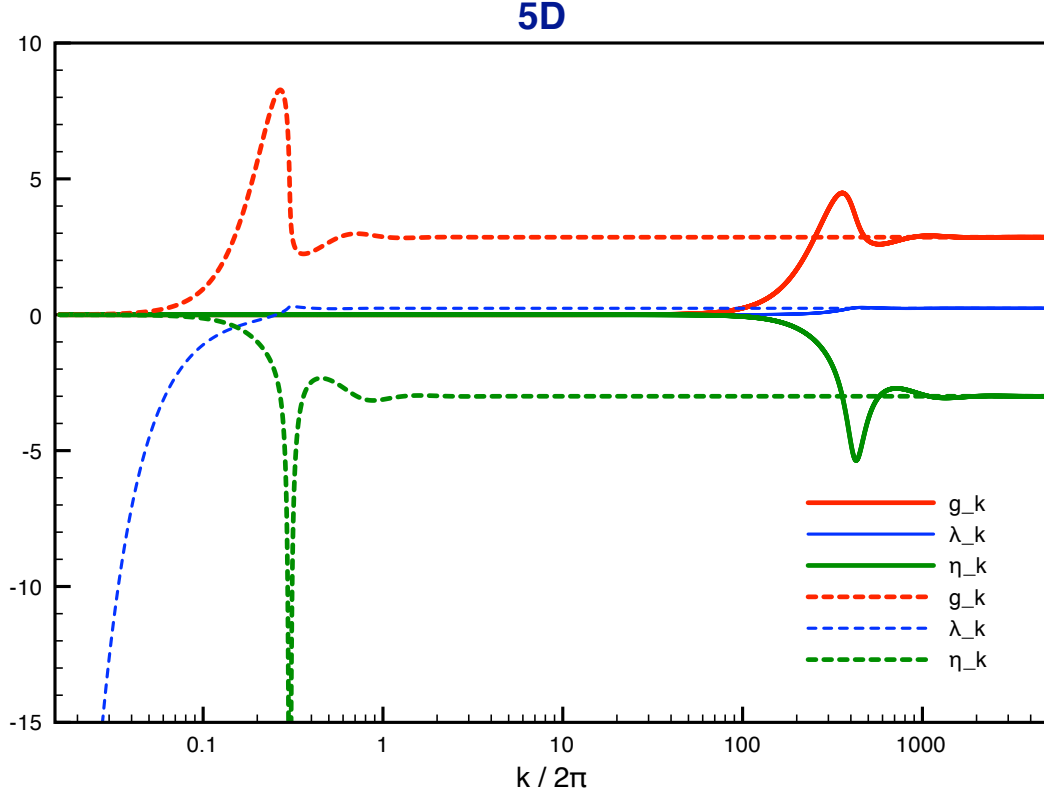


Figure 3.5: Shown are  $g_k$ ,  $\lambda_k$  and  $\eta_k$  in  $D = 5$  for two different trajectories, *i.e.*, for two different starting conditions of the differential equations (2.29) and (2.32) with the functions (3.19) as input. The anomalous dimension  $\eta_{Nk}$  is calculated using Eq. (2.33). For further details see the text below.

The runnings of  $g_k$ ,  $\lambda_k$  and  $\eta_k$  are shown for two different trajectories in Fig. 3.5 in the case of five dimensions. Needless to say that the same kind of comparison is possible (and actually has been performed) for the case of four dimensions. For the starting conditions  $g_{k_{min}} = 10^{-12}$  and  $\lambda_{k_{min}} = 10^{-6}$  at  $k_{min} = 0.1$  the trajectory

(which is a trajectory practically identical to the separatrix) never comes close to the boundary line. Correspondingly,  $g_k$  and  $\lambda_k$  stay very small until the fixed point region is reached at approximately  $k/2\pi \approx 500$ , see the full lines in Fig. 3.5. The anomalous dimension stays very small until the fixed point region is reached where it then quickly oscillates in to the fixed point value  $\eta_* = 2 - D = -3$ . The situation is very different from the RG trajectory corresponding to the dashed lines in Fig. 3.5. Here the starting conditions are  $g_{k_{min}} = 4 \cdot 10^{-3}$  and  $\lambda_{k_{min}} = -45$  at  $k_{min} = 0.1$ . At a value  $k/2\pi \approx 0.3$  the RG trajectory passes close to the boundary line. At this point  $g_k$  rapidly decreases and the anomalous dimension becomes strongly negative. Very soon after this the fixed point region is reached and all quantities oscillate with a very small and further decreasing amplitude around the fixed point values.

Therefore one concludes that strongly negative values of the anomalous dimension are assumed on RG trajectories passing close to the boundary line. In order to test whether this might be a truncation and regulator artefact the case has been investigated in which the function  $B_1(\lambda_k)$  has been neglected. The boundary line becomes then the vertical line  $\lambda_k = 1/2$  (as is also the case for the approximate background field flow). Using now the same starting conditions in the IR the RG trajectory comes the close to the vertical boundary line with a very similar effect on the anomalous dimension. On the other hand, except for regions very close to the boundary line the value and the running of the cosmological constant is of only minor importance.

This concludes the summary of the RG flows for the two investigated forms of the flow equation.

# Chapter 4

## Dimensional Reduction for Einstein-Hilbert Gravity

*“The theory has to be interpreted that extra dimensions beyond the ordinary four dimensions, the three spatial dimensions plus time, are sufficiently small that they haven’t been observed yet.”*  
(E. Witten)

### Contents

---

<b>4.1</b>	<b>Matsubara Formalism and Kaluza-Klein modes . . . . .</b>	<b>30</b>
<b>4.2</b>	<b>Dimensionally Reduced Renormalisation Group Equations . . . . .</b>	<b>32</b>
<b>4.3</b>	<b><math>\beta</math>-Functions and Effective Coupling . . . . .</b>	<b>35</b>
<b>4.4</b>	<b>Discussion of the Limits . . . . .</b>	<b>37</b>
<b>4.5</b>	<b>Renormalisation Group Flows and Phase Diagrams in <math>D = 4 + 1</math> . . . . .</b>	<b>40</b>
4.5.1	Results for the Background Field Flow . . . . .	40
4.5.2	Results following from the Exact Functional Identity . . .	43

---

In this chapter, which constitutes the main part of this thesis, the RG for EH gravity for the case of four extended and one compact dimensions will be treated. The main objective is to provide an explicit example for the realisation of the ADD model. Although the case of only one extra compact dimension is excluded by observation (because then the extension of the extra dimension would be of the size of the solar system) such a scenario is a theoretically sound model. Note, however, that in this simplest version of the ADD model one needs to have an enormously large separation of scales,

$$1/L \ll M_D \quad \text{with} \quad M_D \approx m_{EW} \quad (4.1)$$

being the Planck scale in  $D$  dimensions. From Eq. (1.3) it is evident that for  $n = 1$  there are approximately 32 orders of magnitude between  $1/L$  and  $M_D$ .

The first step in the treatment will be to perform the functional trace in a setting where one dimension is chosen compact, *i.e.*, periodic boundary conditions

apply in one direction. The field modes propagating along the compact dimension are called Kaluza-Klein modes, a suitable formalism to include them in the trace is the Matsubara mode sum known from thermal quantum field theory. As the corresponding formulae are the basis of the dimensionally reduced RG equations to be derived below I will here give a more detailed representation of the relevant expressions for the Matsubara sums although their treatment is quite technical.

## 4.1 Matsubara Formalism and Kaluza-Klein modes

The compact dimension implies periodic boundary conditions on the metric field

$$g_{\mu\nu}(x_1, \dots, x_{D-1}, x_D) = g_{\mu\nu}(x_1, \dots, x_{D-1}, x_D + L) \quad (4.2)$$

where without loss of generality it was assumed that  $D$ th dimension is the compact one. The maximal extension along this dimension has been called  $L$  (in agreement with the discussion in Subsection 1.2.2).

To proceed one should recall the calculations described in Chapter 2. The traces appearing in the FRG equations have been performed by applying a heat kernel expansion to the traces of a function of the covariant background Laplacian, keeping the first two terms and integrating then them over the covariant background field momenta. It is obvious that when considering a compact dimension one has to correspondingly adapt this procedure.

Considering  $D$  dimensions with periodicity as in Eq. (4.2) implies that one has then  $D - 1$  continuous components of the momentum vector and one discrete one. The values for the discrete momentum component resembles formally the Matsubara frequencies for bosons:

$$q_{D,n} = \frac{2\pi n}{L} , \quad (4.3)$$

such that

$$q_D^2 \rightarrow q_{D-1}^2 + (2\pi n/L)^2, \quad (4.4)$$

and correspondingly the  $D$ -dimensional integrals split into a  $(D - 1)$ -dimensional integral and a sum,<sup>1</sup>

$$\int \frac{d^D q}{(2\pi)^D} \rightarrow \frac{1}{L} \sum_n \int \frac{d^{D-1} q}{(2\pi)^{D-1}} . \quad (4.5)$$

Physically, Eq. (4.3) describes the possible momenta of gravitons propagating along the  $D$ th dimension (Kaluza-Klein modes). On a formal level, Eqs. (4.3) and (4.5) are the basis for describing dimensional reduction. The appearing length scale  $L$  will lead to a separation: For  $k \gg 1/L$ , *i.e.*, in the UV, the behaviour of the RG

---

<sup>1</sup>Such Matsubara sums have been introduced very recently (*i.e.*, after the calculations of this thesis have been completed) within Quantum Gravity in Ref. [55] where the Einstein-Hilbert theory has been investigated using the Wetterich equation. The objective of this work is, however, to consider foliated space times.

trajectories will be according to  $D$  dimensions, in the opposite limit according to  $D - 1$  dimensions. Hereby the implementation of the substitution (4.5) into the formalism will allow to derive  $\beta$ -functions and to calculate RG flows which describe the crossover from a  $(D - 1)$ - to a  $D$ -dimensional characteristic.

The modifications in the calculations of the functional traces related to the substitution (4.5) are discussed in Appendix D.3. A recapitulation of one aspect of the previously described formalism is here in order: The angular integrals can be performed leading to one-dimensional integrals, the so-called threshold functions  $l_m^D(w)$ . For completeness, in Appendix E their definition is given. In the same way one can do the angular part of the  $D - 1$ -dimensional momentum integrals. This leads to generalised threshold functions  $l_m^D(w, L)$  which are expressed as a Matsubara sum of one-dimensional integrals, for their definition see Appendix E, where also their limits  $L \rightarrow \infty$  and  $L \rightarrow 0$  are given. In addition, for the Litim regulator the dependence on  $L$  factorises.

However, there is one subtle issue related to the heat kernel expansion. In the integrand of the term linear in the Ricci scalar one additional factor  $1/q^2$  appears as compared to the  $\mathcal{O}(\bar{R}^0)$  term. The existence of such a term (which will later on prove to be the origin of a substantial complication) is evident also from a dimensional analysis because  $\bar{R}$  has mass dimension two. The full expressions resulting from evaluating the trace with the help of a heat kernel expansion are given in Appendix D.3, here in this section I want to focus the description on the problematic term. The substitution (4.5) implies for such a term

$$\begin{aligned} \int \frac{d^D q}{(2\pi)^D} \frac{1}{q_D^2} \dots \bar{R} &\rightarrow \frac{1}{L} \sum_n \int \frac{d^{D-1} q}{(2\pi)^{D-1}} \frac{1}{q_{D-1}^2 + (2\pi n/L)^2} \dots \bar{R} \\ &\propto \frac{1}{L} \sum_n \int_0^\infty dz z^{D/2-3/2} \frac{1}{z + (2\pi n/L)^2} \dots \bar{R} \end{aligned} \quad (4.6)$$

As will become evident below the term  $\frac{1}{z + (2\pi n/L)^2}$  in the part of this expression linear in the Ricci scalar leads to quite complicated sums over  $n$ . Lowering for this part the dimensionality of the trace simplifies the heat kernel expansion sufficiently such that the sums and integrals can be done in a closed form. The approximate formula corresponding to the last line above reads

$$\frac{1}{L} \sum_n \int_0^\infty dz z^{D/2-3/2} \frac{1}{z + (2\pi n/L)^2} \dots \bar{R} \rightarrow \frac{1}{L} \sum_n \int_0^\infty dz z^{D/2-5/2} \dots \bar{R} \quad (4.7)$$

with the full expressions for the heat kernel expansions given in Eqs. (D.31) and (D.32), respectively. Although for completeness also the formulae following from the heat kernel expansion (D.31) will be presented in the next section, the evaluation of the traces will be done using the modified heat kernel expansion (D.32).

## 4.2 Dimensionally Reduced Renormalisation Group Equations

### Background field flow

To obtain the following expression I start from Eq. (D.3) and use Eq. (D.32) for the evaluation of the traces. Some explicit steps of this calculation are given in Appendix D. To proceed let me note that with a few trivial modifications Eq. (D.36) can be rewritten as

$$\begin{aligned}
& 2 \kappa^2 \int d^D x \sqrt{\det \bar{g}_{\mu\nu}} \left( \partial_t Z_{Nk} (-\bar{R}(\bar{g}) + 2 \bar{\lambda}_k) + 2 Z_{Nk} \partial_t \bar{\lambda}_k \right) = \quad (4.8) \\
& = (4 \pi)^{-(D-1)/2} \frac{k^{D-3}}{\Gamma(m+1)} \times \\
& \quad \times \left\{ \int d^D x \sqrt{\det \bar{g}_{\mu\nu}} k^2 \left[ \frac{1}{L} \sum_n \Gamma \left( -\frac{(D-3)}{2} + m \right) \times \right. \right. \\
& \quad \times \left. \left. \left( \frac{1}{2} D(D+1) (\omega_n^2 + 1 - 2 \lambda_k)^{(D-3)/2-m} - 2 D (\omega_n^2 + 1)^{(D-3)/2-m} \right) \right] \right. \\
& \quad + \int d^D x \sqrt{\det \bar{g}_{\mu\nu}} \bar{R} \left[ \frac{1}{L} \sum_n \Gamma \left( -\frac{(D-5)}{2} + m \right) \times \right. \\
& \quad \times \left. \left. \left( \frac{-D(5D^2 - 23D + 20)}{12(D-3)} (\omega_n^2 + 1 - 2 \lambda_k)^{(D-5)/2-m} \right. \right. \right. \\
& \quad \left. \left. \left. + \left( \frac{-D^2 - 4D + 18}{3(D-3)} \right) (\omega_n^2 + 1)^{(D-5)/2-m} \right) \right] \right\} \quad (4.9)
\end{aligned}$$

with

$$\omega_n^2 := \left( \frac{2 \pi n}{k L} \right)^2. \quad (4.10)$$

From this one infers that the  $\beta$ -functions take the form Eq. (2.26) and Eq. (2.28) with the anomalous dimension as in Eq. (2.24) the only difference being that the functions  $A_0(\lambda_k; kL)$  and  $B_0(\lambda_k; kL)$  are deduced from

$$\begin{aligned}
& k^D A_0(\lambda_k; kL) = 8 \pi (4 \pi)^{-(D-1)/2} \frac{\Gamma(-(D-3)/2 + m)}{\Gamma(m+1)} \frac{k^D}{kL} \times \\
& \quad \times \sum_n \left[ \frac{1}{2} D(D+1) (\omega_n^2 + 1 - 2 \lambda_k)^{(D-3)/2-m} - 2 D (\omega_n^2 + 1)^{(D-3)/2-m} \right], \\
& \text{and} \\
& k^{D-2} B_0(\lambda_k; kL) = 16 \pi (4 \pi)^{-(D-1)/2} \frac{\Gamma(-(D-5)/2 + m)}{\Gamma(m+1)} \frac{k^{D-2}}{kL} \times \\
& \quad \times \sum_n \left[ \frac{-D(5D^2 - 23D + 20)}{12(D-3)} (\omega_n^2 + 1 - 2 \lambda_k)^{(D-5)/2-m} \right. \\
& \quad \left. + \left( \frac{-D^2 - 4D + 18}{3(D-3)} \right) (\omega_n^2 + 1)^{(D-5)/2-m} \right]. \quad (4.11)
\end{aligned}$$

Putting  $\mathbf{D} = \mathbf{5}$  and  $\mathbf{m} = \mathbf{2}$  one can perform the sums which results in:

$$A_0(\lambda_k; kL) = \frac{1}{8\pi} \left[ \frac{15}{\sqrt{1-2\lambda_k}} \coth\left(\frac{kL\sqrt{1-2\lambda_k}}{2}\right) - 10 \coth\left(\frac{kL}{2}\right) \right] \quad (4.12)$$

$$B_0(\lambda_k; kL) = -\frac{1}{64\pi} \left[ \frac{25}{1-2\lambda_k} \operatorname{csch}^2\left(\frac{kL\sqrt{1-2\lambda_k}}{2}\right) \times \left( kL + \frac{1}{\sqrt{1-2\lambda_k}} \sinh\left(\frac{kL\sqrt{1-2\lambda_k}}{2}\right) \right) + 18 \operatorname{csch}^2\left(\frac{kL}{2}\right) \left( kL + \sinh(kL) \right) \right]. \quad (4.13)$$

To obtain closed expressions for the functions  $A_0(\lambda_k; kL)$  and  $B_0(\lambda_k; kL)$  it was necessary to employ heat kernel expansion in the form (D.32). Had one used instead the expansion (D.31) one would obtain an unchanged  $A_0(\lambda_k; kL)$  but a different

$$B_0(\lambda_k; kL) = \frac{1}{\pi} \frac{1}{(1-2\lambda_k)^{3/2}} \frac{1}{kL\sqrt{1-2\lambda_k}} \sum_n \left\{ -\frac{5}{(\Omega_n^2+1)^2} + \frac{15}{4} \left( 1 - \frac{1}{2} \frac{1}{\Omega_n^2+1} - \Omega_n^2 \ln\left(1 + \frac{1}{\Omega_n^2}\right) \right) \right\} - \frac{1}{\pi} \frac{1}{kL} \sum_n \left\{ \frac{1}{(\omega_n^2+1)^2} + \frac{5}{2} \left( 1 - \frac{1}{2} \frac{1}{\omega_n^2+1} - \omega_n^2 \ln\left(1 + \frac{1}{\omega_n^2}\right) \right) \right\}, \quad (4.14)$$

with  $\omega_n := \frac{2\pi n}{kL}$  and  $\Omega_n^2 = \frac{\omega_n^2}{1-2\lambda_k}$ ,

for which no closed expression could be found.

## Exact Functional Identity

As it is evident from the discussion in Appendix D the step function contained in the Litim regulator leads to an upper limit in the appearing integrals over the square of the integrated momentum,  $z = q^2$ . Without dimensional reduction the relevant integrals are of the form (*cf.*, Eq. (D.22))

$$\int_0^\infty dz z^{D/2-1} z^m \Theta\left(1 - \frac{z}{k^2}\right) = \int_0^{k^2} dz z^{D/2-1+m}, \quad (4.15)$$

with  $m = -1, 0, 1$ . Now, with the compactification of one dimension the corresponding sums plus integrals read:

$$\begin{aligned} & \frac{1}{L} \sum_{n=-\infty}^{\infty} \int_0^{\infty} dz z^{D/2-3} z^m \left( z + (2\pi n/L)^2 \right)^l \Theta \left( 1 - \frac{z + (2\pi n/L)^2}{k^2} \right) = \\ & = \frac{1}{L} \sum_{n=-[kL/2\pi]}^{[kL/2\pi]} \int_0^{k^2 - (2\pi n/L)^2} dz z^{D/2-3} z^m \left( z + (2\pi n/L)^2 \right)^l, \end{aligned} \quad (4.16)$$

with appropriate values of  $m$  and  $l$ . Due to the step function the upper limit of the integral depends on  $n$  but note that also  $n$  cannot exceed  $kL/2\pi$  due to the regulator. This constraint implies finite sums with  $n_{min} = -[kL/2\pi]$  and  $n_{max} = [kL/2\pi]$  where  $[\dots]$  denotes Gauß's bracket, resp., the floor function.

The sums are now finite, but again the heat kernel expansion (D.32) leads to closed expressions for the functions  $A_0$ ,  $A_1$ ,  $B_0$  and  $B_1$ , whereas the heat kernel expansion (D.31) does not. I will use both forms in the following. Hereby one profits from the Litim regulator: For small and intermediately large values of  $kL$  the sums can be performed easily numerically. For large values of  $kL$  the sums are accurately approximated by the leading order using the Euler-MacLaurin formula, see also Subsection 4.4.

The derivation of the  $\beta$ -functions is then straightforward although quite lengthy, an intermediate step is given once more in Appendix D. Not surprisingly the flow equations have again the form (2.29), (2.32) and (2.33), however, with the functions  $A_0$ ,  $A_1$ ,  $B_0$  and  $B_1$  given by

$$A_0(\lambda_k; kL) = \frac{1}{2\pi} \frac{1}{kL} s_2 \left( \frac{kL}{2\pi} \right) \left( \frac{15}{2} \left( \frac{1}{1-2\lambda_k} \right) - 5 \right), \quad (4.17)$$

$$A_1(\lambda_k; kL) = \frac{1}{2\pi} \frac{1}{kL} s_3 \left( \frac{kL}{2\pi} \right) \frac{5}{4} \left( \frac{1}{1-2\lambda_k} \right), \quad (4.18)$$

$$\begin{aligned} B_0(\lambda_k; kL) = & \frac{1}{\pi} \frac{1}{kL} \left[ s_2 \left( \frac{kL}{2\pi} \right) \left( -5 \left( \frac{1}{1-2\lambda_k} \right)^2 - 1 \right) \right. \\ & \left. + s_1 \left( \frac{kL}{2\pi} \right) \left( \frac{15}{4} \left( \frac{1}{1-2\lambda_k} \right) - \frac{5}{2} \right) \right], \end{aligned} \quad (4.19)$$

$$\begin{aligned} B_1(\lambda_k; kL) = & \frac{1}{\pi} \frac{1}{kL} \left[ s_3 \left( \frac{kL}{2\pi} \right) \left( -\frac{5}{6} \left( \frac{1}{1-2\lambda_k} \right)^2 \right) \right. \\ & \left. + \frac{15}{16} s_2 \left( \frac{kL}{2\pi} \right) \left( \frac{1}{1-2\lambda_k} \right) \right], \end{aligned} \quad (4.20)$$

for the heat kernel expansion (D.32). Hereby

$$s_l(a) := \sum_{-l}^{[a]} \left( 1 - \left( \frac{n}{a} \right)^2 \right)^l, \quad l = 1, 2, 3, \quad (4.21)$$

with  $a = kL/2\pi$  and these functions are normalised such that  $s_l(a) = 1$  for  $a < 1$ . These three sums can be performed explicitly, the corresponding expressions are given in Eq. (D.40) in Appendix D.5.

For the case of the heat kernel expansion (D.31) one obtains instead of the expressions above for  $B_0$  and  $B_1$ :

$$B_0(\lambda_k; kL) = \frac{1}{\pi} \frac{1}{kL} \sum_{-[kL/2\pi]}^{[kL/2\pi]} \left[ \left(1 - \omega_n^2\right)^2 \left( -5 \left(\frac{1}{1-2\lambda_k}\right)^2 - 1 \right) + \left(1 - \omega_n^2 + \omega_n^2 \ln \omega_n^2\right) \left( \frac{15}{4} \left(\frac{1}{1-2\lambda_k}\right) - \frac{5}{2} \right) \right], \quad (4.22)$$

$$B_1(\lambda_k; kL) = \frac{1}{\pi} \frac{1}{kL} \sum_{-[kL/2\pi]}^{[kL/2\pi]} \left[ \left(1 - \omega_n^2\right)^3 \left( -\frac{5}{6} \left(\frac{1}{1-2\lambda_k}\right)^2 \right) + \frac{15}{16} \left(1 - \omega_n^4 + 2 \omega_n^2 \ln \omega_n^2\right) \left(\frac{1}{1-2\lambda_k}\right) \right], \quad (4.23)$$

where the definition (4.10) for  $\omega_n^2$  has been used. The functions  $A_0$  and  $A_1$  do not change.

### 4.3 $\beta$ -Functions and Effective Coupling

For the convenience of the reader the expressions for the  $\beta$ -functions and the anomalous dimension are repeated (*cf.*, Eqs. (2.29), (2.32) and (2.33)):

$$\partial_t \lambda_k = \beta_\lambda(g_k, \lambda_k) = \eta_{Nk} \lambda_k - 2 \lambda_k + g_k \left( A_0(\lambda_k; kL) - \eta_{Nk} A_1(\lambda_k; kL) \right) \quad (4.24)$$

$$\partial_t g_k = \beta_g(g_k, \lambda_k) = (D - 2 + \eta_{Nk}) g_k, \quad \text{with} \quad \eta_{Nk} = \frac{g_k B_0(\lambda_k; kL)}{1 + g_k B_1(\lambda_k; kL)}. \quad (4.25)$$

In the approximate background field flow one has  $A_1 = B_1 = 0$  with  $A_0$  and  $B_0$  given in the case of dimensional reduction in Eqs. (4.12) and (4.13). For the case starting from the exact functional identity the four functions are given in Eqs. (4.17) - (4.20).

A decisive observation is now that in both considered cases, these four functions are proportional to  $1/kL$  for small  $kL$ , for a more detailed discussion of the limits of these functions see the next subsection. And as one sees from Eqs. (4.24) and (4.25) these functions appear always exactly with precisely one factor  $g_k$ . This makes plain that a relation between an effective running (dimensionless) coupling in four space-time dimensions to the one in five space-time dimensions has to take the form

$$\boxed{g_k^{4D} = \frac{g_k^{5D}}{kL} \quad \text{for} \quad kL \ll 1.} \quad (4.26)$$

This identification is corroborated by the following dimensional analysis. Going back to the dimensionful Newton coupling  $G_N$  with canonical dimension  $2 - D$  (*i.e.*,  $G_N^{5D}$  has dimension -3 and  $G_N^{4D}$  dimension -2) it is obvious that dimensional reduction cannot consist only in taking the limit  $L \rightarrow 0$ . Instead one needs to replace the coupling  $G_N^{5D}$  by a coupling of the correct canonical dimension for four dimensions, and because  $L$  is the only scale available one needs to identify  $G_N^{5D}/L$  with  $G_N^{4D}$ . Inserting this identification into Eq. (2.21) one arrives also at the relation Eq. (4.26).

Of course, one does not want to change the coupling “by hand” or in some other discontinuous way. In order to obtain a more appropriate description for the physics of dimensional reduction one is looking for an effective coupling  $g_{k,\text{eff}}$  fulfilling the following requirements:

- It should be well-defined and finite in both limits  $L \rightarrow \infty$  and  $L \rightarrow 0$ .
- It should connect smoothly both limits.
- In the (semi-)classical regime it should behave like  $k^2$  (*i.e.*, like a four-dimensional running coupling) for  $k \ll 1/L$  and like  $k^3$  (*i.e.*, like a five-dimensional running coupling) for  $k \gg 1/L$ .
- The crossover from four- to five-dimensional behaviour should occur for scales  $k \approx 1/L$ .

A definition which fulfils these requirements is given by

$$g_{k,\text{eff}} = g_k \frac{B_0(\lambda_k; kL)}{B_0^\infty} \quad \text{with} \quad B_0^\infty = \lim_{L \rightarrow \infty} B_0(\lambda_k; kL) . \quad (4.27)$$

By construction  $g_{k,\text{eff}} \rightarrow g_k$  for large  $L$ , *i.e.*, it becomes identical to the running (dimensionless) coupling in five space-time dimensions for  $L \gg 1/k$ . In the opposite limit  $L \rightarrow 0$  the effective coupling  $g_{k,\text{eff}}$  stays (on a general RG trajectory) non-vanishing and finite due to the  $1/kL$  divergence of the function  $B_0$ .

In Chapter 3 it was recognised that the influence of the function  $B_1$  on the RG trajectories is of absolutely of minor importance except when a trajectory passes closely to the boundary line  $1/\eta_{Nk} = 0$ . As those trajectories are not in the class of ADD model trajectories I am looking for (see also below) let us neglect for the sake of a qualitatively correct and quantitatively reasonably accurate discussion the function  $B_1$  in the anomalous dimension derived from the exact functional identity (in the corresponding approximate background field flow expression it is anyhow not present). Then one can define an effective anomalous dimension  $\eta_{Nk,\text{eff}}$  which deviates from  $\eta_{Nk}$  only by the scale derivative of the logarithm of the function  $B_0$ :

$$\eta_{Nk,\text{eff}} = \underbrace{B_0^\infty}_{\eta_{Nk}} g_{k,\text{eff}} + \frac{\partial_t B_0(\lambda_k; kL)}{B_0(\lambda_k; kL)} . \quad (4.28)$$

Exploiting the fact that for small  $kL$  one has  $B_0 \propto 1/kL$  and thus

$$\partial_t B_0(\lambda_k; kL) = -B_0(\lambda_k; kL) + \mathcal{O}(kL) \quad (4.29)$$

the relation

$$\eta_{Nk,\text{eff}} = \eta_{Nk} - 1 \quad \text{for } kL \ll 1 \quad (4.30)$$

is evident, *i.e.*, one obtains the lowering of the anomalous dimension by one as it is required by the general formula  $\eta_{Nk} = 2 - D$ . Therefore, based on the definition of  $g_{k,\text{eff}}$  as provided in Eq. (4.27) the five- and the four-dimensional limit,  $L \rightarrow \infty$  and  $L \rightarrow 0$ , resp., are both well-defined.

Changing now the perspective from a varying  $L$  at fixed  $k$  to a varying RG scale  $k$  at fixed size  $L$  of the extra dimension one can get two different types of RG flows for the effective coupling  $g_{k,\text{eff}}$ :

- In the UV, *i.e.*, at large RG scale  $k$ , one starts close to the five-dimensional UV fixed point with  $g_{k,\text{eff}} \approx g_k \approx g_*$ . Still staying in the quantum regime  $k$  becomes smaller than  $1/L$  and one crosses to the four-dimensional UV fixed point, and only later on in the flow one runs into a four-dimensional (semi-)classical regime. Such a trajectory lacks, to the best of my knowledge, a physical interpretation. In any case they are not of the ADD type.
- Also in the second case one starts in the UV very close to the UV fixed point but the five-dimensional (semi-)classical running of  $g_{k,\text{eff}} \approx g_k$  sets in for a scale very much larger than  $1/L$ , *i.e.*, for  $k \gg 1/L$ . For several orders of magnitude one follows the five-dimensional (semi-)classical trajectory until  $k \approx 1/L$ . Then, more or less suddenly, a cross-over from the five-dimensional to the four-dimensional (semi-)classical RG flow takes place. Such a RG trajectory is then a realisation of the ADD model.

## 4.4 Discussion of the Limits

In this section a discussion of the limits  $kL \rightarrow \infty$  and  $kL \rightarrow 0$  will be given. Note that the  $\beta$ -functions and the anomalous dimension depend only on the dimensionless product  $kL$ . Therefore from the mathematical point of view the discussion of the limits of the respective functions in terms of the product  $kL$  is complete. Of course, the physical interpretation changes depending whether the limits are taken for fixed RG scale  $k$  or fixed size of the compact dimensions  $L$ , *cf.*, the discussion in the last section.

For the approximate background field flow and  $kL \gg 1$  one expands the hyperbolic functions in Eqs. (4.12) and (4.13) to obtain

$$A_0(\lambda_k; kL) = \frac{1}{8\pi} \left[ \frac{15}{\sqrt{1-2\lambda_k}} \left( 1 + 2e^{-kL\sqrt{1-2\lambda_k}} \right) - 10 \left( 1 + 2e^{-kL} \right) + \mathcal{O}(e^{-2kL}) \right], \quad (4.31)$$

$$B_0(\lambda_k; kL) = -\frac{1}{32\pi} \left[ \frac{25}{(1-2\lambda_k)^{3/2}} \left( 1 + 2 \left( 1 + kL\sqrt{1-2\lambda_k} \right) e^{-kL\sqrt{1-2\lambda_k}} \right) + 18 \left( 1 + 2 \left( 1 + kL \right) e^{-kL} \right) + \mathcal{O}(e^{-2kL}) \right]. \quad (4.32)$$

A more direct way is to use the Euler-MacLaurin formula for sums ( $B_{2l}$  are the Bernoulli numbers)

$$\sum_{n=a}^b f(n) = \int_a^b f(x) + \frac{1}{2}(f(a) + f(b)) + \sum_{l=1}^{\infty} \frac{B_{2l}}{(2l)!} \left( f^{(2l-1)}(b) - f^{(2l-1)}(a) \right). \quad (4.33)$$

and to perform the limits at the level of the sums. This, of course, provides the same results. In case that the heat kernel expansion (D.31) is used one obtains the same limit for  $A_0$  but the limit for  $B_0$  is now based on Eq. (4.14). The leading order term as calculated with the help of the expansion (4.33) is then given by<sup>2</sup>

$$B_0(\lambda_k; kL) = -\frac{1}{32\pi} \left[ \frac{30}{(1-2\lambda_k)^{3/2}} + \frac{44}{3} + \mathcal{O}(e^{-kL}) \right]. \quad (4.34)$$

As one sees the limits (4.32) and (4.34) differ slightly which has no impact on the qualitative and practically no influence on the quantitative behaviour. However, the five-dimensional UV fixed point is only then precisely assumed if the form Eq. (4.14) with the limiting value (4.34) is employed.

For the approximate background field flow and  $kL \ll 1$  one can either expand the hyperbolic functions or simply exploit the fact that only the zero mode contributes to the Kaluza-Klein mode sums. One obtains

$$A_0(\lambda_k; kL) = \frac{1}{kL} \frac{1}{8\pi} \left[ \frac{30}{1-2\lambda_k} - 20 + \frac{5}{6}(kL)^2 + \mathcal{O}((kL)^4) \right], \quad (4.35)$$

$$B_0(\lambda_k; kL) = -\frac{1}{kL} \frac{1}{8\pi} \left[ \frac{25}{(1-2\lambda_k)^2} + 18 + \mathcal{O}((kL)^4) \right]. \quad (4.36)$$

Needless to say that these limits do not reproduce the four-dimensional UV fixed point due to the fact that several factors entering the calculation are in a non-trivial manner dependent on the number of space-time dimensions. But again the

---

<sup>2</sup>All the limits given in this section have been checked by taking numerically, and when possible analytically, the limits in the sums over Kaluza-Klein modes.

deviations are of no qualitative and minor quantitative importance. To be complete let me mention that the corresponding leading-order limit of Eq. (4.14) is also given by the expression (4.36).

For the case of the expressions derived from the exact functional identity the limit  $kL \rightarrow \infty$  will be discussed first. In this limit the sums in Eqs. (4.17 - 4.23) become Riemann integrals, the respective values are:

$$\begin{aligned}
\int_{-1}^1 \frac{dp}{2\pi} (1-p^2) &= \frac{2}{3\pi}, & \int_{-1}^1 \frac{dp}{2\pi} (1-p^2)^2 &= \frac{8}{15\pi}, \\
\int_{-1}^1 \frac{dp}{2\pi} (1-p^2)^3 &= \frac{16}{35\pi}, & & \\
\int_{-1}^1 \frac{dp}{2\pi} (1-p^2 + p^2 \log p^2) &= \frac{4}{9\pi}, & \int_{-1}^1 \frac{dp}{2\pi} (1-p^4 + 2p^2 \log p^2) &= \frac{16}{45\pi}.
\end{aligned} \tag{4.37}$$

For the case of the heat kernel expansion (D.31) this results as anticipated in the expressions (3.19) for the four functions  $A_0$ ,  $A_1$ ,  $B_0$  and  $B_1$ . Correspondingly, the five-dimensional UV fixed point is precisely reproduced. For the case of the heat kernel expansion (D.32) the limit changes slightly as one has to substitute in the second line of Eq. (4.19), resp., Eq. (4.22)  $4/9\pi \rightarrow 2/3\pi$  and in the second line of Eq. (4.20), resp., Eq. (4.23)  $16/45\pi \rightarrow 8/15\pi$ , *i.e.*, these two terms obtain a weight increased by 50%. Correspondingly the fixed point values are slightly shifted, one has then  $g_* = 2.7650$  and  $\lambda_* = 0.26292$ .

The limit  $kL \rightarrow 0$  is identical for both cases of the heat kernel expansion. In this limit the expressions with the Litim regulator show an interesting feature. For  $kL < 2\pi$  the Kaluza-Klein mode sums degenerate to the zero mode term only. The corresponding  $n = 0$  terms yield:

$$\begin{aligned}
A_0(\lambda_k; kL < 2\pi) &= \frac{1}{kL} \frac{1}{2\pi} \left( \frac{15}{2} c_k - 5 \right), \\
A_1(\lambda_k; kL < 2\pi) &= \frac{1}{kL} \frac{1}{2\pi} \frac{5}{4} c_k, \\
B_0(\lambda_k; kL < 2\pi) &= \frac{1}{kL} \frac{1}{\pi} \left( -5 c_k^2 + \frac{15}{4} c_k - \frac{7}{2} \right), \\
B_1(\lambda_k; kL < 2\pi) &= \frac{1}{kL} \frac{1}{\pi} \left( -\frac{5}{6} c_k^2 + \frac{15}{16} c_k \right),
\end{aligned} \tag{4.38}$$

with  $c_k$  as defined in Eq. (3.15).

And as expected, due to the truncation and to the fact that I use a five-dimensional regulator, these are not exactly the expressions needed to reproduce the four-dimensional UV fixed point in  $g_{k,\text{eff}}$ , *cf.*, Eqs. (3.17).

## 4.5 Renormalisation Group Flows and Phase Diagrams in $D = 4 + 1$

In this section numerical results for the solution of the RG equations with four extended and one compactified dimension will be presented. Some details of the numerical treatment are described in Appendix F.

### 4.5.1 Results for the Background Field Flow

In the case without dimensional reduction the  $\beta$ -functions contain only dimensionless quantities, see *e.g.*, Eqs. (2.29) and (2.32). They constitute a system of differential equations for the dimensionless running coupling constants  $g_k$  and  $\lambda_k$ . Due to this it is evident that the numerical values of the RG scale  $k$  are completely irrelevant. In the case of dimensional reduction the nature of the system of differential equations changes drastically. Now  $L$  provides a length scale, and therefore the cases  $k > 1/L$

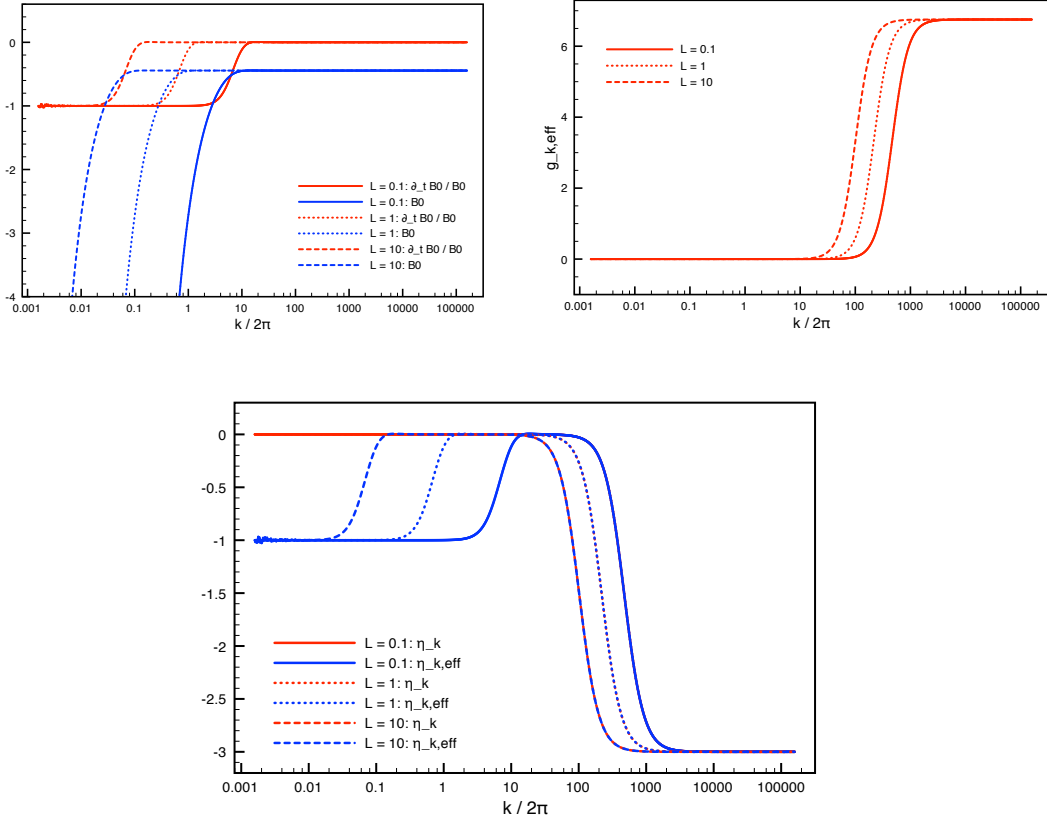


Figure 4.1: Comparison between three different values of  $L$  (0.1 - full lines, 1 - dotted lines and 10 - dashed lines) and all other parameters kept identical. The upper left panel shows the function  $B_0$  (4.13) (blue lines) and its scale derivative (red lines), the upper right panel  $g_{k,\text{eff}}$  (4.27) and the lower panel the anomalous dimensions  $\eta_{Nk}$  (2.33) (red lines) and  $\eta_{Nk,\text{eff}}$  (4.28) (blue lines). For simplicity the cosmological constant  $\lambda_k$  has been set to zero in this test calculation.

and  $k < 1/L$  become different as it is also exemplified by the discussion of the two different limits in the last section. However, there should be a remnant of the original scale invariance: The numerical value of  $L$  is irrelevant to the investigated system in the sense that the results for two different values of  $L$  can be mapped onto each other by a corresponding rescaling of the RG scale  $k$ . I explicitly tested this scenario for the approximate background field flow, see Fig. 4.1, where one clearly sees due to the linear-log presentation the scaling of the results for three different values of  $1/L$ . From now on and without loss of generality I will use  $L = 1$ .

In Fig. 4.2 two examples for the RG scale dependence of the coupling constants are shown. Both sets reach the UV fixed point at different RG scales  $k$  as measured in units of  $1/L$ . To see the approach to the fixed point  $g_k$ ,  $g_{k,\text{eff}}$ ,  $\lambda_k$ ,  $\eta_{Nk}$  or  $\eta_{Nk,\text{eff}}$  are equally suitable. For discriminating the different regions, however,  $\eta_{Nk,\text{eff}}$  is most efficient. For both sets  $\eta_{Nk,\text{eff}} = 2 - D = -3$  in fixed point regime and  $\eta_{Nk,\text{eff}} = -1$  for  $k < 1/L$  indicating a (semi-)classical regime according to  $D - 1 = 4$  dimensions. The both sets are different with respect to the existence of (semi-)classical regime with five-dimensional running: For the set displayed by the full lines there are more than three orders of magnitude between  $1/L$  and the scale where the UV fixed point behaviour starts. Accordingly, there exists for approximately two orders of magnitude a five-dimensional classical regime. Therefore the respective RG trajectory constitutes a realisation of the ADD model. For the set shown with the dashed line the UV fixed point is reached for  $k \approx 8\pi/L$ , and as one sees from the behaviour of  $\eta_{Nk,\text{eff}}$  the separation of scales is too small for a five-dimensional classical regime to exist.

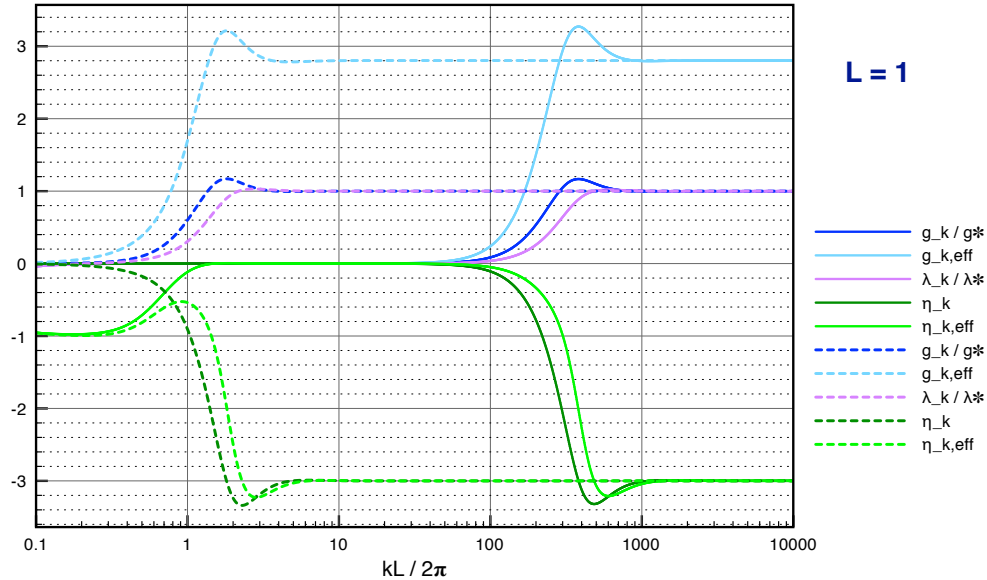


Figure 4.2: Two examples for the RG scale dependence of coupling constants resulting from the Eqs. (2.26) and (2.28) with (4.12) and (4.13) as input: Shown is  $g_k$  (normalised by  $g_*$ ),  $g_{k,\text{eff}}$  (4.27),  $\lambda_k$  (normalised by  $\lambda_*$ ),  $\eta_{Nk}$  (2.24) and  $\eta_{Nk,\text{eff}}$  (4.28). For the set displayed by the dashed lines the UV fixed point is reached for  $k \approx 8\pi/L$ , for the set with the full lines there are more than three orders of magnitude between  $1/L$  and the scale where the UV fixed point behaviour starts.

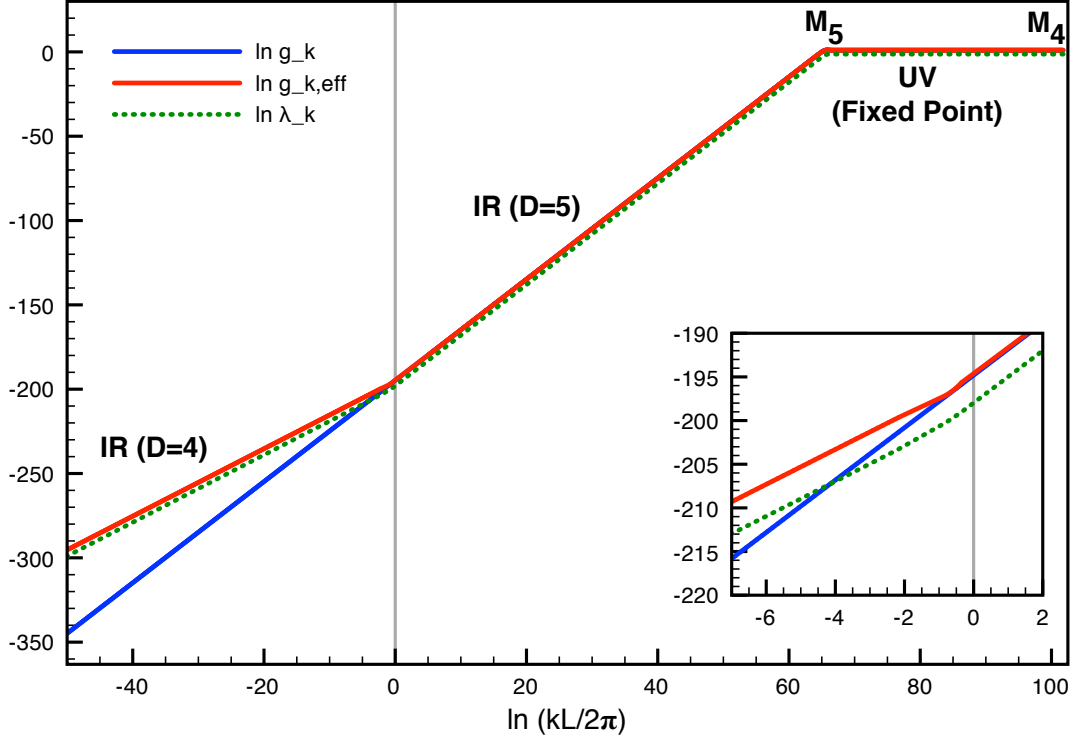


Figure 4.3: A further example for the RG scale dependence of coupling constants: The scale where the UV fixed point is reached is many orders of magnitude larger than  $1/L$ .  $g_k$  and  $\lambda_k$  are solutions of the differential equations (2.26) and (2.28) with the functions (4.12) and (4.13) as input;  $g_{k,\text{eff}}$  is defined in (4.27).

In Fig. 4.3 an example for a RG trajectory being a realisation of the ADD model is given. In the beginning of this chapter we estimated that for  $n = 1$  one has the relation  $M_5 \approx 10^{32}/L$  to obtain  $M_4 \approx 10^{16}M_5$ . In the displayed example the UV fixed point region starts at  $k \approx e^{66} \cdot 2\pi/L \approx 5 \cdot 10^{28} \cdot 2\pi/L$ , *i.e.*, one has  $M_5 \approx 10^{30}/L$  and  $M_4 \approx 10^{15}M_5$ . In between  $2\pi/L$  and the fixed point, both  $g_k$  and  $g_{k,\text{eff}}$  grow like  $k^3$  from a value  $e^{-195} \approx 10^{-85}$  to the fixed point value. For  $k < 1/L$  one sees a clear difference in the power laws:  $g_{k,\text{eff}}$  grows like  $k^2$  according to the four-dimensional behaviour. The dimensionless cosmological constant  $\lambda_k$  shows an interesting behaviour: It possesses also a crossover from a  $k^2$  to a  $k^3$  power law.<sup>3</sup> This can be understood from the explicit expression for  $\beta_\lambda$  and the function  $A_0$  as well as the fact that  $\eta_k$  can be neglected completely in  $\beta_\lambda$  for all  $k \ll M_5$ , *i.e.*, before the fixed point region is reached. For  $\lambda_k < g_{k,\text{eff}}$  one has for  $kL \ll 1$

$$\partial_t \lambda_k \approx g_k A_0 = \text{const.} \times \frac{g_k}{kL} = \text{const.}' \times g_{k,\text{eff}} \quad (4.39)$$

where  $\text{const.}'$  is a number of order one. Therefore,  $\lambda_k \propto k^2$  with a fixed ratio to  $g_{k,\text{eff}}$ . For  $kL$  large but still  $k \ll M_5$  one has  $g_k \approx g_{k,\text{eff}} \propto k^3$  and  $A_0$  being a constant

<sup>3</sup>For a starting value of  $\lambda_k$  very much larger than  $g_{k,\text{eff}}$ , see Fig. 4.5 below.

of order one. Thus also  $\lambda_k$  assumes the power law  $k^3$  until the fixed point region is reached. In the inset of Fig. 4.3 the transition region is shown. Hereby the vertical grey line denotes  $kL = 2\pi$ . One sees that the merger of  $g_k$  and  $g_{k,\text{eff}}$  as well as crossover in power laws for  $g_{k,\text{eff}}$  and  $\lambda_k$  happen at  $kL \approx 2.5$  and therefore a factor two to three lower than naïvely expected.

## 4.5.2 Results following from the Exact Functional Identity

In Fig. 4.4 the RG scale dependence of coupling constants is displayed for the case of the Litim regulator using the same set of starting conditions as for the full lines in Fig. 4.2. Hereby one sees strong similarities between the results of the approximate background field flow and the expressions derived from the exact functional identity but also two differences: At  $k \gtrsim 2\pi$  the anomalous dimension  $\eta_{Nk,\text{eff}}$  shows oscillations characteristic to the “onset” of Kaluza-Klein modes. This effect is purely due to the regulator and of minor importance. The other difference, namely a much more drastic overshooting of  $g_k$  before it reaches its UV fixed point value, might be of more significance *cf.*, the discussion on phenomenological applications in the next chapter.

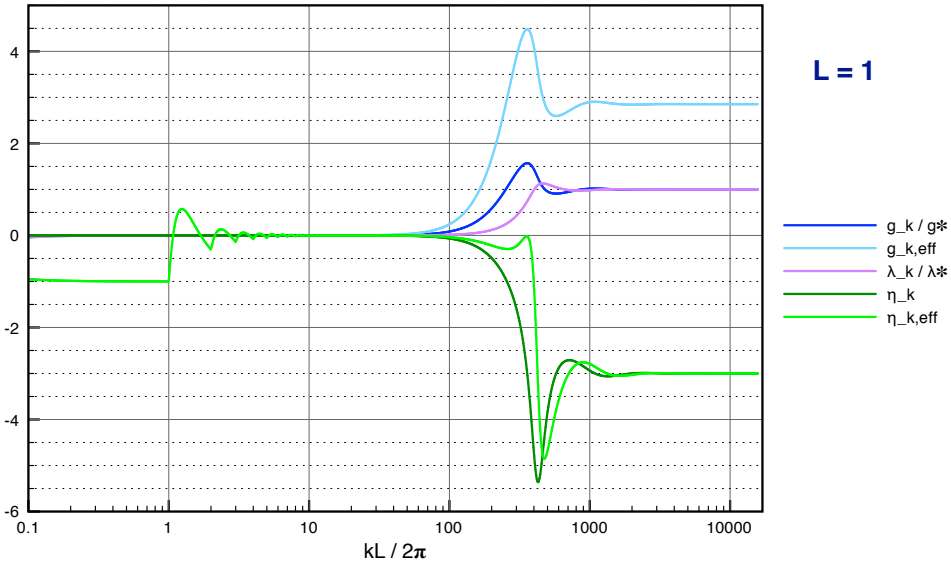


Figure 4.4: Same example as the full lines in Fig. 4.2 for the RG scale dependence of coupling constants but now for the  $\beta$ -functions (2.29) and (2.32) derived from the exact functional identity with the functions (4.17) - (4.20) as input.

In Fig. 4.5 the coupling constants derived from the exact functional identity are displayed. If the same starting conditions had been chosen as in Fig. 4.3 for the approximate background field flow the two versions of results would be practically indistinguishable with the given resolution of these figures. Therefore, an even smaller value of  $g_k$  was chosen as starting point in the IR. In the examples of Fig. 4.5 one has even larger ratios of scales as in Fig. 4.3:  $1/L$  and  $M_5$  differ by 32 to 33 orders of magnitude. This demonstrates that also for the  $\beta$ -functions derived from

the exact functional identity one can obtain RG trajectories with a separation of scales as required by the  $n = 1$  ADD model.

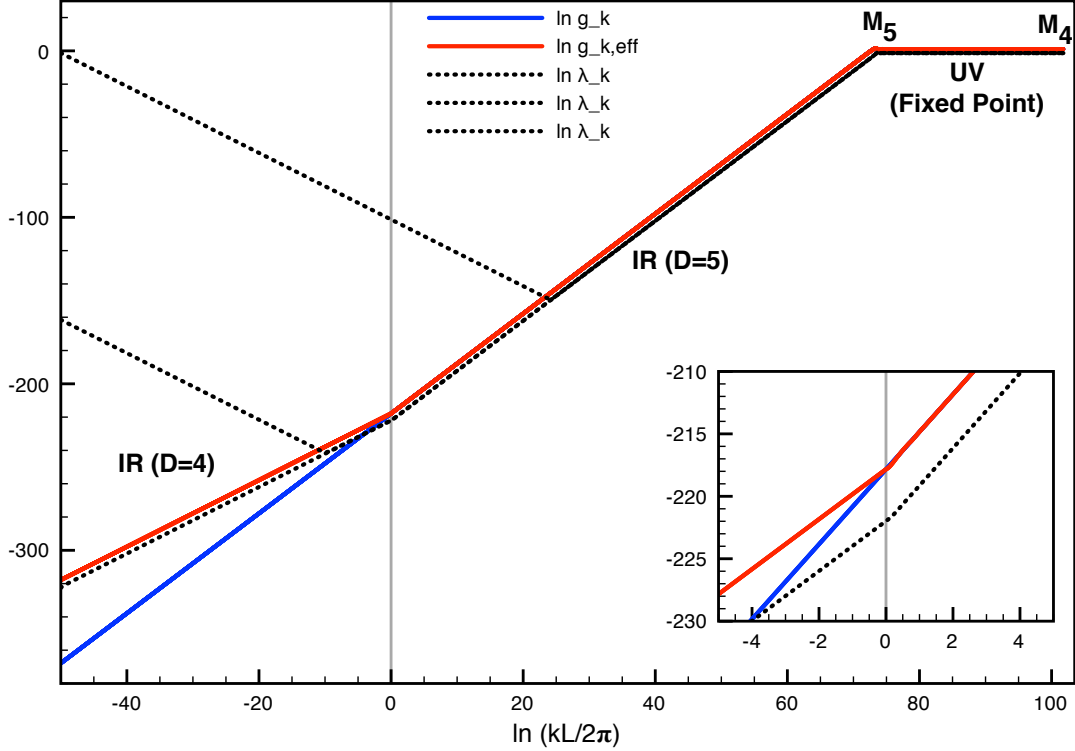


Figure 4.5: Similar to Fig. 4.3 but now for the coupling constants derived from the exact functional identity, and for  $\lambda_k$  several starting conditions are displayed.  $g_k$  and  $\lambda_k$  are solutions of the differential equations (2.29) and (2.32) with the functions (4.17) - (4.20) as input.  $g_{k,\text{eff}}$  is defined in (4.27).

For Fig. 4.5 three different starting values of the dimensionless cosmological constant  $\lambda_k$  have been chosen. Hereby it is important to note that the influence on the running of  $g_k$  is absolutely negligible: The three curves for  $g_k$  as well as the three curves for  $g_{k,\text{eff}}$  are exactly on top of each other. If the absolute value of  $\lambda_k$  is chosen as small as  $g_{k,\text{eff}}$  or even smaller one sees the crossover from a  $k^2$  to a  $k^3$  power law as in Fig. 4.3. If the starting value of  $\lambda_k$  is chosen very much larger than  $g_{k,\text{eff}}$  then it shows for increasing  $k$  first a power-law decrease with  $1/k^2$  as then the leading term in  $\beta_\lambda$  is such that  $\partial_t \lambda_k \approx -2\lambda_k$ . After it falls below the value of  $g_{k,\text{eff}}$  it follows the power-law increase of  $g_{k,\text{eff}}$  until both reach together their respective UV fixed point value. This is demonstrated here with starting values of  $\lambda_k = 0.4$  and  $\lambda_k = 10^{-70}$ , the difference between the both cases being that the latter has a part where it increases like  $k^2$  in the four-dimensional classical regime. In the former case the increase of  $\lambda_k$  starts only in the five-dimensional classical regime. In the calculations also starting conditions  $\lambda_k = -0.4$  and  $\lambda_k = -10^{-70}$  have been chosen. Plotting then the logarithm of the absolute values of  $\lambda_k$  produces indistinguishable

curves from the respective cases of positive  $\lambda_k$  except the locations of the respective minima: In the cases when starting with negative values for  $\lambda_k$  one has at exactly these locations the zero crossing.

However, the most important observation is the following: Comparing the two respective insets in the two figures 4.3 and 4.5 (which display a zoom around the value  $k = 2\pi/L$  indicated in both figures by the vertical grey line) shows a significant deviation. For the Litim regulator the merger of  $g_k$  and  $g_{k,\text{eff}}$  as well as crossover in power laws for  $g_{k,\text{eff}}$  and  $\lambda_k$  happens quite precisely at the naïvely expected scale  $k = 2\pi/L$ .

The difference of an approximate factor two in between these two calculations is certainly noteworthy. One has to conclude that within the employed truncations, for a given extension  $L$  of the compact dimension, the RG results for the precise scale of the dimensional crossover depends on the regulator.

In Fig. 4.6 the phase diagram for the running gravitational coupling  $g_{k,\text{eff}}$  and the cosmological constant  $\lambda_k$  in 4+1 dimensions within the approach based on the exact functional identity is shown. The third axis is  $\ln(kL/2\pi)$ . Here only trajectories have been displayed which are possible realisations of the ADD model. The separatrix is given by the red line. In the part which is visible in this linear plot it follows the five-dimensional running, for this trajectory one has  $M_5L \approx 7000$ . Therefore that part of the other RG trajectories running parallel to the separatrix flows according to the five-dimensional  $\beta$ -functions. All displayed trajectories follow the five-dimensional (semi-)classical running before they enter the fixed point regime. Note, however, that the separation of scales is quite small to allow for a linear representation:  $M_5L \approx 31$  for the blue,  $\approx 28$  for the green,  $\approx 24$  for the purple and  $\approx 23$  for the orange lines. Choosing larger separations of scales the crossover behaviour would be invisible in a linear plot, *cf.*, the log-log plot in Fig. 4.5. At  $k = 2\pi/L$  the trajectories depart from the four-dimensional running. One recognises that there is a regime where the change from four- to five-dimensional (semi-) classical running takes place. As one can see (*cf.*, also Fig. 4.4) this intermediate regime is up to values of  $k \approx 3 \cdot 2\pi/L$ .

From this section one can infer the following most relevant information: For RG trajectories being a realisation of the ADD model one has a quite sharp crossover from four- to five-dimensional behaviour which, when employing the Litim regulator, takes place in the interval  $2\pi < kL < 6\pi$ . However, the calculated position of the crossover is regulator dependent as the comparison to the approximate background field flow demonstrates. Reaching from the IR the fixed point regime the gravitational coupling is rapidly changing and oscillates around the fixed point value before it freezes to it. The width of this region is approximately one order of magnitude. The values of Newton's coupling and of the cosmological constant are to a high precision the ones of the five-dimensional RG equations because the corresponding Matsubara sums are quite accurately presented already by their limiting values.

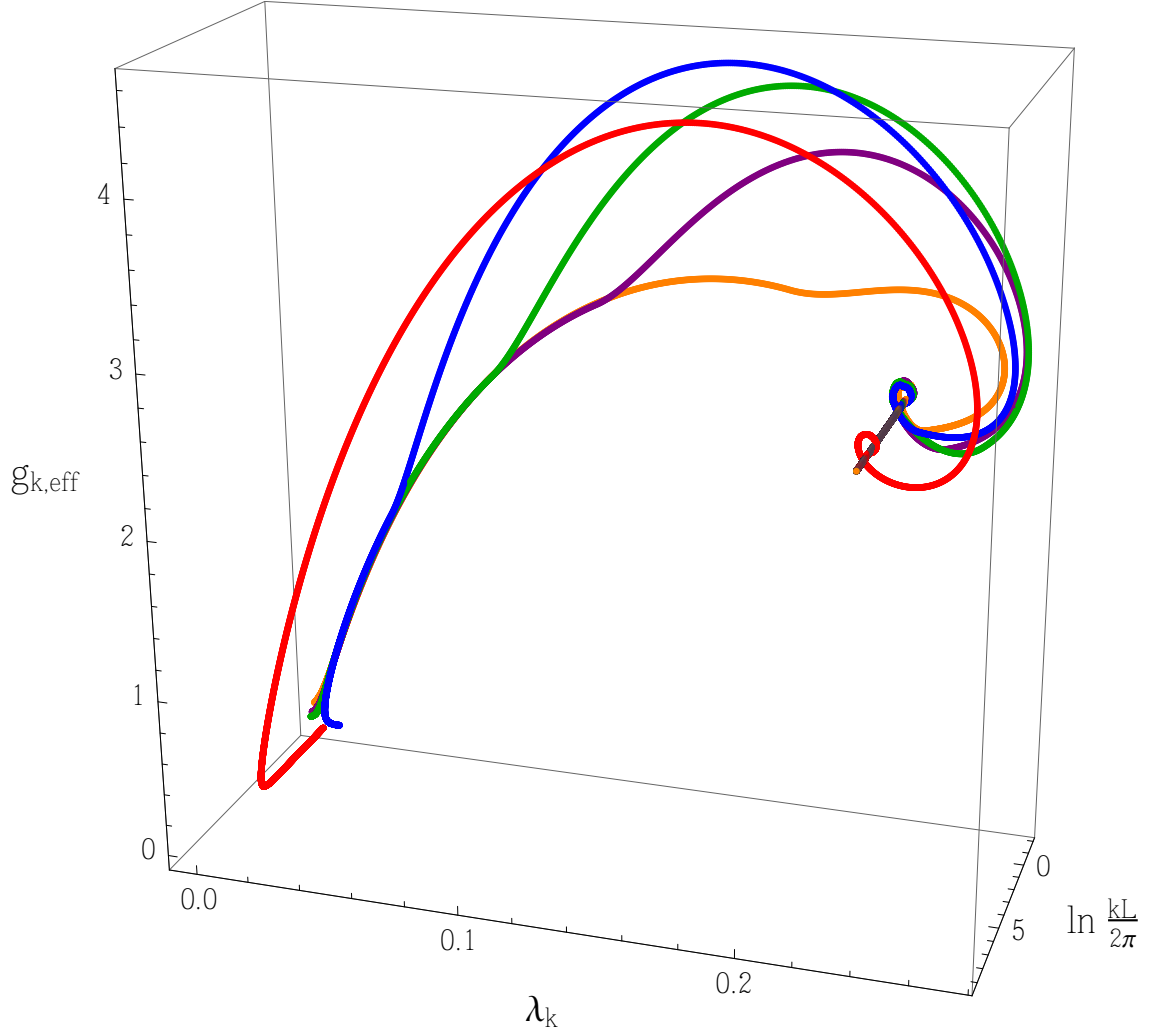


Figure 4.6: Shown is the phase diagram for the running gravitational coupling  $g_{k,\text{eff}}$  and the cosmological constant  $\lambda_k$  in  $4 + 1$  dimensions in function of  $\ln(kL/2\pi)$ . Displayed are RG trajectories corresponding to different values for  $M_5 L$ : 7000 (red line), 31 (blue line), 28 (green line), 24 (purple line) and 23 (orange line). The red line shows the separatrix and, in the part visible in this linear representation, the five-dimensional running. These trajectories are physical and except the separatrix show a clearly visible four- to five-dimensional crossover occurring at  $kL = 2\pi$ . They are solutions of the differential equations (2.29) and (2.32) with the functions (4.17), (4.18), (4.22) and (4.23) as input.  $g_{k,\text{eff}}$  is defined in (4.27).

# Chapter 5

## Conclusions

*“Imagination is more important than knowledge.”*

*(A. Einstein)*

### Contents

---

<b>5.1 Phenomenological Implications . . . . .</b>	<b>47</b>
<b>5.2 Concluding Remarks and Outlook . . . . .</b>	<b>48</b>

---

## 5.1 Phenomenological Implications

The basic idea of the ADD model is to bring the scale of gravity down to the EW scale, or at least down to only slightly above the EW scale. As already mentioned in the introduction besides many other implications, particle production processes may then be significantly enhanced by virtual graviton exchange.

Of course, in this context the value and scale dependence of the gravitational coupling play a significant role. Hereby one can identify for RG trajectories representing a realisation of the ADD model two transition regions. The first one is the one where the running of the gravitational coupling and the cosmological constant changes from a (semi-)classical four-dimensional to a (semi-)classical higher-dimensional behaviour. The second one is the transition from the (semi-)classical to the quantum, *i.e.*, fixed point, regime. If the latter is brought down to the electroweak scale this opens up the possibility that quantum gravity might be tested at the LHC. But also the first transition region can, at least in principle, be searched for in experiments. The most significant change in the behaviour of gravity would be the modification from an inverse-square law of the gravitational force to a power-law  $F \propto 1/r^{2+n}$  in  $4 + n$  space-time dimensions. Here, however, one has to note that an observed deviation from Newton’s gravitational law is not immediately identical to a precise measurement of the size of the compact dimension(s). In this thesis I even found quite a sizeable regulator dependence of the scale of the dimensional crossover even for a given size  $L$  of the compact dimension.

On the other hand, at the higher-dimensional Planck scale the values of the running gravitational constant could have been directly calculated from the higher-dimensional  $\beta$ -functions. This becomes evident already from the fact that for the

RG trajectories of interest the Matsubara sums are in the fixed point region already extremely close to their limiting values. In the best investigated examples of this thesis the starting conditions of the RG flow were chosen such that a separation of  $1/L$  and  $M_5$  by 30 to 33 orders of magnitude resulted. Then the mode sums are to any achievable numerical precision identical to their limiting values. In view of the fact that also for larger values of the number of extra dimensions,  $1/L$  and  $M_D \approx m_{EW}$  stay significantly separated, this conclusion seems robust. Therefore, for an analysis of the phenomenological implications of the asymptotic safety scenario at highest achievable accelerator energies it is sufficient to simply investigate the running of the gravitational constant in  $D = 4 + n$  dimensional quantum gravity. Given the very general appearance of complex scaling exponents in the asymptotic safety scenario the resulting rapid changes of the gravitational constant will provide an unique “fingerprint”.

## 5.2 Concluding Remarks and Outlook

To summarise, in this thesis I discussed the application of the asymptotic safety scenario to EH quantum gravity in the case of four extended and one compactified dimensions. All investigations were done in the EH theory and in deDonder gauge. As tools I used an approximate background field flow and an exact functional equation with the Litim regulator.

In the main chapter I presented results for corresponding RG trajectories. Some of them possess the separation of scales as required by the ADD model [31, 32]: These RG trajectories can be considered as realisations of this model. Especially, they provide an explicit example for an UV completion of the ADD model.

The investigations presented in this thesis can be considered only as first steps leading to studies of the ADD model assumptions within the asymptotic safety scenario of EH quantum gravity. The case of only one compact dimension while the true Planck scale is at or only slightly above the EW scale is excluded by experiment: The compact extra dimension would have a size comparable to the solar system. However, an ADD model with two and more compactified dimensions is still viable. Introducing several compact dimensions lead immediately to the question of the topological properties of the compactified space. In a first investigation one certainly will assume the easiest case, namely the topology of a torus with  $n = D - 4$  independent periodic boundary conditions. This will lead then to nested Matsubara sums. The techniques developed in this thesis should allow to treat the cases of a few (*e.g.*, two to four) nested sums in a efficient manner.

Nevertheless, the bottom line is that if there are “large” extra dimensions in nature this, first, might open up the exciting possibility of testing quantum gravity at the LHC [33–35]. Should a strong scale-dependence of the gravitational constant be measured then one can interpret this as evidence for the asymptotic safety scenario at work in quantum gravity. Second, a deviation from the inverse-square law of the gravitational force should become visible at the  $\mu\text{m}$  to nm scale. Hereby, the length

scale of the crossover in between the two power laws will be related to the size  $L$  of the compact dimensions. The crossover length scale is by definition observable, the size  $L$  is directly related to the excitation energies of Kaluza-Klein modes and thus also a physical length scale. Therefore, these both length scales (and automatically the ratio in between them) are expected to be independent of the renormalisation scheme and scale. However, in this theses the RG scale where the crossover happens was different for the employed two different regulators. This result clearly requires a better understanding and deserves therefore a more profound investigation.



# Appendix A

## Notations and Definitions

In this thesis I used units such that  $\hbar = 1$  and  $c = 1$ . One has then  $G_N = 1/m_{\text{Pl}}^2$  with  $m_{\text{Pl}} = 1.22093(7) \cdot 10^{19}$  GeV [3].

The definition of the expectation value of the full metric is given in Eq. (2.12). With this metric one obtains for the Ricci scalar, the Ricci tensor, the Riemann tensor and the Christoffel symbols the following relations:

$$\overbrace{R}^{\text{Ricci scalar}} = g^{\mu\nu} \underbrace{R_{\mu\nu}}_{\text{Ricci tensor}} \quad (\text{A.1})$$

with

$$\overbrace{R^{\mu}_{\nu\lambda\rho}}^{\text{Riemann tensor}} = \partial_\lambda \Gamma^{\mu}_{\nu\rho} - \partial_\rho \Gamma^{\mu}_{\nu\lambda} + \Gamma^{\mu}_{\sigma\lambda} \Gamma^{\sigma}_{\nu\rho} - \Gamma^{\mu}_{\sigma\rho} \Gamma^{\sigma}_{\nu\lambda}, \quad (\text{A.2})$$

and contracting first and third indices yields:

$$\underbrace{R_{\nu\rho}}_{\text{Ricci tensor}} = \partial_\lambda \Gamma^{\lambda}_{\nu\rho} - \partial_\rho \Gamma^{\lambda}_{\nu\lambda} + \Gamma^{\lambda}_{\sigma\lambda} \Gamma^{\sigma}_{\nu\rho} - \Gamma^{\lambda}_{\sigma\rho} \Gamma^{\sigma}_{\nu\lambda} \quad (\text{A.3})$$

where

$$\underbrace{\Gamma^{\mu}_{\nu\lambda}}_{\text{Christoffel symbols}} = \frac{1}{2} g^{\mu\rho} (\partial_\nu g_{\rho\lambda} + \partial_\lambda g_{\rho\nu} - \partial_\rho g_{\nu\lambda}). \quad (\text{A.4})$$

The variations of the Riemann and the Ricci tensor are given by

$$\delta R^{\mu}_{\nu\lambda\rho} = \partial_\lambda \delta \Gamma^{\mu}_{\nu\rho} - \partial_\rho \delta \Gamma^{\mu}_{\nu\lambda} + \delta \Gamma^{\mu}_{\sigma\lambda} \Gamma^{\sigma}_{\nu\rho} + \Gamma^{\mu}_{\sigma\lambda} \delta \Gamma^{\sigma}_{\nu\rho} - \delta \Gamma^{\mu}_{\sigma\rho} \Gamma^{\sigma}_{\nu\lambda} - \Gamma^{\mu}_{\sigma\rho} \delta \Gamma^{\sigma}_{\nu\lambda} \quad (\text{A.5})$$

and

$$\delta R_{\mu\nu} = \frac{1}{2} g^{\lambda\eta} (D_\nu D_\mu \delta g_{\lambda\eta} - D_\lambda D_\nu \delta g_{\eta\mu} - D_\lambda D_\mu \delta g_{\eta\nu} + D_\lambda D_\eta \delta g_{\mu\nu}), \quad (\text{A.6})$$

where  $D_\nu$  is the covariant derivative such that  $D_\nu V^\mu = \partial_\nu V^\mu + \Gamma^{\mu}_{\nu\lambda} V^\lambda$ .

The covariant gauge fixing functional can be written as [11]

$$\Gamma_{k,gf} = \kappa^2 Z_{Nk} \frac{1}{\alpha} \int d^D x \sqrt{\det \bar{g}_{\mu\nu}} \bar{g}^{\mu\nu} (\mathcal{F}_\mu^{\alpha\beta} g_{\alpha\beta}) (\mathcal{F}_\nu^{\rho\sigma} g_{\rho\sigma}) , \quad (\text{A.7})$$

where  $\alpha$  is a gauge parameter and the tensor  $\mathcal{F}_\mu^{\alpha\beta}$  depends on the background covariant derivative,

$$\mathcal{F}_\mu^{\alpha\beta} = \delta_\mu^\beta \bar{g}^{\alpha\gamma} \bar{D}_\gamma - \frac{1}{2} \bar{g}^{\alpha\beta} \bar{D}_\mu . \quad (\text{A.8})$$

An important property of the tensor  $\mathcal{F}_\mu^{\alpha\beta}$  is that it vanishes when contracted with the background metric

$$\mathcal{F}_\mu^{\alpha\beta} \bar{g}_{\alpha\beta} = 0 . \quad (\text{A.9})$$

Landau-deWitt gauge corresponds to the limit  $\alpha \rightarrow 0$ , deDonder gauge to  $\alpha = 1$ . In this thesis I used deDonder gauge.

# Appendix B

## Derivation of the Functional Renormalisation Group Equations

### Contents

---

<b>B.1 An exact functional identity for the effective average action . . . . .</b>	<b>53</b>
<b>B.2 Background field flow in proper-time regularisation . . .</b>	<b>55</b>

---

Throughout this thesis I employed two forms of the FRG, an exact functional identity and an approximated background field flow. Both are functional differential equations for the effective average action. Here, I provide a brief presentation of the derivation of the Wetterich equation and a discussion of the Litim regulator as well as an alternative derivation of the approximated background field flow in proper-time regularisation.

### B.1 An exact functional identity for the effective average action

As the Wetterich equation is an exact equation an appropriate starting point is the generating functional  $Z[J]$  where  $J(x)$  is a source coupled to the field(s). Taking the logarithm provides the generating functional of the connected Green functions  $W[J]$ . A Legendre transform leads to the effective action  $\Gamma[\bar{\Phi}]$  which is the generating functional of the one-particle irreducible Green functions. In the Wilsonian RG approach one also performs these three steps, however, with a  $k$ -dependent regulator function included, *i.e.*, one starts with<sup>1</sup>

$$Z_k[J] = \int \mathcal{D}\Phi \exp(-S[\Phi] - \Delta S_k[\Phi] + J \cdot \Phi) . \quad (\text{B.1})$$

---

<sup>1</sup>In this thesis only Euclidean Quantum Field Theories are considered, *i.e.*, it is always assumed that a Wick rotation has been performed. In addition, I will use the deWitt notation  $J \cdot \Phi = \int d^D x J(x)\Phi(x)$ .

In this functional integral the term  $\Delta S_k[\Phi]$  is included to provide a smooth momentum cutoff such that the UV modes are unchanged and the IR modes are suppressed. The standard choice is a quadratic cutoff which, in momentum space, reads

$$\Delta S_k[\Phi] = \frac{1}{2} \int \frac{d^D q}{(2\pi)^D} \Phi(-q) R_k(q^2) \Phi(q) . \quad (\text{B.2})$$

For the UV modes one thus requires

$$\lim_{q^2/k^2 \rightarrow \infty} R_k(q^2) = 0 \quad (\text{B.3})$$

and for the IR modes

$$R_k(q^2) \xrightarrow{q^2/k^2 \rightarrow 0} \infty , \quad (\text{B.4})$$

*cf.* also the discussion in Ref. [56].

The flow for the generating functional  $W_k$  is then straightforwardly determined to be

$$\partial_t W_k[J] = \partial_t \ln Z_k[J] = -\langle \partial_t \Delta S_k \rangle = -\frac{1}{2} \int \frac{d^D q}{(2\pi)^D} \partial_t R_k(q^2) \langle \Phi(q) \Phi(-q) \rangle . \quad (\text{B.5})$$

Next one introduces the Legendre transformed functional

$$\Gamma_k[\bar{\Phi}] = \sup_J (J \cdot \bar{\Phi} - \ln Z_k[J] - \Delta S_k[\bar{\Phi}]) \quad (\text{B.6})$$

where  $\bar{\Phi}$  is the expectation value of  $\Phi$  for a fixed external current  $J$ ,  $\bar{\Phi} = \langle \Phi \rangle_J$ . Returning for clarity for the time being to a real-space representation one employs then the definition of the connected two-point function

$$G(x, y) := \frac{\delta^2 \ln Z_k[J]}{\delta J(x) \delta J(y)} \quad (\text{B.7})$$

and the fact that the quantum equation of motion

$$J(x) = \frac{\delta \Gamma_k[\bar{\Phi}]}{\delta \bar{\Phi}(x)} + (R_k \cdot \bar{\Phi})(x) \quad (\text{B.8})$$

leads to

$$G(x, y) = \left( \frac{\delta^2 \Gamma_k[\bar{\Phi}]}{\delta \bar{\Phi}(x) \delta \bar{\Phi}(y)} + R_k(x - y) \right)^{-1} \quad (\text{B.9})$$

to show that in momentum space the equation

$$\partial_t \Gamma_k[\bar{\Phi}] = \frac{1}{2} \int \frac{d^D q}{(2\pi)^D} \left( \frac{\delta^2 \Gamma_k[\bar{\Phi}]}{\delta \bar{\Phi}(q) \delta \bar{\Phi}(-q)} + R_k(q^2) \right)^{-1} \partial_t R_k(q^2) \quad (\text{B.10})$$

is fulfilled. In case discrete indices are present they have to be summed over. Denoting by  $\text{Tr}$  these sums as well as the integrals leads then to the compact notation for the Wetterich equation [22]

$$\boxed{\partial_t \Gamma_k = \frac{1}{2} \text{Tr} \left( \left( \Gamma_k^{(2)} + R_k \right)^{-1} \partial_t R_k \right)} \quad (\text{B.11})$$

with

$$\Gamma_k^{(2)} := \frac{\delta^2 \Gamma_k[\bar{\Phi}]}{\delta \bar{\Phi}(q) \delta \bar{\Phi}(-q)} . \quad (\text{B.12})$$

Throughout this thesis the Litim regulator

$$\boxed{R_k(q^2) = (k^2 - q^2) \Theta(k^2 - q^2)} \quad (\text{B.13})$$

has been used. Its scale derivative can be straightforwardly calculated

$$\partial_t R_k(q^2) = 2 k^2 \Theta(k^2 - q^2) . \quad (\text{B.14})$$

## B.2 Background field flow in proper-time regularisation

Here an alternative derivation of the background field flow in proper-time regularisation is summarised following the presentation in Ref. [45]. To arrive at this flow one may start with the observation that in every Quantum Field Theory the one-loop contribution to the effective action can be expressed as a logarithm of a determinant. Denoting all the fields of the theory as  $\Phi$  and with  $S_\Phi^{(2)}$  the matrix of the second functional derivatives of the action  $S_\Phi$  w.r.t.  $\Phi$  one obtains

$$\Gamma^{(1\text{-loop})}[\Phi] = \frac{1}{2} \ln \det S_\Phi^{(2)} - \ln \det S_{gh}^{(2)} \quad (\text{B.15})$$

where  $S_\Phi$  is assumed to contain potential gauge fixing terms.  $S_{gh}^{(2)}$  denotes the second derivative of the ghost term associated to this gauge fixing term.

In the next step one introduces the proper time presentation

$$\ln \det S^{(2)} = \text{Tr} \ln S^{(2)} \rightarrow - \int_{1/\Lambda^2}^{\infty} \frac{ds}{s} \text{Tr} \exp(-s S^{(2)}) . \quad (\text{B.16})$$

UV singularities are then regularised by introducing a corresponding cutoff  $\Lambda$ . In the simplest case one substitutes the lower limit of the  $s$ -integral by  $1/\Lambda^2$ . Also in this form of the RG one wants to follow the idea of the Wilsonian RG and introduces a scale  $k$  which acts as an IR cutoff. Again, in the simplest case one substitutes then the upper limit of the  $s$ -integral by  $1/k^2$ . In this thesis I will use, however, a quite general class of proper time regulator functions in order to allow for a comparison to [44, 45]:

$$\text{Tr} \left( \ln S^{(2)} \right)_{\text{reg.}} = - \int_0^{\infty} \frac{ds}{s} f_k^m(s) \text{Tr} \exp(-s S^{(2)}) . \quad (\text{B.17})$$

The regulator functions  $f_k^m(s)$  depend on an additional parameter  $m$  and are for all  $m$  chosen such that they interpolate smoothly from zero for  $s \gg 1/k^2$  to one for small  $s$ . For the calculations in this thesis the family of regulator functions

$$f_k^m(s) = e^{(-Z s k^2)} \sum_{\mu=0}^m \frac{1}{\mu!} (Z s k^2)^\mu \quad (\text{B.18})$$

have been used. Here  $Z$  denotes a wave function renormalisation function. The advantage of introducing it into the regulator will become evident in Appendix D. In the following also the scale derivative of these functions will be needed. Employing the usual definitions

$$t = \ln k, \quad k \frac{\partial}{\partial k} = \frac{\partial}{\partial t} =: \partial_t, \quad (\text{B.19})$$

one gets

$$\partial_t f_k^m(s) = -2 \frac{1}{m!} (Z s k^2)^{m+1} e^{-Z s k^2}. \quad (\text{B.20})$$

In

$$\partial_t \text{Tr} \left( \ln S^{(2)} \right)_{\text{reg.}} = - \int_0^\infty \frac{ds}{s} \partial_t f_k^m(s) \text{Tr} \exp(-s S^{(2)}) \quad (\text{B.21})$$

the integral can be performed resulting in

$$\partial_t \text{Tr} \left( \ln S^{(2)} \right)_{\text{reg.}} = 2 \text{Tr} \left( \frac{Z k^2}{S^{(2)} + Z k^2} \right)^{m+1}. \quad (\text{B.22})$$

Regularising the determinants in Eq. (B.15) as described above makes the one-loop effective action  $\Gamma_k[\Phi] := S_\Phi + \Gamma_k^{(1\text{-loop})}[\Phi]$  dependent on the scale  $k$ :

$$\partial_t \Gamma_k[\Phi] = \partial_t \Gamma_k^{(1\text{-loop})}[\Phi] = -\frac{1}{2} \text{Tr} \int_0^\infty \frac{ds}{s} \partial_t f_k^m(s) (e^{-s S_\Phi^{(2)}} - 2 e^{-s S_{gh}^{(2)}}). \quad (\text{B.23})$$

This is still a one-loop expression. The underlying idea to implement the RG improvement is now to turn this into a self-consistent and thus non-perturbative equation by replacing on the r.h.s.  $S_\Phi^{(2)}$  by  $\Gamma_k^{(2)}$ , the second derivative of the fully dressed and scale- dependent  $\Gamma_k$  which then has to be calculated self-consistently:

$$\boxed{\partial_t \Gamma_k[\Phi] = -\frac{1}{2} \text{Tr} \int_0^\infty \frac{ds}{s} \partial_t f_k^m(s) \left( e^{-s \Gamma_k^{(2)}} - 2 e^{-s S_{gh}^{(2)}} \right)}. \quad (\text{B.24})$$

This form of the RG equation (with ghost quantum corrections neglected, see also Subsection 2.2.2) will be used in the following section for EH gravity.

# Appendix C

## Second Variation of the Effective Action

### Contents

---

C.1 Basic Variations . . . . .	57
C.2 Tensor Decomposition of $\Gamma_k^{(2)}$ . . . . .	58

---

### C.1 Basic Variations

For the first and second variations of the effective average action, there are a few terms which should be computed first. Looking to Eqs. (2.16) and (A.7) one can see that when doing a variation over  $\hat{S}_k[g; \bar{g}]$  terms like  $\delta\sqrt{\det g_{\mu\nu}}$  and  $\delta(\sqrt{\det g_{\mu\nu}} R)$  will appear. For this reason I will start with them.

For the variation of the first term one gets:

$$\begin{aligned} \delta\sqrt{\det g_{\mu\nu}} &= \delta e^{\frac{1}{2} \text{tr} \ln g} \\ &= \frac{1}{2} \sqrt{\det g_{\mu\nu}} g^{\mu\nu} h_{\mu\nu} . \end{aligned} \quad (\text{C.1})$$

And for the variation of the second term:

$$\begin{aligned} \delta(\sqrt{\det g_{\mu\nu}} R) &= (\delta\sqrt{\det g_{\mu\nu}}) R + \sqrt{\det g_{\mu\nu}} (\delta R) \\ &= (\delta e^{\frac{1}{2} \text{tr} \ln g}) R + \sqrt{\det g_{\mu\nu}} (\delta(g^{\mu\nu} R_{\mu\nu})) \\ &= \frac{1}{2} \sqrt{\det g_{\mu\nu}} h_{\mu}^{\mu} R \\ &+ \sqrt{\det g_{\mu\nu}} (-h^{\mu\nu} R_{\mu\nu} + D^{\alpha} D^{\mu} h_{\alpha\mu} - D^2 h_{\mu}^{\mu}) . \end{aligned} \quad (\text{C.2})$$

For the second variation of  $\delta\sqrt{\det g_{\mu\nu}}$  after some computations one finds:

$$\delta^2 \sqrt{\det g_{\mu\nu}} = \frac{1}{4} \sqrt{\det g_{\mu\nu}} h_{\mu}^{\mu} h_{\mu}^{\mu} - \frac{1}{2} \sqrt{\det g_{\mu\nu}} h^{\mu\nu} h_{\mu\nu} . \quad (\text{C.3})$$

And for the second variation of  $\delta(\sqrt{\det g_{\mu\nu}} R)$  :

$$\begin{aligned}
\delta^2(\sqrt{\det g_{\mu\nu}} R) &= \frac{1}{4}\sqrt{\det g_{\mu\nu}} h_\mu^\mu h_\mu^\mu R - \frac{1}{2}\sqrt{\det g_{\mu\nu}} h^{\mu\nu} h_{\mu\nu} R \\
&+ \sqrt{\det g_{\mu\nu}} h_\mu^\mu (-h^{\mu\nu} R_{\mu\nu} + D^\alpha D^\mu h_{\alpha\mu} - D^2 h_\mu^\mu) \\
&+ \sqrt{\det g_{\mu\nu}} [2h^{\mu\rho} h_\rho^\nu R_{\mu\nu} - \frac{1}{2}h^{\mu\nu} (D^\alpha D_\mu h_{\alpha\nu} + D^\alpha D_\nu h_{\alpha\mu} \\
&- D^2 h_{\mu\nu} - D_\nu D_\mu h_\alpha^\alpha) - \frac{1}{2}h_\lambda^\lambda D^\alpha D^\mu h_{\alpha\mu} \\
&+ \frac{1}{2}h_\rho^\rho D^\alpha D_\alpha h_\lambda^\lambda] . \tag{C.4}
\end{aligned}$$

Varying the gauge fixing action (A.7) provides the gauge fixing condition

$$F_\nu := \sqrt{2} \kappa \mathcal{F}_\nu^{\alpha\beta} [\bar{g}] h_{\alpha\beta} \stackrel{!}{=} 0 . \tag{C.5}$$

For further use I note that

$$\frac{\partial F_\nu}{\partial h_{\alpha\beta}} = \sqrt{2} \kappa \mathcal{F}_\nu^{\alpha\beta} [\bar{g}] . \tag{C.6}$$

Finally, the ghost action is given by

$$\Gamma_{gh}[h, c, \bar{c}; \bar{g}] = -\kappa^{-1} \int d^D x \sqrt{\det \bar{g}_{\mu\nu}} \bar{c}_\mu \bar{g}^{\mu\nu} \frac{\partial F_\nu}{\partial h_{\alpha\beta}} \mathcal{L}_c(\bar{g}_{\alpha\beta} + h_{\alpha\beta}) , \tag{C.7}$$

where the Lie derivative  $\mathcal{L}_c$  can be written as:

$$\mathcal{L}_c \gamma_{\alpha\beta} = \gamma_{\beta\nu} D_\alpha c^\nu + \gamma_{\alpha\nu} D_\beta c^\nu , \tag{C.8}$$

with  $\gamma_{\alpha\beta}$  being the full metric. As usual one can reexpress the ghost action in terms of the Faddeev-Popov operator

$$\begin{aligned}
\Gamma_{gh}[h, c, \bar{c}; \bar{g}] &= -\sqrt{2} \int d^D x \sqrt{\det \bar{g}_{\mu\nu}} \bar{c}_\mu \mathcal{M}[\gamma; \bar{g}]^\mu{}_\nu c^\nu , \tag{C.9} \\
\mathcal{M}[\gamma; \bar{g}]^\mu{}_\nu &= (\bar{g}^{\mu\beta} \bar{g}^{\alpha\gamma} \bar{D}_\gamma \gamma_{\beta\nu} D_\alpha + \bar{g}^{\mu\beta} \bar{g}^{\alpha\gamma} \bar{D}_\gamma \gamma_{\alpha\nu} D_\beta - \bar{g}^{\mu\lambda} \bar{g}^{\sigma\rho} \bar{D}_\lambda \gamma_{\rho\nu} D_\sigma) .
\end{aligned}$$

## C.2 Tensor Decomposition of $\Gamma_k^{(2)}$

In both, the background field flow (2.8) and the exact functional equation (2.1), the second variation of the effective average action appears on the respective right hand sides. The first and second variations of the two terms in the EH action are derived in Appendix C.1. Based on these results the second variation of the effective average action  $\Gamma_k[g; \bar{g}]$  within the deDonder gauge ( $\alpha = 1$ ) can be straightforwardly calculated. As explained in the last paragraph of Subsection 2.2.1 the background

metric has to be identified with the physical metric, *i.e.*, in Eqs. (2.8) and (2.1) the second variation of  $\Gamma_k[\bar{g}; \bar{g}]$  enters. It is given by

$$\begin{aligned} \frac{1}{2} \delta^2 \Gamma_k[\bar{g}; \bar{g}] &= \kappa^2 Z_{Nk} \int d^D x \sqrt{\det \bar{g}_{\mu\nu}} \left[ \left( \frac{1}{4} h_\mu^\mu h_\mu^\mu - \frac{1}{2} h^{\mu\nu} h_{\mu\nu} \right) \left( -\bar{R} + 2\bar{\lambda}_k \right) \right. \\ &+ h_\mu^\mu h^{\mu\nu} \bar{R}_{\mu\nu} - h^{\mu\rho} h_\rho^\nu \bar{R}_{\mu\nu} + h^{\mu\nu} \bar{R}^\alpha{}_{\mu\nu}{}^\lambda h_{\alpha\lambda} \\ &\left. - \frac{1}{2} h^{\mu\nu} \bar{D}^2 h_{\mu\nu} + \frac{1}{4} h_\mu^\mu \bar{D}^2 h_\mu^\mu \right]. \end{aligned} \quad (\text{C.10})$$

Next I decompose the fluctuating metric into a traceless part and a trace part. The idea is to diagonalise partly the effective average action. For this one defines

$$h_{\mu\nu} =: \hat{h}_{\mu\nu} + \frac{1}{D} \bar{g}_{\mu\nu} h, \quad h := h_\mu^\mu \quad (\text{C.11})$$

where the  $\hat{h}_{\mu\nu}$  is representing the traceless part. Consequently,  $\bar{g}^{\mu\nu} \hat{h}_{\mu\nu} = 0$ , and one may rewrite the second variation as

$$\begin{aligned} \frac{1}{2} \delta^2 \Gamma_k[\bar{g}; \bar{g}] &= \kappa^2 Z_{Nk} \int d^D x \sqrt{\det \bar{g}_{\mu\nu}} \left[ \frac{1}{2} \hat{h}^{\mu\nu} \left( -\bar{D}^2 + \bar{R} - 2\bar{\lambda}_k \right) \hat{h}_{\mu\nu} \right. \\ &- \left( \frac{D-2}{4D} \right) h \left( -\bar{D}^2 - 2\bar{\lambda}_k + \bar{R} \left( \frac{D-4}{D} \right) \right) h \\ &\left. + \left( \frac{D-4}{D} \right) \hat{h}^{\mu\nu} \bar{R}_{\mu\nu} h + \hat{h}^{\mu\nu} \hat{h}_{\alpha\lambda} \bar{R}^\alpha{}_{\mu\nu}{}^\lambda - \hat{h}^{\mu\rho} \hat{h}_{\rho\nu} \bar{R}_\mu{}^\nu \right]. \end{aligned} \quad (\text{C.12})$$

Until now the computations were background independent. To simplify further I will exploit the relations (2.17) and (2.18) (valid for a maximally symmetric space) to simplify Eq. (C.12),

$$\begin{aligned} \delta^2 \Gamma_k[\bar{g}; \bar{g}] &= \kappa^2 Z_{Nk} \int d^D x \sqrt{\det \bar{g}_{\mu\nu}} \left[ \hat{h}^{\mu\nu} \left( -\bar{D}^2 - 2\bar{\lambda}_k + C_T \bar{R} \right) \hat{h}_{\mu\nu} \right. \\ &\left. - \left( \frac{D-2}{2D} \right) h \left( -\bar{D}^2 - 2\bar{\lambda}_k + C_S \bar{R} \right) h \right], \end{aligned} \quad (\text{C.13})$$

where I introduced a short notation for the following terms:

$$C_T = \left( \frac{D^2 - 3D + 4}{D(D-1)} \right) \quad (\text{C.14})$$

and

$$C_S = \left( \frac{D-4}{D} \right). \quad (\text{C.15})$$

For the second variation of the ghost action one obtains

$$S_{gh}^{(2)}[g; \bar{g}]^\mu{}_\nu = -\sqrt{2} \mathcal{M}[g; \bar{g}]^\mu{}_\nu . \quad (\text{C.16})$$

The Faddeev-Popov operator  $\mathcal{M}[\bar{g}; \bar{g}]^\mu{}_\nu$  in this equation also simplifies in the maximally symmetric space:

$$\mathcal{M}[\bar{g}; \bar{g}]^\mu{}_\nu = -C_V \delta^\mu{}_\nu \bar{R} + \delta^\mu{}_\nu \bar{D}^2 \quad (\text{C.17})$$

with

$$C_V = -\left(\frac{1}{D}\right) . \quad (\text{C.18})$$

# Appendix D

## Trace Evaluations and Heat Kernel Expansion

### Contents

---

<b>D.1</b>	<b>Background Field Flow . . . . .</b>	<b>61</b>
<b>D.2</b>	<b>Exact Functional Identity . . . . .</b>	<b>65</b>
<b>D.3</b>	<b>Tracing with a Compact Dimension . . . . .</b>	<b>67</b>
<b>D.4</b>	<b>Dimensionally Reduced Background Field Flow . . . . .</b>	<b>69</b>
<b>D.5</b>	<b>Exact Functional Identity: Dimensional Reduction . . . . .</b>	<b>71</b>

---

As a first step for deriving the  $\beta$ -functions one notes that in both, the background field flow (2.8) and the exact functional equation (2.1), the l.h.s. can be written within the EH theory as

$$\partial_t \Gamma_k[\bar{g}; \bar{g}] = 2 \kappa^2 \int d^D x \sqrt{\det \bar{g}_{\mu\nu}} \left( (\partial_t Z_{Nk}) (-\bar{R}(\bar{g}) + 2 \bar{\lambda}_k) + 2 Z_{Nk} \partial_t \bar{\lambda}_k \right) . \quad (\text{D.1})$$

To evaluate the traces in Eqs. (2.8) and (2.1) one needs to consider the cases of the approximate background field flow and of the exact functional identity separately.

### D.1 Background Field Flow

The computation of the r.h.s. of Eq. (2.8) requires to identify the three different regulator functions in Eqs. (B.18) and (B.20):

$$\begin{aligned} \text{traceless tensor: } Z &\rightarrow Z_{Nk} \kappa^2 , \\ \text{scalar (trace part): } Z &\rightarrow -\frac{D-2}{2D} Z_{Nk} \kappa^2 , \\ \text{vector (ghost part): } Z &\rightarrow \sqrt{2} . \end{aligned}$$

Plugging in the respective three versions of Eq. (B.20) into Eq. (2.8) and using Eq. (C.13) as well as Eq. (C.17), one obtains

$$\begin{aligned}
& \partial_t \Gamma_k[\bar{g}; \bar{g}] = \\
& = \text{Tr}_T \int_0^\infty \frac{ds}{s} \frac{1}{m!} (Z_{Nk} \kappa^2 s k^2)^{m+1} \exp\left(-Z_{Nk} \kappa^2 s (-\bar{D}^2 + k^2 - 2\bar{\lambda}_k + C_T \bar{R})\right) \\
& + \text{Tr}_S \int_0^\infty \frac{ds}{s} \frac{1}{m!} \left(-\frac{D-2}{2D} Z_{Nk} \kappa^2 s k^2\right)^{m+1} \times \\
& \quad \times \exp\left(Z_{Nk} \kappa^2 \frac{D-2}{2D} s (-\bar{D}^2 + k^2 - 2\bar{\lambda}_k + C_S \bar{R})\right) \\
& - 2 \text{Tr}_V \int_0^\infty \frac{ds}{s} \frac{1}{m!} (\sqrt{2} s k^2)^{m+1} \exp\left(-s \sqrt{2} (-\bar{D}^2 + k^2 + C_V \bar{R})\right), \quad (D.2)
\end{aligned}$$

and expanding up to linear order in  $\bar{R}$

$$\begin{aligned}
& \partial_t \Gamma_k[\bar{g}; \bar{g}] \approx \\
& \approx \text{Tr}_T \int_0^\infty \frac{ds}{s} \frac{1}{m!} (Z_{Nk} \kappa^2 s k^2)^{m+1} \exp\left(-Z_{Nk} \kappa^2 s (-\bar{D}^2 + k^2 - 2\bar{\lambda}_k)\right) \times \\
& \quad \times (1 - Z_{Nk} \kappa^2 s C_T \bar{R}) \\
& + \text{Tr}_S \int_0^\infty \frac{ds}{s} \frac{1}{m!} \left(-\frac{D-2}{2D} Z_{Nk} \kappa^2 s k^2\right)^{m+1} \times \\
& \quad \times \exp\left(\frac{D-2}{2D} Z_{Nk} \kappa^2 s (-\bar{D}^2 + k^2 - 2\bar{\lambda}_k)\right) \left(1 + \frac{D-2}{2D} Z_{Nk} \kappa^2 s C_S \bar{R}\right) \\
& - 2 \text{Tr}_V \int_0^\infty \frac{ds}{s} \frac{1}{m!} (\sqrt{2} s k^2)^{m+1} \exp\left(-s \sqrt{2} (-\bar{D}^2 + k^2)\right) (1 - s \sqrt{2} C_V \bar{R}). \quad (D.3)
\end{aligned}$$

Next I compute the trace of the three exponentials separately using the formulae for the heat kernel expansion [11, 45]

$$\begin{aligned}
\text{Tr}[W(-\bar{D}^2)] & = (4\pi)^{-D/2} \text{tr}(I) \left( Q_{D/2}[W] \int d^D x \sqrt{\det \bar{g}_{\mu\nu}} \right. \\
& \quad \left. + \frac{1}{6} Q_{D/2-1}[W] \int d^D x \sqrt{\det \bar{g}_{\mu\nu}} \bar{R} + \mathcal{O}(\bar{R}^2) \right) \quad (D.4)
\end{aligned}$$

and

$$Q_n[W] = \frac{1}{\Gamma(n)} \int_0^\infty dz z^{n-1} W(z), \quad (D.5)$$

where  $W$  is an appropriately chosen function.<sup>1</sup> For the tensor trace this yields

$$\begin{aligned}
& \text{Tr}_T \exp \left( -Z_{Nk} \kappa^2 s (-\bar{D}^2 + k^2 - 2\bar{\lambda}_k) \right) = \\
& = (4\pi)^{-D/2} \text{tr}_T(I) \times \\
& \times \left( \frac{1}{\Gamma(D/2)} \int_0^\infty dz z^{D/2-1} \exp \left( -Z_{Nk} \kappa^2 s (z + k^2 - 2\bar{\lambda}_k) \right) \int d^D x \sqrt{\det \bar{g}_{\mu\nu}} \right. \\
& + \frac{1}{6} \frac{1}{\Gamma(D/2 - 1)} \int_0^\infty dz z^{D/2-2} \exp \left( -Z_{Nk} \kappa^2 s (z + k^2 - 2\bar{\lambda}_k) \right) \int d^D x \sqrt{\det \bar{g}_{\mu\nu}} \bar{R} \\
& \left. + \mathcal{O}(\bar{R}^2) \right), \tag{D.6}
\end{aligned}$$

with  $\text{tr}_T(I) = \frac{1}{2}(D-1)(D+2)$ . Analogously for the scalar trace

$$\begin{aligned}
& \text{Tr}_S \exp \left( \frac{D-2}{2D} Z_{Nk} \kappa^2 s (-\bar{D}^2 + k^2 - 2\bar{\lambda}_k) \right) = \\
& = (4\pi)^{-D/2} \text{tr}_S(I) \times \\
& \times \left[ \frac{1}{\Gamma(D/2)} \int_0^\infty dz z^{D/2-1} \exp \left( \frac{D-2}{2D} Z_{Nk} \kappa^2 s (z + k^2 - 2\bar{\lambda}_k) \right) \int d^D x \sqrt{\det \bar{g}_{\mu\nu}} \right. \\
& + \frac{1}{6} \frac{1}{\Gamma(D/2 - 1)} \int_0^\infty dz z^{D/2-2} \exp \left( \frac{D-2}{2D} Z_{Nk} \kappa^2 s (z + k^2 - 2\bar{\lambda}_k) \right) \times \\
& \quad \left. \times \int d^D x \sqrt{\det \bar{g}_{\mu\nu}} \bar{R} + \mathcal{O}(\bar{R}^2) \right], \tag{D.7}
\end{aligned}$$

with  $\text{tr}_S(I) = 1$  and

$$\begin{aligned}
& \text{Tr}_V \exp \left( -s \sqrt{2} (-\bar{D}^2 + k^2) \right) = \\
& = (4\pi)^{-D/2} \text{tr}_V(I) \times \\
& \times \left[ \frac{1}{\Gamma(D/2)} \int_0^\infty dz z^{D/2-1} \exp \left( -s \sqrt{2} (z + k^2) \right) \int d^D x \sqrt{\det \bar{g}_{\mu\nu}} \right. \\
& + \frac{1}{6} \frac{1}{\Gamma(D/2 - 1)} \int_0^\infty dz z^{D/2-2} \exp \left( -s \sqrt{2} (z + k^2) \right) \int d^D x \sqrt{\det \bar{g}_{\mu\nu}} \bar{R} \\
& \left. + \mathcal{O}(\bar{R}^2) \right], \tag{D.8}
\end{aligned}$$

---

<sup>1</sup>Here it is helpful to note that the functional  $Q_n[W]$  is directly related to an integral over covariant background momenta  $q$ :

$$\int \frac{d^D q}{(2\pi)^D} W(q^2) = \frac{(4\pi)^{-D/2}}{\Gamma(D/2)} \int_0^\infty dz z^{D/2-1} W(z) = (4\pi)^{-D/2} Q_{D/2}[W].$$

The condition to be fulfilled by the otherwise arbitrary function  $W$  is the requirement that the integral above is well-defined.

with  $\text{tr}_V(I) = D$ .

Putting all terms together, performing first the integral over  $s$  and afterwards the integral over  $z$ , the resulting equation can be written as

$$\begin{aligned}
& 2 \kappa^2 \int d^D x \sqrt{\det \bar{g}_{\mu\nu}} \left( \partial_t Z_{Nk} (-\bar{R}(\bar{g}) + 2 \bar{\lambda}_k) + 2 Z_{Nk} \partial_t \bar{\lambda}_k \right) \approx \\
& \approx (4\pi)^{-D/2} \frac{\Gamma(m+1-D/2)}{\Gamma(m+1)} (k^2)^{m+1} \times \\
& \times \left( \frac{1}{(k^2 - 2 \bar{\lambda}_k)^{(m+1-D/2)}} \frac{1}{2} D(D+1) - 2D \frac{1}{(k^2)^{(m+1-D/2)}} \right) \int d^D x \sqrt{\det \bar{g}_{\mu\nu}} \\
& + (4\pi)^{-D/2} \frac{\Gamma(m+2-D/2)}{\Gamma(m+1)} (k^2)^{m+1} \times \\
& \times \left( \frac{1}{(k^2 - 2 \bar{\lambda}_k)^{(m+2-D/2)}} \frac{1}{12} (-5D+7)D - \frac{1}{3} (D+6) \frac{1}{(k^2)^{(m+2-D/2)}} \right) \times \\
& \times \int d^D x \sqrt{\det \bar{g}_{\mu\nu}} \bar{R}. \tag{D.9}
\end{aligned}$$

This equation can be split into two independent equations, one for the part independent of the Ricci scalar and one for the part linear in the Ricci scalar:

$$\begin{aligned}
& 2 \kappa^2 \left( (\partial_t Z_{Nk}) 2 \bar{\lambda}_k + 2 Z_{Nk} (\partial_t \bar{\lambda}_k) \right) = \\
& = (4\pi)^{-D/2} \frac{\Gamma(m+1-D/2)}{\Gamma(m+1)} k^D \left( \frac{\frac{1}{2} D(D+1)}{(1 - 2 \bar{\lambda}_k/k^2)^{(m+1-D/2)}} - 2D \right) \tag{D.10}
\end{aligned}$$

and

$$\begin{aligned}
& -2 \kappa^2 (\partial_t Z_{Nk}) = \\
& = (4\pi)^{-D/2} \frac{\Gamma(m+2-D/2)}{\Gamma(m+1)} k^{D-2} \left( \frac{\frac{1}{12} (-5D+7)D}{(1 - 2 \bar{\lambda}_k/k^2)^{(m+2-D/2)}} - \frac{1}{3} (D+6) \right). \tag{D.11}
\end{aligned}$$

Rewriting the last two equations in terms of the dimensionless Newton's constant  $g_k \equiv k^{D-2} G_k \equiv k^{D-2} Z_{Nk}^{-1} G_N$  and the dimensionless cosmological constant  $\lambda_k \equiv k^{-2} \bar{\lambda}_k$  leads to the following system of equations

$$\begin{aligned}
\partial_t \left( Z_{Nk} \lambda_k k^2 \right) & = 8 \pi g_k k^2 Z_{Nk} (4\pi)^{-D/2} \frac{\Gamma(m+1-D/2)}{\Gamma(m+1)} \times \\
& \times \left( \frac{\frac{1}{2} D(D+1)}{(1 - 2 \lambda_k)^{(m+1-D/2)}} - 2D \right) \tag{D.12}
\end{aligned}$$

and

$$\begin{aligned}
\partial_t Z_{Nk} & = -16 \pi g_k Z_{Nk} (4\pi)^{-D/2} \frac{\Gamma(m+2-D/2)}{\Gamma(m+1)} \times \\
& \times \left( \frac{\frac{1}{12} (-5D+7)D}{(1 - 2 \lambda_k)^{(m+2-D/2)}} - \frac{1}{3} (D+6) \right), \tag{D.13}
\end{aligned}$$

which relates directly to the  $\beta$ -functions as given in Sec. 2.3

## D.2 Exact Functional Identity

Before performing the analogous evaluation of the traces for the Wetterich equation a note on the regulator function needs to be given. Starting from

$$\tilde{R}_k(q^2) = q^2 r(y) \quad \text{with} \quad y = \frac{q^2}{k^2}, \quad (\text{D.14})$$

and

$$\partial_t \tilde{R}_k(q^2) = -2y r'(y) q^2 \quad (\text{D.15})$$

one obtains the Litim regulator (*cf.*, Eq. (2.3)) if the dimensionless regulator function  $r(y)$  is given by

$$r_{opt}(y) = \left( \frac{1}{y} - 1 \right) \Theta(1-y). \quad (\text{D.16})$$

The corresponding scale derivative reads

$$\partial_t \tilde{R}_k(q^2) = 2k^2 \Theta(1-y). \quad (\text{D.17})$$

The full regulator including the factor  $Z_k$ , *i.e.*, the running wave function renormalisation constant, is given by:

$$R_k = Z_k \tilde{R}_k(-\bar{D}^2) = Z_k(-\bar{D}^2) r_{opt}(y) \quad \text{with} \quad y = \frac{-\bar{D}^2}{k^2}, \quad (\text{D.18})$$

which results in a scale derivative

$$\partial_t R_k = -\eta_{Nk,gh} R_k + Z_k 2k^2 \Theta(1-y). \quad (\text{D.19})$$

The Wetterich equation for the Einstein-Hilbert theory explicitly reads:

$$\begin{aligned} & 2\kappa^2 \int d^D x \sqrt{\det \bar{g}_{\mu\nu}} \left( \partial_t Z_{Nk} (-\bar{R}(\bar{g}) + 2\bar{\lambda}_k) + 2Z_{Nk} \partial_t \bar{\lambda}_k \right) = \\ & = \frac{1}{2} \text{Tr}_T \left[ \left( \kappa^2 Z_{Nk} (-\bar{D}^2 - 2\bar{\lambda}_k + C_T \bar{R}) + Z_{Nk} \kappa^2 (-\bar{D}^2) r_{opt}(y) \right)^{-1} \times \right. \\ & \quad \left. \times \left( -\eta_{Nk} Z_{Nk} \kappa^2 (-\bar{D}^2) r_{opt}(y) + Z_{Nk} \kappa^2 2k^2 \Theta(1-y) \right) \right] \\ & + \frac{1}{2} \text{Tr}_S \left[ \left( \kappa^2 Z_{Nk} c_D (-\bar{D}^2 - 2\bar{\lambda}_k + C_S \bar{R}) + c_D Z_{Nk} \kappa^2 (-\bar{D}^2) r_{opt}(y) \right)^{-1} \times \right. \\ & \quad \left. \times \left( -\eta_{Nk} c_D Z_{Nk} \kappa^2 (-\bar{D}^2) r_{opt}(y) + c_D Z_{Nk} \kappa^2 2k^2 \Theta(1-y) \right) \right] \\ & - 2 \frac{1}{2} \text{Tr}_V \left[ \left( \sqrt{2} (-\bar{D}^2 + C_V \bar{R}) + \sqrt{2} (-\bar{D}^2) r_{opt}(y) \right)^{-1} \times \right. \\ & \quad \left. \times \left( -\eta_{gh} \sqrt{2} (-\bar{D}^2) r_{opt}(y) + \sqrt{2} 2k^2 \Theta(1-y) \right) \right], \quad (\text{D.20}) \end{aligned}$$

where  $c_D = -(D-2)/2D$  and for the employed truncation one puts additionally  $\eta_{gh} = 0$ .

Once again one expands up to linear order in  $\bar{R}$  and employs the heat kernel expansion. Using the abbreviations

$$\begin{aligned}\bar{c}_k &:= \frac{1}{k^2 - 2\bar{\lambda}_k}, \\ t_k(z) &:= \left( -\eta_{Nk} (k^2 - z) + 2k^2 \right) \Theta \left( 1 - \frac{z}{k^2} \right),\end{aligned}\quad (\text{D.21})$$

one obtains

$$\begin{aligned}& 2\kappa^2 \int d^D x \sqrt{\det \bar{g}_{\mu\nu}} \left( \partial_t Z_{Nk} (-\bar{R}(\bar{g}) + 2\bar{\lambda}_k) + 2Z_{Nk} \partial_t \bar{\lambda}_k \right) = \\ &= \frac{1}{2} (4\pi)^{-D/2} \frac{1}{2} (D-1)(D+2) \left\{ \frac{1}{\Gamma(D/2)} \int_0^\infty dz z^{D/2-1} \times \right. \\ &\quad \left. \times \left[ t_k(z) \left( \bar{c}_k - \bar{c}_k^2 C_T \bar{R} \right) \right] \int d^D x \sqrt{\det \bar{g}_{\mu\nu}} \right. \\ &\quad \left. + \frac{1}{6} \frac{1}{\Gamma(D/2-1)} \int_0^\infty dz z^{D/2-2} t_k(z) \bar{c}_k \int d^D x \sqrt{\det \bar{g}_{\mu\nu}} \bar{R} \right\} \\ &+ \frac{1}{2} (4\pi)^{-D/2} \left\{ \frac{1}{\Gamma(D/2)} \int_0^\infty dz z^{D/2-1} \left[ t_k(z) \left( \bar{c}_k - \bar{c}_k^2 C_S \bar{R} \right) \right] \times \right. \\ &\quad \left. \times \int d^D x \sqrt{\det \bar{g}_{\mu\nu}} \right. \\ &\quad \left. + \frac{1}{6} \frac{1}{\Gamma(D/2-1)} \int_0^\infty dz z^{D/2-2} t_k(z) \bar{c}_k \int d^D x \sqrt{\det \bar{g}_{\mu\nu}} \bar{R} \right\} \\ &- (4\pi)^{-D/2} D \left\{ \frac{1}{\Gamma(D/2)} \int_0^\infty dz z^{D/2-1} \left[ 2k^2 \Theta \left( 1 - \frac{z}{k^2} \right) \left( \frac{1}{k^2} - \frac{C_V \bar{R}}{k^4} \right) \right] \times \right. \\ &\quad \left. \times \int d^D x \sqrt{\det \bar{g}_{\mu\nu}} \right. \\ &\quad \left. + \frac{1}{6} \frac{1}{\Gamma(D/2-1)} \int_0^\infty dz z^{D/2-2} \left[ 2k^2 \Theta \left( 1 - \frac{z}{k^2} \right) \left( \frac{1}{k^2} \right) \right] \int d^D x \sqrt{\det \bar{g}_{\mu\nu}} \bar{R} \right\}\end{aligned}\quad (\text{D.22})$$

where the integrals over  $z$  can be performed easily.

After all the computations one arrives at the following flow equation:

$$\begin{aligned}
& 2 \kappa^2 \int d^D x \sqrt{\det \bar{g}_{\mu\nu}} \left( \partial_t Z_{Nk} (-\bar{R}(\bar{g}) + 2 \bar{\lambda}_k) + 2 Z_{Nk} \partial_t \bar{\lambda}_k \right) = \\
&= (4\pi)^{-D/2} \frac{k^D}{\Gamma(D/2)} \left( \frac{(D+1)}{(D+2)} \frac{(-\eta_{Nk} + D + 2) k^2}{(k^2 - 2 \bar{\lambda}_k)} - 4 \right) \int d^D x \sqrt{\det \bar{g}_{\mu\nu}} \\
&+ (4\pi)^{-D/2} \frac{k^D}{\Gamma(D/2)} \left( -\frac{(D-1)}{(D+2)} (-\eta_{Nk} + D + 2) \frac{k^2}{(k^2 - 2 \bar{\lambda}_k)^2} \right. \\
&\quad \left. + \frac{(D+1)}{12} (-\eta_{Nk} + D) \frac{1}{(k^2 - 2 \bar{\lambda}_k)} - 2 D k^2 \left( \frac{2}{D^2} + \frac{1}{6} \right) \right) \times \\
&\quad \times \int d^D x \sqrt{\det \bar{g}_{\mu\nu}} \bar{R} . \tag{D.23}
\end{aligned}$$

Again it is straightforward to read off the  $\beta$ -functions as given in Sec. 2.3.

### D.3 Tracing with a Compact Dimension

From  $D$  dimensions one is chosen compact, and thus the periodic boundary conditions as in Eq. (4.2) arise. Therefore  $D - 1$  components of the momentum vector are continuous, one is discrete:

$$q_{D,n} = \frac{2\pi n}{L} . \tag{D.24}$$

The traces involve then a  $(D - 1)$ -dimensional integral and a sum, and as explained in Sect. 4.1 one substitutes

$$\int \frac{d^D q}{(2\pi)^D} \rightarrow \frac{1}{L} \sum_n \int \frac{d^{D-1} q}{(2\pi)^{D-1}} . \tag{D.25}$$

In Chapter 2 and in the derivations in this Appendix, the identity

$$\int \frac{d^D q}{(2\pi)^D} W(q^2) = (4\pi)^{-D/2} \frac{1}{\Gamma(D/2)} \int_0^\infty dz z^{D/2-1} W(z) \tag{D.26}$$

has been implicitly used, *i.e.*, all momentum integrals have been already expressed as integrals over  $z = q^2$ . Hereby,  $W(z)$  is an arbitrary function except the requirement that the integral should be well-defined and finite. Likewise, the integrals (D.5) can be equivalently written as momentum integrals, *e.g.*,

$$(4\pi)^{-D/2} Q_{D/2}[W] = \int \frac{d^D q}{(2\pi)^D} W(q^2) . \tag{D.27}$$

The (back-)substitution of  $Q_{D/2-1}[W]$  is slightly more subtle,

$$(4\pi)^{-D/2} Q_{D/2-1}[W] = (D/2 - 1) \int \frac{d^D q}{(2\pi)^D} \frac{1}{q^2} W(q^2) . \tag{D.28}$$

In total this amounts to rewrite the heat kernel expansion as

$$\begin{aligned}
\text{Tr}[W(-\bar{D}^2)] &= \text{tr}(I) \left( \int \frac{d^D q}{(2\pi)^D} W(q^2) \int d^D x \sqrt{\det \bar{g}_{\mu\nu}} \right. \\
&\quad + \frac{1}{6} \left( \frac{D}{2} - 1 \right) \int \frac{d^D q}{(2\pi)^D} \frac{1}{q^2} W(q^2) \int d^D x \sqrt{\det \bar{g}_{\mu\nu}} \bar{R} \\
&\quad \left. + \mathcal{O}(\bar{R}^2) \right), \tag{D.29}
\end{aligned}$$

in which then the substitution (D.25) can be straightforwardly applied

$$\begin{aligned}
\text{Tr}[W(-\bar{D}^2)] &= \text{tr}(I) \left( \frac{1}{L} \sum_n \int \frac{d^{D-1} q}{(2\pi)^{D-1}} W(q^2) \int d^D x \sqrt{\det \bar{g}_{\mu\nu}} \right. \\
&\quad + \frac{1}{6} \left( \frac{D}{2} - 1 \right) \frac{1}{L} \sum_n \int \frac{d^{D-1} q}{(2\pi)^{D-1}} \frac{1}{q^2} W(q^2) \int d^D x \sqrt{\det \bar{g}_{\mu\nu}} \bar{R} \\
&\quad \left. + \mathcal{O}(\bar{R}^2) \right). \tag{D.30}
\end{aligned}$$

Doing the angular integrals, *i.e.*, applying Eq. (D.26) for  $D \rightarrow D - 1$ , one gets

$$\begin{aligned}
\text{Tr}[W(-\bar{D}^2)] &= \text{tr}(I) (4\pi)^{-(D-1)/2} \frac{1}{\Gamma(D/2 - 1/2)} \times \\
&\quad \times \left( \frac{1}{L} \sum_n \int_0^\infty dz z^{D/2-3/2} W(z + q_{D,n}^2) \int d^D x \sqrt{\det \bar{g}_{\mu\nu}} \right. \\
&\quad + \frac{1}{6} \left( \frac{D}{2} - 1 \right) \frac{1}{L} \sum_n \int_0^\infty dz z^{D/2-3/2} \frac{1}{z + q_{D,n}^2} W(z + q_{D,n}^2) \times \\
&\quad \left. \times \int d^D x \sqrt{\det \bar{g}_{\mu\nu}} \bar{R} + \mathcal{O}(\bar{R}^2) \right). \tag{D.31}
\end{aligned}$$

As described in Chapter 4 the term  $\frac{1}{z + q_{D,n}^2}$  in the part of this expression linear in  $\bar{R}$  leads to logarithms in the sums over  $n$ . Decreasing for this part the dimensionality of the trace simplifies the expressions enough such that the sums can be performed in a closed form. The corresponding approximate formula for the heat kernel expansion

reads

$$\begin{aligned}
\text{Tr}[W(-\bar{D}^2)] &= \text{tr}(I)(4\pi)^{-(D-1)/2} \frac{1}{\Gamma(D/2 - 1/2)} \times \\
&\times \left( \frac{1}{L} \sum_n \int_0^\infty dz z^{D/2-3/2} W(z + q_{D,n}^2) \int d^D x \sqrt{\det \bar{g}_{\mu\nu}} \right. \\
&+ \frac{1}{6} \left( \frac{D}{2} - 1 \right) \frac{1}{L} \sum_n \int_0^\infty dz z^{D/2-5/2} W(z + q_{D,n}^2) \times \\
&\left. \times \int d^D x \sqrt{\det \bar{g}_{\mu\nu}} \bar{R} + \mathcal{O}(\bar{R}^2) \right). \tag{D.32}
\end{aligned}$$

## D.4 Dimensionally Reduced Background Field Flow

Starting from Eq. (D.3) and using Eq. (D.32) for the evaluation of the traces yields

$$\begin{aligned}
2\kappa^2 \int d^D x \sqrt{\det \bar{g}_{\mu\nu}} \left( \partial_t Z_{Nk} (-\bar{R}(\bar{g}) + 2\bar{\lambda}_k) + 2Z_{Nk} \partial_t \bar{\lambda}_k \right) &= \tag{D.33} \\
= \text{tr}_T(I) \frac{1}{L} \sum_n u_D \int_0^\infty dz z^{(D-3)/2} (d_k(z; \bar{\lambda}_k))^{m+1} \int d^D x \sqrt{\det \bar{g}_{\mu\nu}} \\
- \text{tr}_T(I) C_T \frac{m+1}{k^2} \frac{1}{L} \sum_n u_D \int_0^\infty dz z^{(D-3)/2} (d_k(z; \bar{\lambda}_k))^{m+2} \int d^D x \sqrt{\det \bar{g}_{\mu\nu}} \bar{R} \\
+ \text{tr}_T(I) \frac{(D/2-1)}{6} \frac{1}{L} \sum_n u_D \int_0^\infty dz z^{(D-5)/2} (d_k(z; \bar{\lambda}_k))^{m+1} \int d^D x \sqrt{\det \bar{g}_{\mu\nu}} \bar{R} \\
+ \text{tr}_S(I) \frac{1}{L} \sum_n u_D \int_0^\infty dz z^{(D-3)/2} (d_k(z; \bar{\lambda}_k))^{m+1} \int d^D x \sqrt{\det \bar{g}_{\mu\nu}} \\
- \text{tr}_S(I) C_S \frac{m+1}{k^2} \frac{1}{L} \sum_n u_D \int_0^\infty dz z^{(D-3)/2} (d_k(z; \bar{\lambda}_k))^{m+2} \int d^D x \sqrt{\det \bar{g}_{\mu\nu}} \bar{R} \\
+ \text{tr}_S(I) \frac{(D/2-1)}{6} \frac{1}{L} \sum_n u_D \int_0^\infty dz z^{(D-5)/2} (d_k(z; \bar{\lambda}_k))^{m+1} \int d^D x \sqrt{\det \bar{g}_{\mu\nu}} \bar{R} \\
- 2 \text{tr}_V(I) \frac{1}{L} \sum_n u_D \int_0^\infty dz z^{(D-3)/2} (d_k(z; 0))^{m+1} \int d^D x \sqrt{\det \bar{g}_{\mu\nu}} \\
+ 2 \text{tr}_V(I) C_V \frac{m+1}{k^2} \frac{1}{L} \sum_n u_D \int_0^\infty dz z^{(D-3)/2} (d_k(z; 0))^{m+2} \int d^D x \sqrt{\det \bar{g}_{\mu\nu}} \bar{R} \\
- 2 \text{tr}_V(I) \frac{(D/2-1)}{6} \frac{1}{L} \sum_n u_D \int_0^\infty dz z^{(D-5)/2} (d_k(z; 0))^{m+1} \int d^D x \sqrt{\det \bar{g}_{\mu\nu}} \bar{R} .
\end{aligned}$$

where the abbreviations

$$\begin{aligned}
u_D &:= \frac{(4\pi)^{-(D-1)/2}}{\Gamma((D-1)/2)}, \\
d_k(z; \bar{\lambda}_k) &:= \left( \frac{k^2}{z + \left(\frac{2\pi n}{L}\right)^2 + k^2 - 2\bar{\lambda}_k} \right),
\end{aligned} \tag{D.34}$$

have been used.

The integrals over  $z$  can be done straightforwardly:

$$\begin{aligned}
& 2\kappa^2 \int d^D x \sqrt{\det \bar{g}_{\mu\nu}} \left( \partial_t Z_{Nk} (-\bar{R}(\bar{g}) + 2\bar{\lambda}_k) + 2Z_{Nk} \partial_t \bar{\lambda}_k \right) = \\
& = (\text{tr}_T(I) + \text{tr}_S(I)) (4\pi)^{-(D-1)/2} \frac{1}{L} \sum_n \frac{\Gamma(-(D-3)/2 + m)}{\Gamma(m+1)} (k^2)^{m+1} \times \\
& \times \left( \left( \frac{2\pi n}{L} \right)^2 + k^2 - 2\bar{\lambda}_k \right)^{(D-3)/2-m} \int d^D x \sqrt{\det \bar{g}_{\mu\nu}} \\
& - (\text{tr}_T(I) C_T + \text{tr}_S(I) C_S) (4\pi)^{-(D-1)/2} \frac{1}{L} \sum_n \frac{\Gamma(-(D-5)/2 + m)}{\Gamma(m+1)} (k^2)^{m+1} \times \\
& \times \left( \left( \frac{2\pi n}{L} \right)^2 + k^2 - 2\bar{\lambda}_k \right)^{(D-5)/2-m} \int d^D x \sqrt{\det \bar{g}_{\mu\nu}} \bar{R} \\
& + (\text{tr}_T(I) + \text{tr}_S(I)) (4\pi)^{-(D-1)/2} \frac{1}{L} \sum_n \frac{D-2}{6(D-3)} \frac{\Gamma(-(D-5)/2 + m)}{\Gamma(m+1)} (k^2)^{m+1} \times \\
& \times \left( \left( \frac{2\pi n}{L} \right)^2 + k^2 - 2\bar{\lambda}_k \right)^{(D-5)/2-m} \int d^D x \sqrt{\det \bar{g}_{\mu\nu}} \bar{R} \\
& - 2 \text{tr}_V(I) (4\pi)^{-(D-1)/2} \frac{1}{L} \sum_n \frac{\Gamma(-(D-3)/2 + m)}{\Gamma(m+1)} (k^2)^{m+1} \times \\
& \times \left( \left( \frac{2\pi n}{L} \right)^2 + k^2 \right)^{(D-3)/2-m} \int d^D x \sqrt{\det \bar{g}_{\mu\nu}} \\
& + 2 \text{tr}_V(I) C_V (4\pi)^{-(D-1)/2} \frac{1}{L} \sum_n \frac{\Gamma(-(D-5)/2 + m)}{\Gamma(m+1)} (k^2)^{m+1} \times \\
& \times \left( \left( \frac{2\pi n}{L} \right)^2 + k^2 \right)^{(D-5)/2-m} \int d^D x \sqrt{\det \bar{g}_{\mu\nu}} \bar{R} \\
& - 2 \text{tr}_V(I) (4\pi)^{-(D-1)/2} \frac{1}{L} \sum_n \frac{D-2}{6(D-3)} \frac{\Gamma(-(D-5)/2 + m)}{\Gamma(m+1)} (k^2)^{m+1} \times \\
& \times \left( \left( \frac{2\pi n}{L} \right)^2 + k^2 \right)^{(D-5)/2-m} \int d^D x \sqrt{\det \bar{g}_{\mu\nu}} \bar{R}.
\end{aligned} \tag{D.35}$$

This equation can be simplified

$$\begin{aligned}
& 2\kappa^2 \int d^D x \sqrt{\det \bar{g}_{\mu\nu}} \left( \partial_t Z_{Nk} (-\bar{R}(\bar{g}) + 2\bar{\lambda}_k) + 2Z_{Nk} \partial_t \bar{\lambda}_k \right) = \\
& = \int d^D x \sqrt{\det \bar{g}_{\mu\nu}} \left\{ (4\pi)^{-(D-1)/2} \frac{(k^2)^{(D-1)/2} \Gamma(-\frac{(D-3)}{2} + m)}{\Gamma(m+1)} \times \right. \\
& \quad \times \frac{1}{L} \sum_n \left[ \frac{1}{2} D(D+1) (\omega_n^2 + 1 - 2\lambda_k)^{(D-3)/2-m} \right. \\
& \quad \quad \left. \left. - 2D (\omega_n^2 + 1)^{(D-3)/2-m} \right] \right\} \\
& + \int d^D x \sqrt{\det \bar{g}_{\mu\nu}} \bar{R} \left\{ (4\pi)^{-(D-1)/2} \frac{(k^2)^{(D-3)/2} \Gamma(-\frac{(D-5)}{2} + m)}{\Gamma(m+1)} \times \right. \\
& \quad \times \frac{1}{L} \sum_n \left[ \frac{-D(5D^2 - 23D + 20)}{12(D-3)} (\omega_n^2 + 1 - 2\lambda_k)^{(D-5)/2-m} \right. \\
& \quad \quad \left. \left. + \left( \frac{-D^2 - 4D + 18}{3(D-3)} \right) (\omega_n^2 + 1)^{(D-5)/2-m} \right] \right\}
\end{aligned} \tag{D.36}$$

where the definition (4.10) for  $\omega_n^2$  has been used.

## D.5 Exact Functional Identity: Dimensional Reduction

Starting point is the expression (D.20) but now the traces are performed with the help of either Eq. (D.31) or (D.32). After some algebra and using the definitions (D.34) or (D.21) as well as

$$\tilde{t}_k(z, n) := -\eta_{Nk}(k^2 - (2\pi n/L)^2 - z) + 2k^2 \quad \text{and} \quad \tilde{q}^2 := k^2 - (2\pi n/L)^2 \tag{D.37}$$

one arrives then at

$$\begin{aligned}
& 2\kappa^2 \int d^D x \sqrt{\det \bar{g}_{\mu\nu}} \left( \partial_t Z_{Nk} (-\bar{R}(\bar{g}) + 2\bar{\lambda}_k) + 2Z_{Nk} \partial_t \bar{\lambda}_k \right) = \\
& = \int d^D x \sqrt{\det \bar{g}_{\mu\nu}} \frac{1}{L} \sum_{n^2 \leq (kL/2\pi)^2} u_D \int_0^{\tilde{q}^2} dz z^{(D-3)/2} \left( \frac{1}{4} D(D+1) \tilde{t}_k(z, n) \bar{c}_k - 2D \right) \\
& + \int d^D x \sqrt{\det \bar{g}_{\mu\nu}} \bar{R} \frac{1}{L} \sum_{n^2 \leq (kL/2\pi)^2} u_D \int_0^{\tilde{q}^2} dz z^{(D-3)/2} \\
& \quad \left[ \left( \left( -\frac{1}{4} (D-1)(D+2) C_T - \frac{1}{2} C_S \right) \tilde{t}_k(z, n) \bar{c}_k^2 + 2DC_V \right) \right. \\
& \quad \left. + \frac{1}{z + (2\pi n/L)^2} \left( \left( \frac{1}{48} D(D+1)(D-2) \right) \tilde{t}_k(z, n) \bar{c}_k - \frac{1}{6} D(D-2) \right) \right]
\end{aligned} \tag{D.38}$$

where the difference in the two types of traces (D.31) or (D.32) is in keeping or neglecting the term in red. Setting  $D = 5$  and performing the integrals over  $z$  one arrives straightforwardly at the expressions for given in Sect. 4.2. There the following definition has been used

$$s_l(a) = \sum_{-l}^{l-1} \left( 1 - \left( \frac{n}{a} \right)^2 \right)^l, \quad l = 1, 2, 3, \quad (\text{D.39})$$

where  $a = kL/2\pi$  and  $s_l(a) = 1$  for  $a < 1$ . The sums can be performed:

$$\begin{aligned} s_1(a) &= (1 + 2[a]) \left( 1 - \frac{[a]}{3a^2} (1 + [a]) \right), \\ s_2(a) &= (1 + 2[a]) \left( 1 - \frac{[a]}{15a^4} (1 + [a]) \left( 1 + 10a^2 - 3[a](1 + [a]) \right) \right), \\ s_3(a) &= (1 + 2[a]) \left( 1 - \frac{[a]}{105a^6} (1 + [a]) \times \right. \\ &\quad \left. \times \left( 5 + 21(a^2 + 5a^4) + 3[a](1 + [a]) \left( -5 - 21a^2 + 5[a](1 + [a]) \right) \right) \right), \end{aligned} \quad (\text{D.40})$$

the limits for  $a \rightarrow \infty$  are

$$\begin{aligned} s_1(a) &\rightarrow \frac{4}{3} a, \\ s_2(a) &\rightarrow \frac{16}{15} a, \\ s_3(a) &\rightarrow \frac{32}{35} a. \end{aligned} \quad (\text{D.41})$$

# Appendix E

## Threshold Functions

Following Refs. [6, 24] in this Appendix the so-called threshold functions are introduced and some of their properties are discussed. First, the case without dimensional reduction is considered.

The basic threshold function in  $D$  dimensions is defined as

$$l_0^D(w) := \frac{1}{4} v_D^{-1} k^{-D} \int \frac{d^D q}{(2\pi)^D} \frac{\partial_t (R_k(q^2)/Z_k)}{q^2 + R_k(q^2)/Z_k + k^2 w} \quad (\text{E.1})$$

where  $v_D^{-1} = 2(4\pi)^{D/2} \Gamma(D/2)$  and the regulator  $R_k$  is defined in Eq. (D.18). Comparing this expression with the ones given in Appendix D.2 reveals that in the cases treated in this thesis one has  $w = -2\lambda_k$ . The substitution  $y = q^2/k^2$  and performing the angular integrals yields

$$l_0^D(w) = \frac{1}{2} \int_0^\infty dy y^{D/2-1} \frac{y \partial_t r(y)}{y(1+r(y)) + w}. \quad (\text{E.2})$$

For the Litim regulator, *i.e.*, for  $r_{opt}(y) = (1/y - 1) \Theta(1 - y)$ , one obtains

$$l_0^D(w) = \frac{1}{1+w} \int_0^1 dy y^{D/2-1} = \frac{2}{D} \frac{1}{1+w}. \quad (\text{E.3})$$

Higher threshold functions can be defined by taking derivatives

$$\partial_w l_m^D(w) = -(\delta_{m,0} + m) l_{m+1}^D(w) \quad (\text{E.4})$$

or equivalently

$$l_m^D(w) = \frac{1}{2} (\delta_{m,0} + m) \int_0^\infty dy y^{D/2-1} \frac{y \partial_t r(y)}{(y(1+r(y)) + w)^{m+1}}. \quad (\text{E.5})$$

In the case of dimensional reduction applying the substitution (4.5),

$$\int \frac{d^D q}{(2\pi)^D} \rightarrow \frac{1}{L} \sum_n \int \frac{d^{D-1} q}{(2\pi)^{D-1}}, \quad (\text{E.6})$$

motivates to introduce the following generalised threshold function<sup>1</sup>

$$l_0^D(w, L) = \frac{v_{D-1}}{v_D} \frac{1}{kL} \sum_n \int_0^\infty dy y^{D/2-3/2} \frac{-(y + \omega_n^2)^2 r'(y + \omega_n^2)}{(y + \omega_n^2)(1 + r(y + \omega_n^2)) + w} \quad (\text{E.7})$$

where  $\partial_t r(y) = -2yr'(y)$  has been substituted and the definition (4.10), *i.e.*,  $\omega_n = 2\pi n/kL$  has been used. The higher threshold functions are again related to  $l_0^D(w, L)$  by deriving it  $n$  times. By construction their limiting values are given by:

$$\begin{aligned} l_m^D(w, L \rightarrow \infty) &= l_m^D(w), \\ l_m^D(w, L \rightarrow 0) &= \frac{v_{D-1}}{v_D} \frac{1}{kL} l_m^{D-1}(w). \end{aligned} \quad (\text{E.8})$$

The latter limit is evident from the fact that for  $L \rightarrow 0$  only the zero mode contributes to the sum.

For the Litim regulator the dependence on  $L$  factorizes,

$$l_0^D(w, L) = \frac{2}{D-1} \frac{1}{1+w} \frac{v_{D-1}}{v_D} \frac{1}{kL} \sum_n (1 - \omega_n^2)^{D/2-1/2} \Theta(1 - \omega_n^2) \quad (\text{E.9})$$

and for higher threshold functions

$$l_m^D(w, L) = \frac{D}{D-1} l_m^D(w) \frac{v_{D-1}}{v_D} \frac{1}{kL} \sum_n (1 - \omega_n^2)^{D/2-1/2} \Theta(1 - \omega_n^2). \quad (\text{E.10})$$

For  $D = 5$  the sum can be performed explicitly,

$$\sum_n (1 - \omega_n^2)^2 \Theta(1 - \omega_n^2) = \sum_{n=-[a]}^{[a]} (1 - n^2/a^2)^2 = s_2(a) \quad (\text{E.11})$$

with  $a = kL/2\pi$  and  $s_2(a)$  being defined in Eq. (D.39), see also the explicit form (D.40).

---

<sup>1</sup>In Ref. [24] those functions have been introduced for non-vanishing temperatures  $T$ . Substituting  $T \rightarrow 1/L$  and  $\tau \rightarrow 2\pi/kL$  in the corresponding expressions of Ref. [24] provides the ones given here.

# Appendix F

## Numerical treatment

In Chapters 3 and 4 the UV fixed points have been determined from the roots of the  $\beta$ -functions with the SOLVE function of MATHEMATICA. The RG flows have been calculated by solving the differential equations by either using the function NDSOLVE of MATHEMATICA or by a FORTRAN code containing a self-written fourth-order Runge-Kutta algorithm. In the cases both methods have been applied to the same parameter set the results agreed very well. Also other numerical checks have been passed with high precision, *e.g.*, the numerical solution of the differential equations reproduced the UV fixed point values typically with a precision of  $\mathcal{O}(10^{-8})$ . Where available I compared my results to those available in the literature, and was therefore able to verify them.

In most cases the flow has been integrated from the IR to the UV. It has been checked that the opposite direction of the flow generates the same trajectory as long as one does not start too close to the UV fixed point. Typically the flow has been started at  $k_{min} = 0.1$  and terminated at  $k_{max} = 10^5$  with  $\mathcal{O}(10^4)$  steps in between, except for Figs. 4.3 and 4.5 where  $k_{min} = 10^{-21}$  and  $k_{max} = 10^{45}$  has been used with  $10^7$  Runge-Kutta steps.

In cases the sums over Kaluza-Klein modes could not be expressed in a closed form they have been performed numerically. As the sums originating from the exact functional identity are finite this has been straightforwardly possible. For  $kL > 10^8$  the sums then have been simply substituted by the limiting expressions. For the sums within approximate background field flow convergence has been tested and a numerical accuracy at the level of  $10^{-8}$  was obtained by adjusting the numerical limits of the sums accordingly.



# References

- [1] A. Einstein, “The Foundation of the General Theory of Relativity,” *Annalen Phys.* **49** (1916) 769 [*Annalen Phys.* **14** (2005) 517].
- [2] C. D. Hoyle, D. J. Kapner, B. R. Heckel, E. G. Adelberger, J. H. Gundlach, U. Schmidt and H. E. Swanson, “Sub-millimeter tests of the gravitational inverse-square law,” *Phys. Rev. D* **70** (2004) 042004, [[hep-ph/0405262](#)];  
D. J. Kapner, T. S. Cook, E. G. Adelberger, J. H. Gundlach, B. R. Heckel, C. D. Hoyle and H. E. Swanson, “Tests of the gravitational inverse-square law below the dark-energy length scale,” *Phys. Rev. Lett.* **98** (2007) 021101, [[hep-ph/0611184](#)].
- [3] J. Beringer *et al.* [Particle Data Group Collaboration], “Review of Particle Physics (RPP),” *Phys. Rev. D* **86** (2012) 010001.
- [4] M. Reuter and F. Saueressig, “Renormalization group flow of quantum gravity in the Einstein-Hilbert truncation,” *Phys. Rev. D* **65** (2002) 065016, [[hep-th/0110054](#)].
- [5] S. Weinberg, in “General Relativity: An Einstein centenary survey,” Eds. S. W. Hawking and W. Israel, Cambridge University Press (1979), p. 790.
- [6] J. Berges, N. Tetradis and C. Wetterich, “Nonperturbative renormalization flow in quantum field theory and statistical physics,” *Phys. Rept.* **363** (2002) 223, [[hep-ph/0005122](#)].
- [7] J. Polonyi, “Lectures on the functional renormalization group method,” *Central Eur. J. Phys.* **1** (2003) 1, [[hep-th/0110026](#)].
- [8] D. F. Litim and J. M. Pawłowski, “On gauge invariant Wilsonian flows,” [hep-th/9901063](#).
- [9] J. M. Pawłowski, “Aspects of the functional renormalisation group,” *Annals Phys.* **322** (2007) 2831, [[hep-th/0512261](#)].
- [10] H. Gies, “Introduction to the functional RG and applications to gauge theories,” *Lect. Notes Phys.* **852** (2012) 287, [[hep-ph/0611146](#)].
- [11] M. Reuter, “Nonperturbative evolution equation for quantum gravity,” *Phys. Rev. D* **57** (1998) 971, [[hep-th/9605030](#)].

- [12] O. Lauscher and M. Reuter, “Ultraviolet fixed point and generalized flow equation of quantum gravity,” *Phys. Rev. D* **65** (2002) 025013, [hep-th/0108040].
- [13] O. Lauscher and M. Reuter, “Is quantum Einstein gravity nonperturbatively renormalizable?,” *Class. Quant. Grav.* **19** (2002) 483, [hep-th/0110021].
- [14] O. Lauscher and M. Reuter, “Flow equation of quantum Einstein gravity in a higher derivative truncation,” *Phys. Rev. D* **66** (2002) 025026, [hep-th/0205062].
- [15] M. Niedermaier, “The Asymptotic safety scenario in quantum gravity: An Introduction,” *Class. Quant. Grav.* **24** (2007) R171, [gr-qc/0610018].
- [16] M. Niedermaier and M. Reuter, “The Asymptotic Safety Scenario in Quantum Gravity,” *Living Rev. Rel.* **9** (2006) 5.
- [17] R. Percacci, “A Short introduction to asymptotic safety,” hep-th/1110.6389.
- [18] M. Reuter and F. Saueressig, “Quantum Einstein Gravity,” *New J. Phys.* **14** (2012) 055022, [hep-th/1202.2274].
- [19] K. Falls, D. F. Litim, K. Nikolakopoulos and C. Rahmede, “A bootstrap towards asymptotic safety,” hep-th/1301.4191.
- [20] J. Ambjorn, A. Goerlich, J. Jurkiewicz and R. Loll, “Nonperturbative Quantum Gravity,” hep-th/1203.3591.
- [21] D. Coumbe and J. Laiho, “Exploring the Phase Diagram of Lattice Quantum Gravity,” *PoS LATTICE 2011* (2011) 334, [hep-lat/1201.2864].
- [22] C. Wetterich, “Exact evolution equation for the effective potential,” *Phys. Lett. B* **301** (1993) 90.
- [23] D. F. Litim, “Optimization of the exact renormalization group,” *Phys. Lett. B* **486** (2000) 92, [hep-th/0005245].
- [24] D. F. Litim, “Optimized renormalization group flows,” *Phys. Rev. D* **64** (2001) 105007, [hep-th/0103195].
- [25] D. F. Litim, “Mind the gap,” *Int. J. Mod. Phys. A* **16** (2001) 2081, [hep-th/0104221].
- [26] D. F. Litim, “Critical exponents from optimized renormalization group flows,” *Nucl. Phys. B* **631** (2002) 128, [hep-th/0203006].
- [27] D. F. Litim, “Derivative expansion and renormalization group flows,” *JHEP* **0111** (2001) 059, [hep-th/0111159].
- [28] D. F. Litim, “Convergence and stability of the renormalization group,” hep-th/0208117.

- [29] D. F. Litim, “Fixed points of quantum gravity,” *Phys. Rev. Lett.* **92** (2004) 201301, [hep-th/0312114].
- [30] P. Fischer and D. F. Litim, “Fixed points of quantum gravity in extra dimensions,” *Phys. Lett. B* **638** (2006) 497, [hep-th/0602203].
- [31] N. Arkani-Hamed, S. Dimopoulos and G. R. Dvali, “The Hierarchy problem and new dimensions at a millimeter,” *Phys. Lett. B* **429** (1998) 263, [hep-ph/9803315].
- [32] N. Arkani-Hamed, S. Dimopoulos and G. R. Dvali, “Phenomenology, astrophysics and cosmology of theories with submillimeter dimensions and TeV scale quantum gravity,” *Phys. Rev. D* **59** (1999) 086004, [hep-ph/9807344].
- [33] D. F. Litim and T. Plehn, “Signatures of gravitational fixed points at the LHC,” *Phys. Rev. Lett.* **100** (2008) 131301, [hep-ph/0707.3983].
- [34] D. F. Litim and T. Plehn, “Virtual gravitons at the LHC,” In \*Karlsruhe 2007, SUSY 2007\* 628-631, [hep-ph/0710.3096].
- [35] E. Gerwick, D. Litim and T. Plehn, “Asymptotic safety and Kaluza-Klein gravitons at the LHC,” *Phys. Rev. D* **83** (2011) 084048, [hep-ph/1101.5548].
- [36] D. F. Litim, “Renormalisation group and the Planck scale,” *Phil. Trans. Roy. Soc. Lond. A* **369** (2011) 2759, [hep-th/1102.4624].
- [37] J. Hewett and T. Rizzo, “Collider Signals of Gravitational Fixed Points,” *JHEP* **0712** (2007) 009, [hep-ph/0707.3182].
- [38] G. F. Giudice, R. Rattazzi and J. D. Wells, “Quantum gravity and extra dimensions at high-energy colliders,” *Nucl. Phys. B* **544** (1999) 3, [hep-ph/9811291].
- [39] J. Wang and C. S. Li, “Updated predictions for graviton and photon associated production at the LHC,” *Phys. Rev. D* **86** (2012) 116008, [hep-ph/1209.6257].
- [40] D. F. Litim and D. Zappala, “Ising exponents from the functional renormalisation group,” *Phys. Rev. D* **83** (2011) 085009, [hep-th/1009.1948].
- [41] D. F. Litim and J. M. Pawłowski, “Predictive power of renormalization group flows: A Comparison,” *Phys. Lett. B* **516** (2001) 197, [hep-th/0107020].
- [42] D. F. Litim and J. M. Pawłowski, “Completeness and consistency of renormalisation group flows,” *Phys. Rev. D* **66** (2002) 025030, [hep-th/0202188].
- [43] D. F. Litim, “Towards functional flows for hierarchical models,” *Phys. Rev. D* **76** (2007) 105001, [hep-th/0704.1514].

- [44] S. -B. Liao, “On connection between momentum cutoff and the proper time regularizations,” *Phys. Rev. D* **53** (1996) 2020, [hep-th/9501124].
- [45] A. Bonanno and M. Reuter, “Proper time flow equation for gravity,” *JHEP* **0502** (2005) 035, [hep-th/0410191].
- [46] M. Reuter and C. Wetterich, “Effective average action for gauge theories and exact evolution equations,” *Nucl. Phys. B* **417** (1994) 181.
- [47] F. Freire, D. F. Litim and J. M. Pawłowski, “Gauge invariance and background field formalism in the exact renormalization group,” *Phys. Lett. B* **495** (2000) 256, [hep-th/0009110].
- [48] D. F. Litim and J. M. Pawłowski, “Wilsonian flows and background fields,” *Phys. Lett. B* **546** (2002) 279, [hep-th/0208216].
- [49] K. Groh and F. Saueressig, “Ghost wave-function renormalization in Asymptotically Safe Quantum Gravity,” *J. Phys. A* **43** (2010) 365403, [hep-th/1001.5032].
- [50] A. Eichhorn and H. Gies, “Ghost anomalous dimension in asymptotically safe quantum gravity,” *Phys. Rev. D* **81** (2010) 104010, [hep-th/1001.5033].
- [51] A. Eichhorn, “Faddeev-Popov ghosts in quantum gravity beyond perturbation theory,” hep-th/1301.0632.
- [52] P. Fischer and D. F. Litim, “Fixed points of quantum gravity in higher dimensions,” *AIP Conf. Proc.* **861** (2006) 336, [hep-th/0606135].
- [53] D. Litim and A. Satz, “Limit cycles and quantum gravity,” hep-th/1205.4218.
- [54] N. Christiansen, D. F. Litim, J. M. Pawłowski and A. Rodigast, “Fixed points and infrared completion of quantum gravity,” hep-th/1209.4038.
- [55] S. Rechenberger and F. Saueressig, “A functional renormalization group equation for foliated spacetimes,” hep-th/1212.5114.
- [56] D. F. Litim, “Fixed Points of Quantum Gravity and the Renormalisation Group,” hep-th/0810.3675.

# Acknowledgements

Many persons have contributed to the work of this thesis, I am grateful to all of them.

First of all, with great pleasure I thank my advisor, Daniel F. Litim, who introduced me to such an overwhelmingly and outstandingly interesting topic! He always made the most complicated problems look easier to me. It was delightful to have the opportunity to work with somebody like Daniel! I really enjoyed all our discussions, being in Sussex, Graz, or anywhere else.

Secondly, I thank my co-advisor, Bernd-Jochen Schaefer, for the helpful discussions, hints and the critical reading of my thesis.

During the work of this thesis I had gladly many occasions to discuss with very interesting physicists, and for some of them I want to take the chance to mention explicitly here: Holger Gies, Jan Martin Pawłowski, Frank Saueressig and my good old friend, John Swain. Here, specially, I would like to thank Jan for many conversations and advices.

My thanks also go to my colleagues from the SICQFT group in Graz, but one person in particular, Hèlios Sanchis-Alepuz (right now at the University of Giessen), with whom I had joyful discussions about classical gravity.

As part of this work was also done at the University of Sussex, where I spent several very pleasant visits, I would like to thank the Department of Physics and Astronomy and my colleagues there for their kind hospitality. In special, I want to mention Kevin Geoffrey Falls and Edouard Marchais for their very helpful and interesting discussions in the beginning of my thesis. It was always a lot of fun to talk with them!

Financial support from the Paul-Urban Foundation at the University of Graz is acknowledged.

Last, but not least, I would like to thank my family for all their support and trust! And of course, my beloved husband, who was always there for me, specially when I was deeply drowning in my higher dimensional world... Thank you for all the energy, support and love when I most needed!

